

WORLD METEOROLOGICAL ORGANIZATION

GLOBAL ATMOSPHERE WATCH

WORLD DATA CENTRE FOR GREENHOUSE GASES



**GLOBAL
ATMOSPHERE
WATCH**

WMO WDCGG DATA SUMMARY

WDCGG No. 43

GAW DATA
Volume IV-Greenhouse and Related Gases

PUBLISHED BY
JAPAN METEOROLOGICAL AGENCY
IN CO-OPERATION WITH
WORLD METEOROLOGICAL ORGANIZATION

March 2020



CONTENTS

	Page
PREFACE	1
1. CARBON DIOXIDE	3
2. METHANE	9
3. NITROUS OXIDE	15
4. HALOCARBONS AND OTHER HALOGENATED SPECIES	21
5. CARBON MONOXIDE	27
APPENDICES	33
A ANALYSIS	34
B CALIBRATION AND STANDARD SCALES	36
C LIST OF OBSERVATIONAL STATIONS	53
D LIST OF CONTRIBUTORS	64
E LIST OF ABBREVIATIONS	83
F LIST OF WMO/WDCGG PUBLICATIONS	87
REFERENCES	89

PREFACE

Global observations of greenhouse gases are essential for understanding of the global carbon cycle and the role these gases play in driving climate change. Ongoing observational efforts have shown gradually increasing levels of various greenhouse gases in the atmosphere, and independent scientific analysis has repeatedly suggested that increased gas emissions driven by anthropogenic activity (such as fossil fuel combustion and deforestation) since the industrial era have led to detectable tropospheric warming. To prevent further warming urgent actions should be taken to reduce emissions and those actions must be based on scientifically robust information. Against this background, there is increased demand for greenhouse gas data to satisfy scientific requirements and provide reliable information to policy makers.

The World Data Centre for Greenhouse Gases (WDCGG) has been operated by the Japan Meteorological Agency (JMA) since 1990 in response to a request from the World Meteorological Organization (WMO). It holds the status of a World Data Centre (WDC) under the WMO Global Atmosphere Watch (GAW) programme for the collection, archiving and distribution of data on greenhouse and related gases (such as CO) in the atmosphere and oceans from surface stations worldwide, mobile platforms and satellite. The data are provided online with a requirement for acknowledgment or co-authorship accreditation if used in a publication (see the website for details).

Information on the global state of major greenhouse gases in the atmosphere is regularly published in the WMO Greenhouse Gas Bulletin, to which WDCGG contributes via the calculation of related global mean mole fractions, long-term trends and growth rates. The WMO WDCGG Data Summary reports on the global means covered in the Bulletin and on latitudinal or hemispheric means, individual observational data used in global analysis. In addition to the gases, covered by the Bulletin, this summary contains information on CO and certain halogenated species.

This issue of the Data Summary covers observational data collected at surface stations and on certain ships for the period from 1968 to 2017 based on monthly mean data submitted to WDCGG by September 2018. The observation data and the results of related analysis indicate that concentrations of major greenhouse gases (CO₂, CH₄, N₂O, SF₆ and certain HCFCs and HFCs) are increasing, while those of certain ozone-depleting substances (e.g., CFCs) are not. The global mean mole fractions of CO₂, CH₄ and N₂O reached new highs of 405.5±0.1 ppm, 1859±2 ppb and 329.9±0.1 ppb in 2017, corresponding to 146%, 257% and 122% of pre-industrial levels, respectively. More detailed information is provided in the main text. The value-added analytical information presented in this Data Summary is expected to support scientific research, assessment and policy-making in relation to environmental issues.

Finally, WDCGG would like to thank all data contributors worldwide for their efforts in maintaining accurate long-term observations and for their ongoing data submission. Contributors include the National Oceanic and Atmospheric Administration (NOAA) Earth System Research Laboratory (ESRL) and its cooperative air-sampling network, the Advanced Global Atmospheric Gases Experiment (AGAGE), and a variety of other observational stations operating under the framework of GAW and other monitoring programmes as listed in Appendix D. All organizations submitting data to WDCGG are acknowledged as invaluable contributors to the Data Summary.

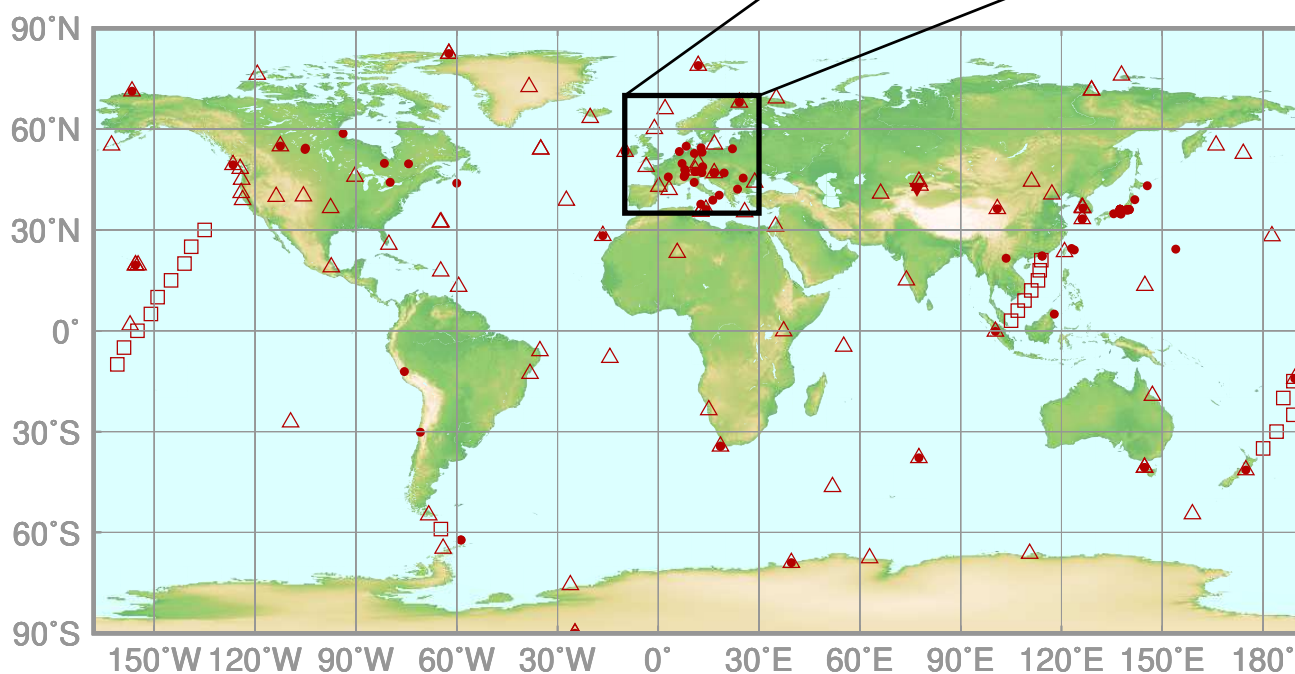
Mailing address:

WMO World Data Centre for Greenhouse Gases (WDCGG)
c/o Japan Meteorological Agency
1-3-4, Otemachi, Chiyoda-ku, Tokyo 100-8122, Japan
E-mail: wdcgg@met.kishou.go.jp
Telephone: +81-3-3287-3439
Facsimile: +81-3-3211-8309
Website: <https://gaw.kishou.go.jp/>

1.

CARBON DIOXIDE (CO₂)

- : CONTINUOUS STATION
- △ : FLASK STATION
- : FLASK MOBILE (SHIP)
- ▼ : REMOTE SENSING STATION



This map shows locations of the stations that have submitted data for monthly mean mole fractions.

CO₂ Monthly Data

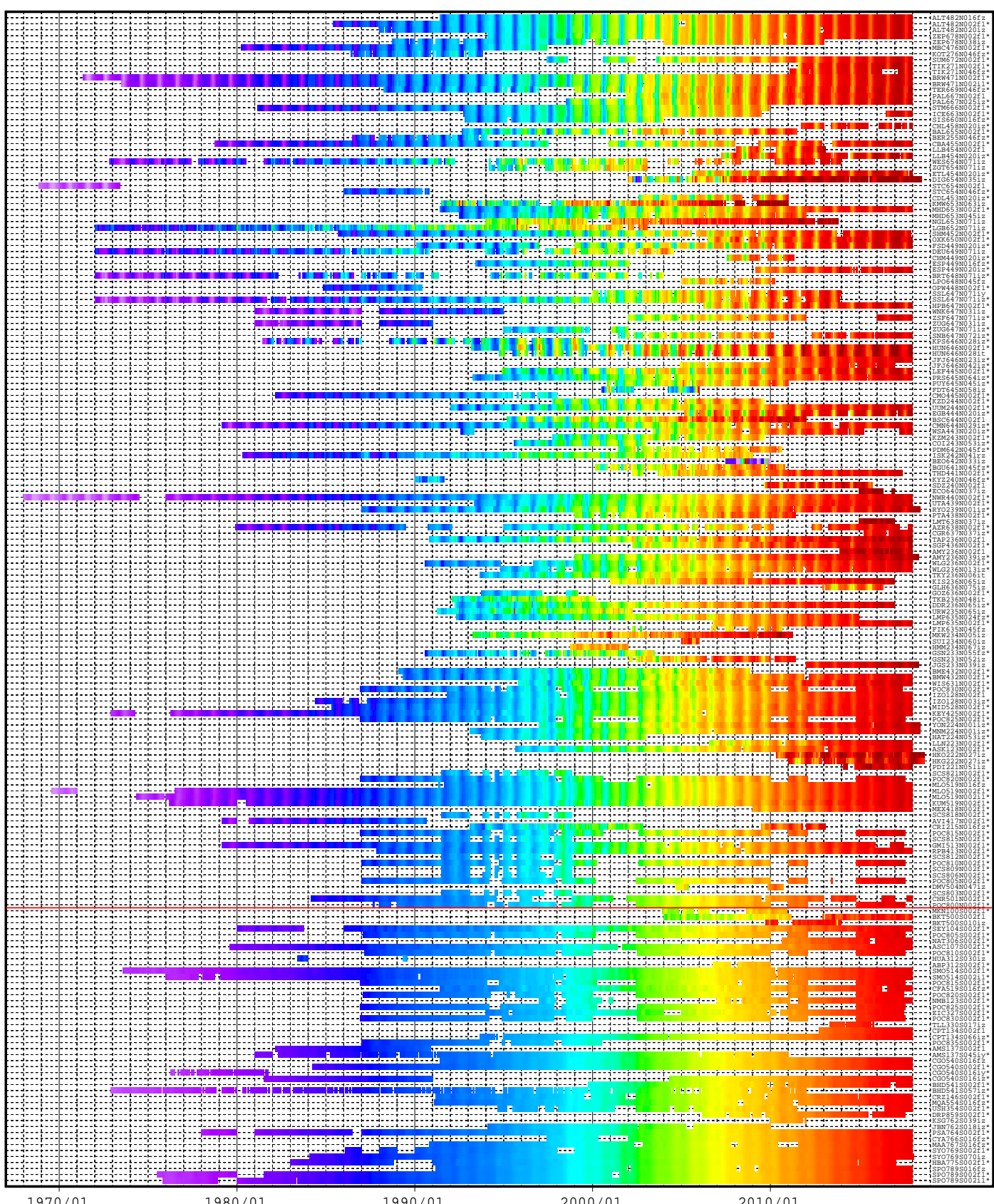
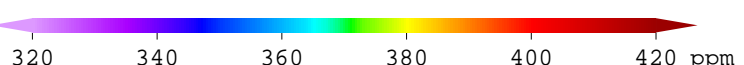
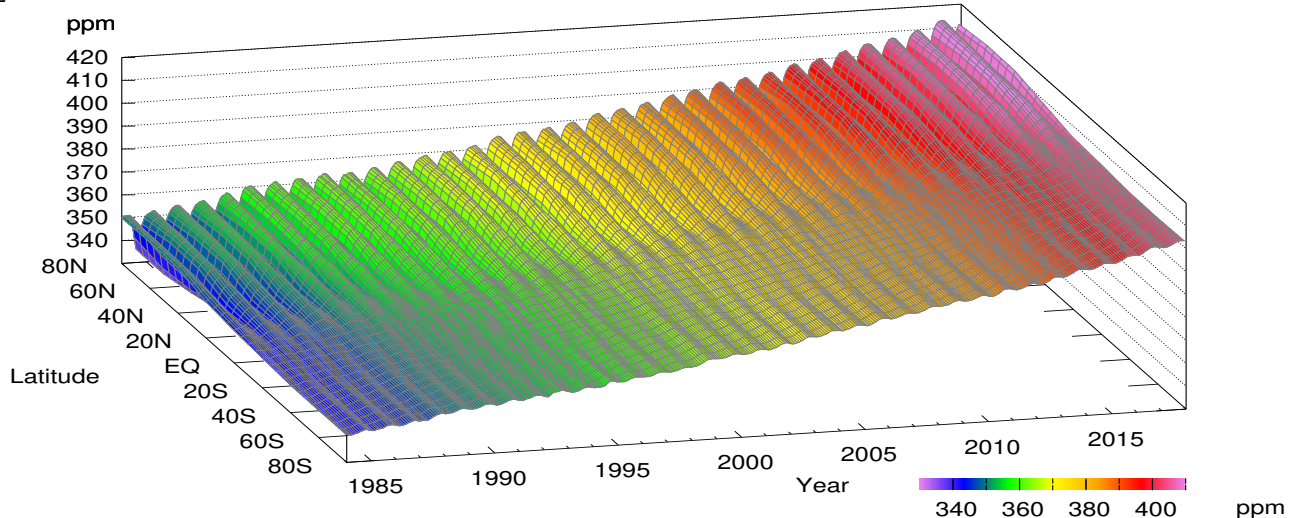
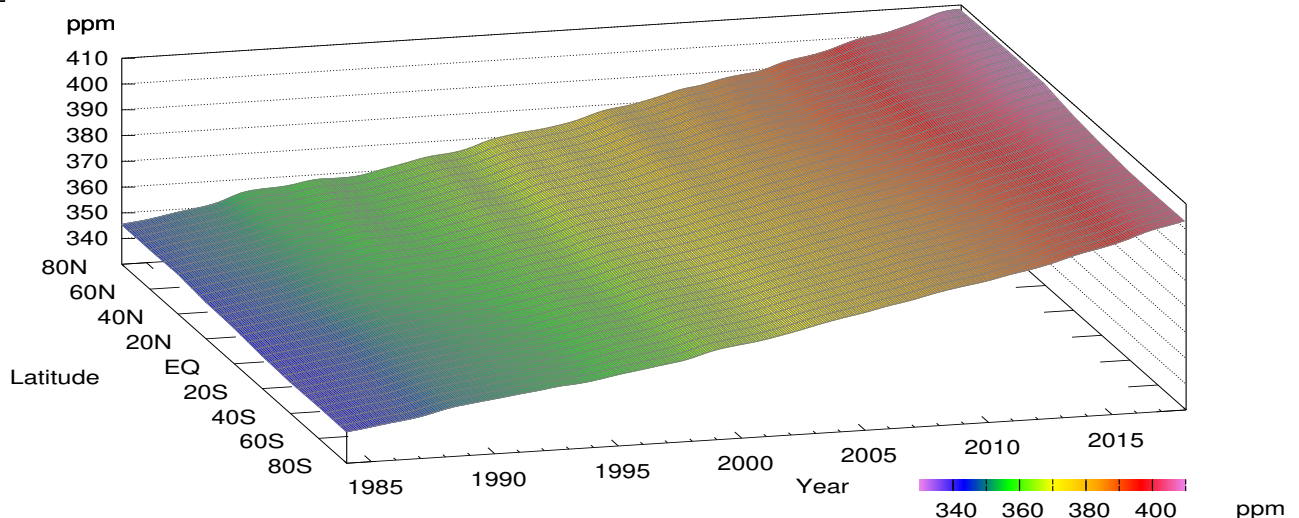


Plate 1.1 Monthly mean CO₂ mole fractions that have been reported to the WDCGG. The mole fractions are illustrated in different colors. The sites are listed in order from north to south. The red line indicates the equator. In cases where data are reported for two or three different altitudes, only the data at the highest altitudes are illustrated. In cases where monthly means are not reported, the WDCGG calculates them from hourly or other mole fractions reported to the WDCGG by simple arithmetic mean. The data from the sites with an asterisk at the end of the station index were used for the analyses shown in Plate 1.2. (see Appendix A)

CO₂ mole fraction



CO₂ deseasonalized mole fraction



CO₂ growth rate

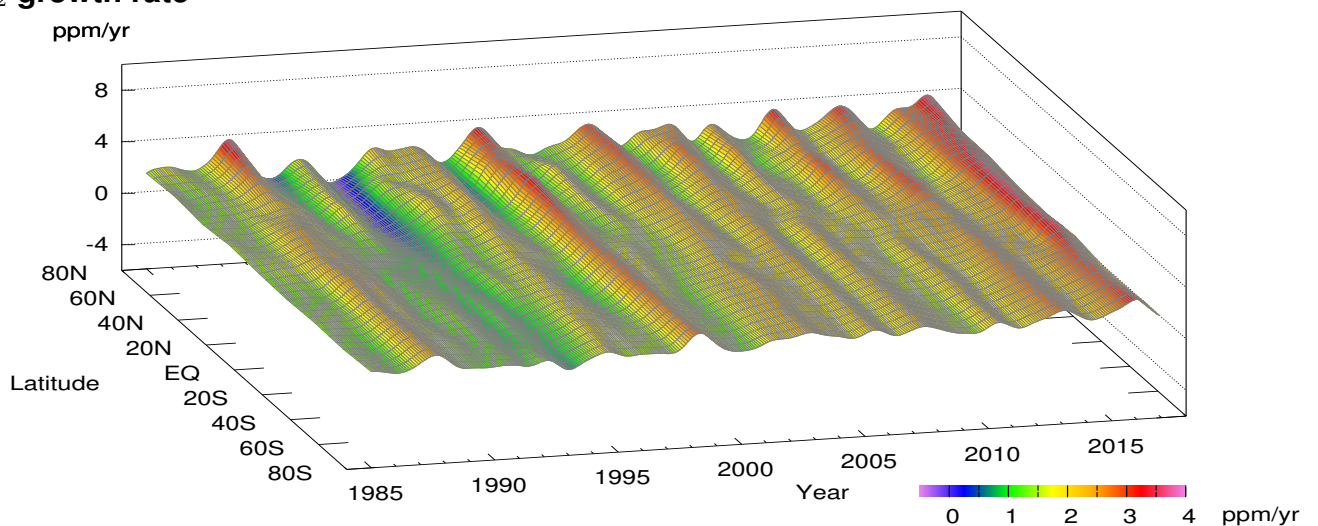


Plate 1.2 Variation of zonally averaged monthly mean CO₂ mole fractions (top), deseasonalized long-term trends (middle), and growth rates (bottom). The zonally averaged mole fractions were calculated for each 20° zone. The deseasonalized trends and growth rates were derived as described in Appendix A.

1. CARBON DIOXIDE (CO₂)

Atmospheric mole fractions of carbon dioxide (CO₂) – the most significant contributor to global warming – have been increasing since the beginning of the industrial era in around 1750. The global mean mole fraction of CO₂ reached a new high of 405.5 ± 0.1 ppm in 2017, representing an increase of 2.2 ppm from previous year. This mole fraction constitutes 146% of the pre-industrial level of 278 ppm which is inferred from ice-core studies. CO₂ is responsible for around 66% of radiative forcing (relative to the pre-industrial era) caused by long-lived greenhouse gases (WMO, 2018a).

The increase in mole fractions is primarily attributable to human activity, particularly fossil fuel combustion, cement production and land use changes. Around half of anthropogenic CO₂ emissions are removed by biosphere and ocean, and the rest remains in the atmosphere. The balance between emissions and sinks determines the annual CO₂ increment in the atmosphere. Figure 1.1 shows the observed growth rate of atmospheric mole fractions with red columns and theoretical growth rates derived under an assumption that all annual anthropogenic carbon remains in the atmosphere with a green line. The lack of correlation between two time-series suggests significant interannual variations in the land and/or ocean sink. A comprehensive understanding of the mechanisms

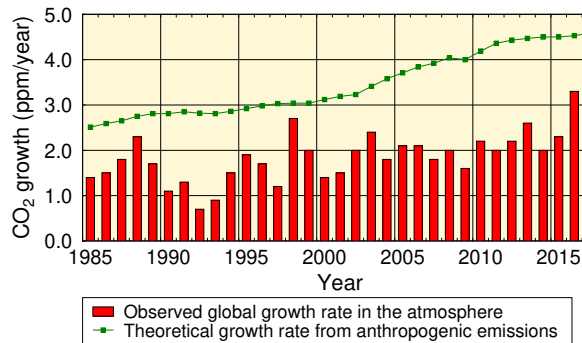


Fig. 1.1 Annual mean growth rates of CO₂ in the atmosphere, calculated from observational data (red columns) and the theoretical one driven by anthropogenic emissions (green curve). The theoretical growth rates were calculated taking CO₂ emissions as a proxy (from Global Carbon Project (Le Quéré et al., 2018)), expressed as moles divided by the total mass of gas in the atmosphere (5.2 petatonnes) converted to moles based on the mean molar mass of dry air (about 29.0 g/mol). The observed growth rates were calculated by the WDCGG. CO₂ abundance from observational data is expressed as mole fractions with respect to dry air, while that estimated from anthropogenic emissions is based on the atmosphere, including water vapor, usually in a proportion less than 1%.

that control various CO₂ sources and sinks as well as their current state is of key importance in providing a scientific foundation for strategies to combat climate change.

Global mean mole fractions

Figure 1.2 shows global mean mole fractions (top) and related growth rate (bottom) in blue dots. The red line in the top panel shows the remaining component after removal of seasonal cycles from the time series of blue dots (referred to here as the long-term trend). Details of the analysis are provided in Appendix A.

Throughout the period for which observation data are available, the mole fraction shows a continuous increase accompanied by characteristic seasonal cycles, with higher values from boreal winter to spring and lower values in summer. The seasonal cycle is mainly driven by activity of the terrestrial biosphere; plant photosynthesis is active in summer and large amounts of CO₂ are consumed, while plant respiration and organic-matter decomposition in soil become dominant in winter and emissions exceed the amount absorbed.

The characteristics of activity in the terrestrial biosphere

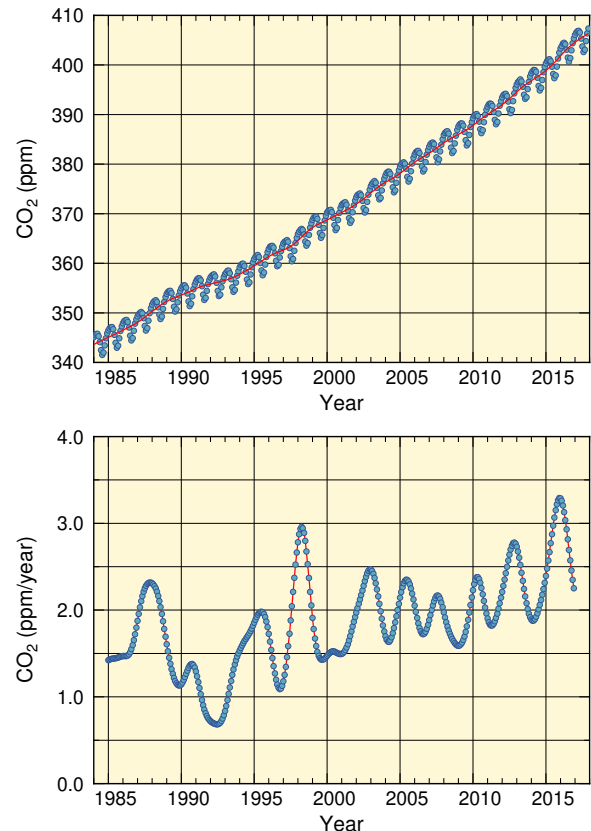


Fig. 1.2 Globally averaged monthly mean mole fraction of CO₂ from 1984 to 2017 and the deseasonalized long-term trend shown as a red line (top), and its growth rate (bottom).

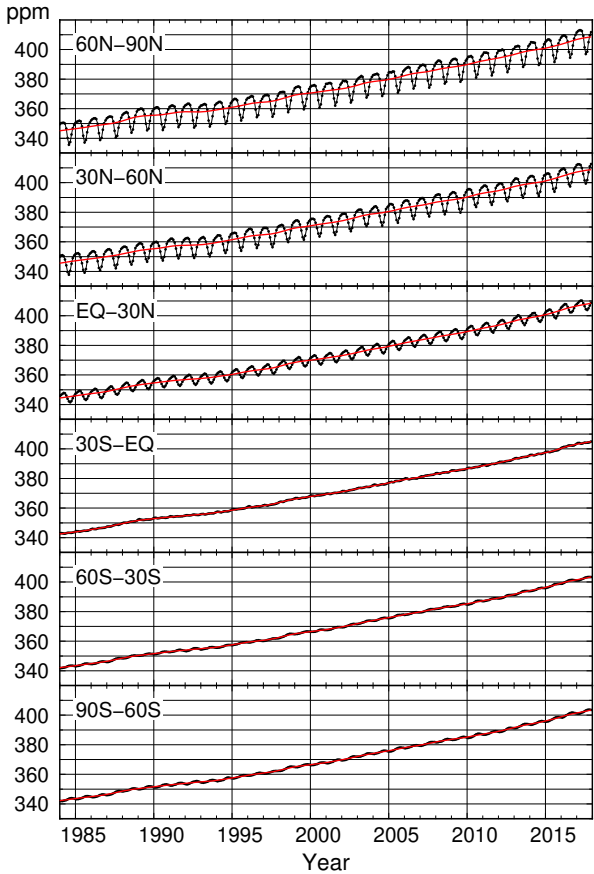


Fig. 1.3 Monthly mean mole fractions of CO₂ from 1984 to 2017 averaged over each 30° latitudinal zone (black) and their deseasonalized long-term trends (red).

show significant interannual fluctuations, as reflected in the growth rate variations shown in the bottom panel of Figure 1.2. This rate has been particularly high during El Niño events, such as those of 1986 – 1988, 1997/1998, 2002/2003, 2009/2010 and 2014 – 2016. Usually, El Niño conditions are associated with high temperatures and droughts in tropical land areas. These temperatures enhance plant respiration and organic-matter decomposition in soil, thereby increasing CO₂ emissions, while droughts suppress CO₂ consumption by plant photosynthesis and induce forest/peat fires, which also increases CO₂ emissions. The growth rate was exceptionally low during the El Niño event of 1991/1992. This is largely attributed to the eruption of Mt. Pinatubo in June 1991, which caused low-temperature anomalies on a global scale and a terrestrial biospheric change opposite to the one described above.

Latitudinal dependence of mole fractions

Figure 1.3 shows mole fractions averaged over six 30° latitudinal bands (60 – 90°N, 30 – 60°N, etc.) with black lines. The long-term trends are shown by the red lines in each panel, and are collectively shown in the top panel of Figure 1.4. The bottom panel of Figure 1.4 shows the

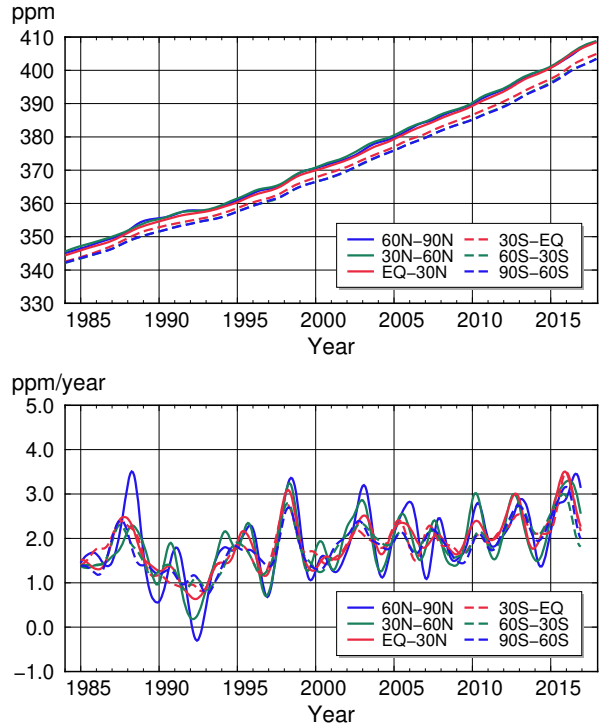


Fig. 1.4 Long-term trends of the CO₂ mole fractions for each 30° latitudinal zone (top) and their growth rates (bottom).

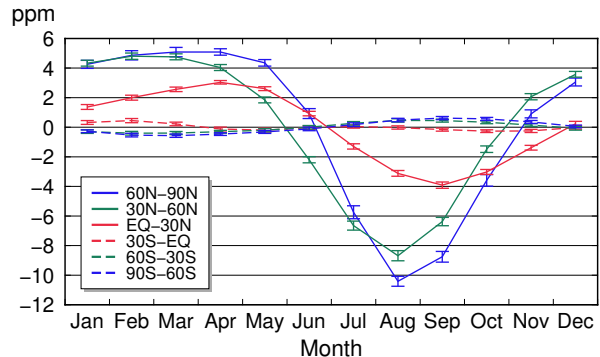


Fig. 1.5 Average seasonal cycles of the CO₂ mole fractions for each 30° latitudinal zone obtained by subtracting long-term trends from the zonal mean time series. Vertical error bars represent the range of $\pm 1\sigma$ which was calculated for each month (period 1984 to 2017).

growth rates in each latitudinal belt. Figure 1.5 shows the average seasonal cycles of CO₂ in those six bands. Figure 1.6 presents monthly mean mole fractions for four months of 2017 at individual stations which were included in the calculation of the global average mole fraction as a function of latitude.

As shown in Figure 1.4, mole fractions are higher on average in the Northern Hemisphere, largely due to higher concentrations of human activity in land areas there. However, values increase in a similar way in every latitudinal band. This suggests that, although the major

sources and sinks of CO₂ are located in the Northern Hemisphere, changes in mole fractions occur on a global scale due to atmospheric transport.

Figure 1.5 indicates that the seasonal cycles have a large amplitude in northern regions, mainly because the Northern Hemisphere has larger continental areas and an extensive terrestrial biosphere. These large variations are also evident in Figure 1.6. In contrast, low seasonal variability is shown in southern regions. In the mid- and high southern latitudes, seasonal cycles have an opposite phase to those of northern regions. In the low southern latitudes, however, their phase is similar to those of northern regions, suggesting that mole fractions in the former are more readily affected by the northern hemispheric air.

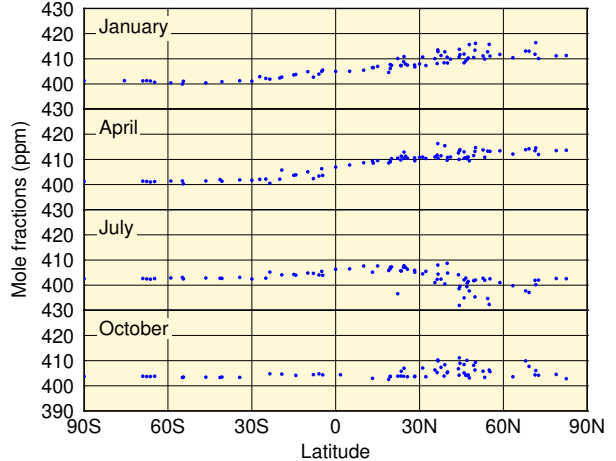


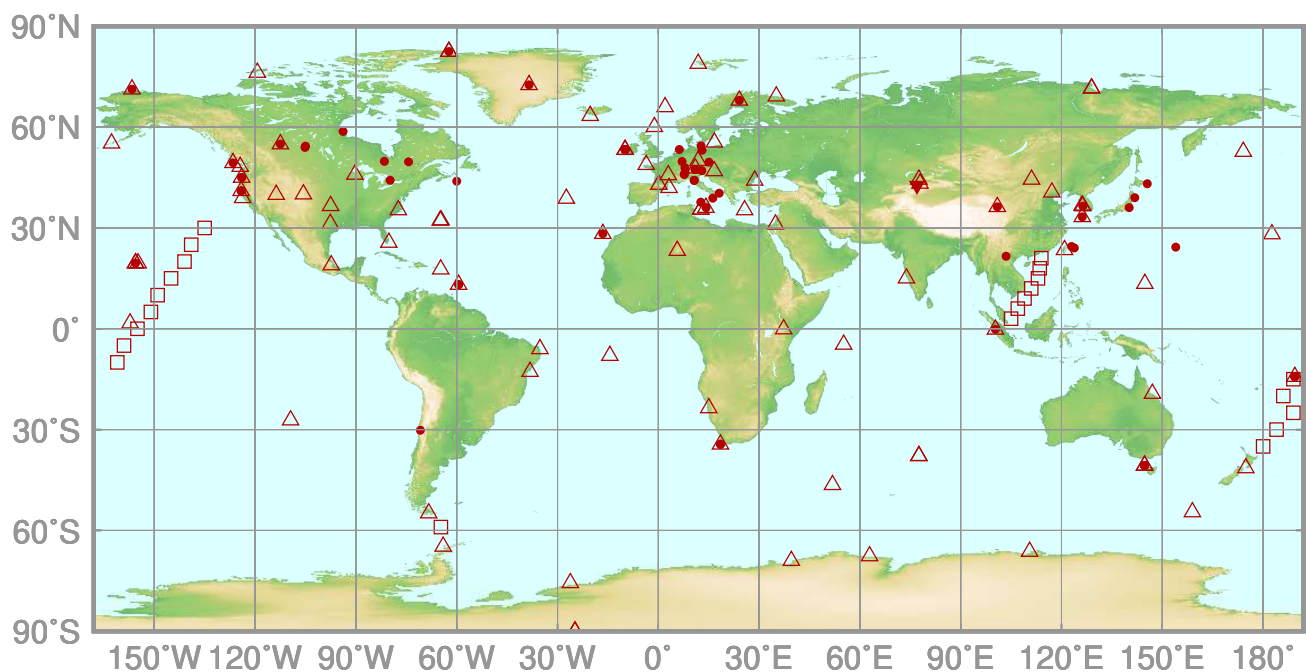
Fig. 1.6 Latitudinal distributions of the monthly mean mole fractions of CO₂ in January, April, July and October 2017 at individual stations.

2.

METHANE

(CH₄)

- : CONTINUOUS STATION
- △ : FLASK STATION
- : FLASK MOBILE (SHIP)
- ▼ : REMOTE SENSING STATION



This map shows locations of the stations that have submitted data for monthly mean mole fractions.

CH₄ Monthly Data

1600 1700 1800 1900 2000 ppb

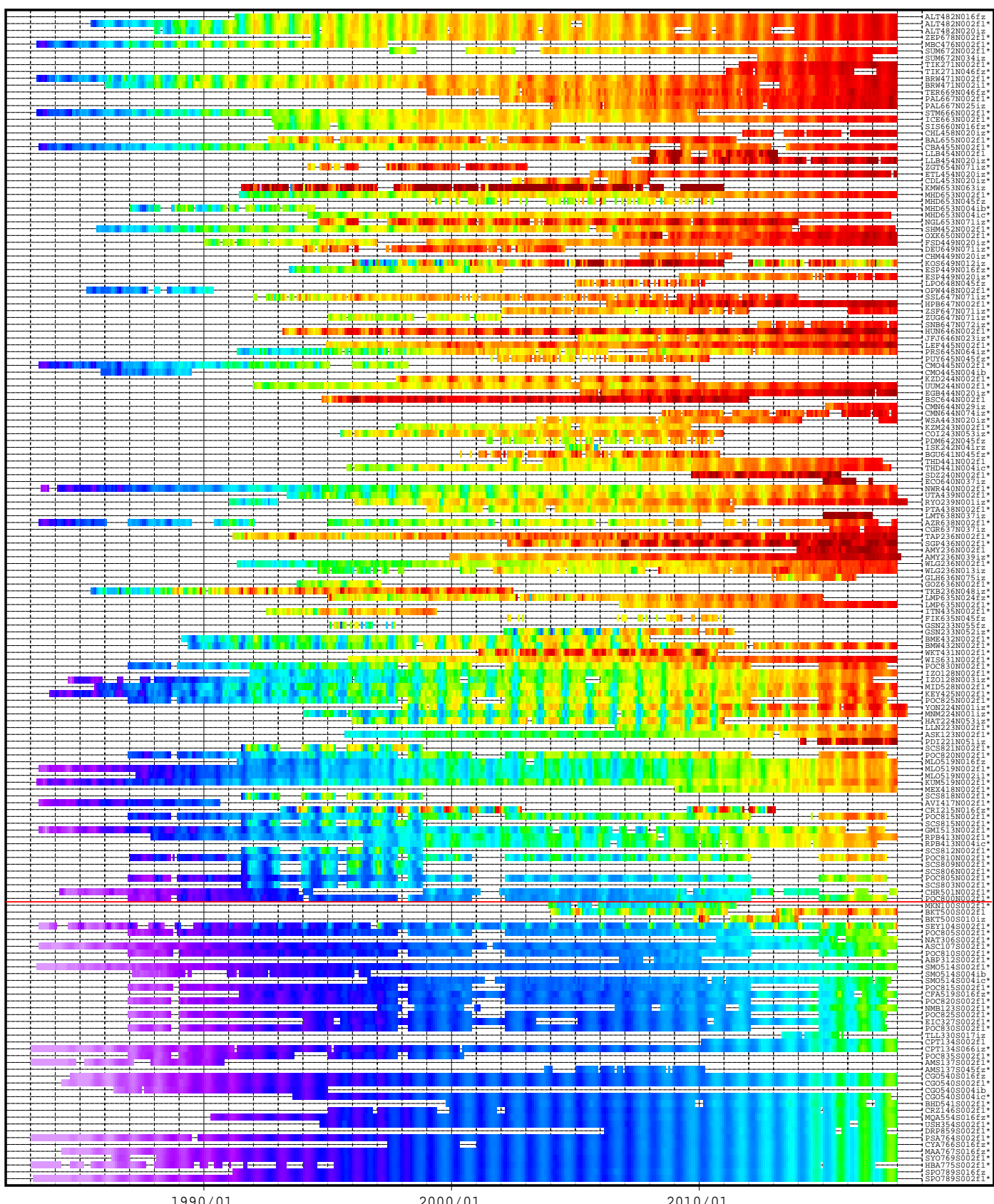
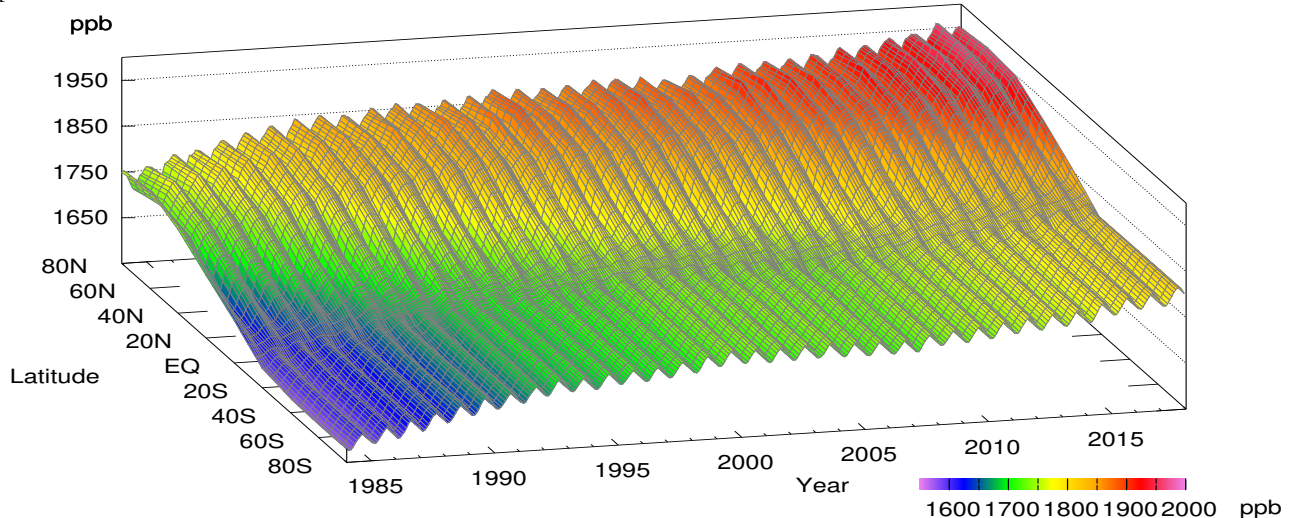


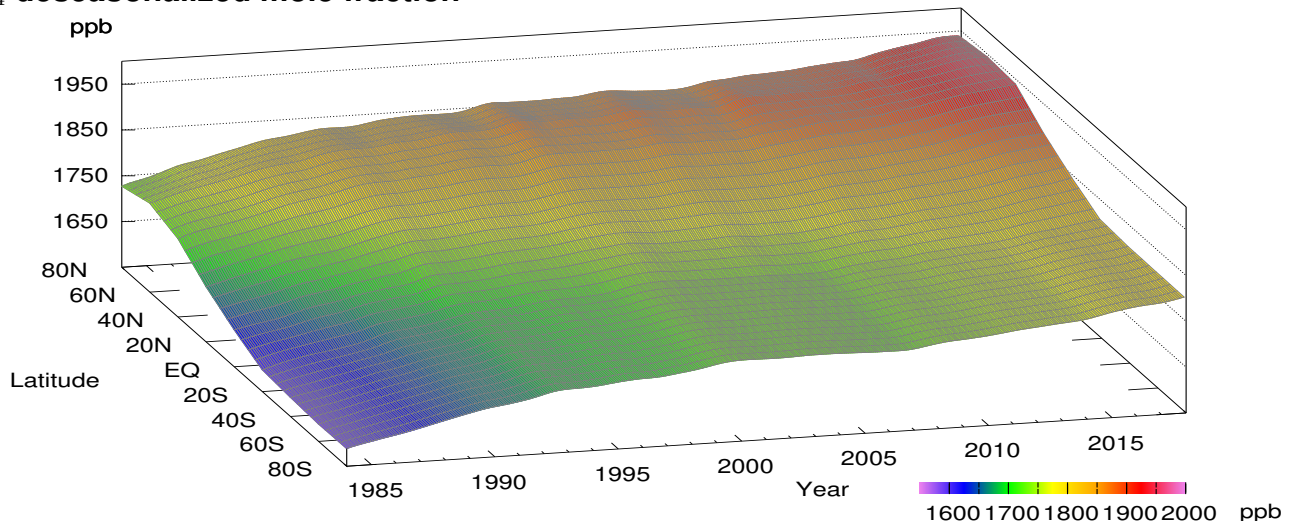
Plate 2.1 Monthly mean CH₄ mole fractions that have been reported to the WDCGG. The mole fractions are illustrated in different colors.

The sites are listed in order from north to south. The red line indicates the equator. In cases where monthly means are not reported, the WDCGG calculates them from hourly or other mole fractions reported to the WDCGG by simple arithmetic mean. The data from the sites with an asterisk at the end of the station index were used for the analyses shown in Plate 2.2. (see Appendix A)

CH_4 mole fraction



CH_4 deseasonalized mole fraction



CH_4 growth rate

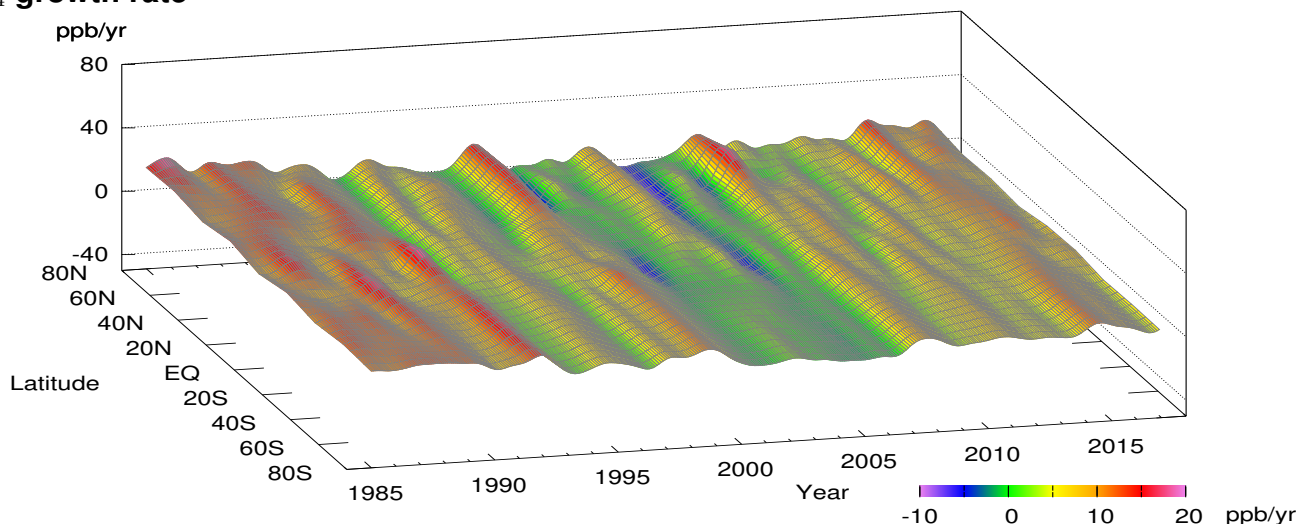


Plate 2.2 Variation of zonally averaged monthly mean CH_4 mole fractions (top), deseasonalized long-term trends (middle), and growth rates (bottom). The zonally averaged mole fractions were calculated for each 20° zone. The deseasonalized trends and growth rates were derived as described in Appendix A.

2. METHANE (CH_4)

Atmospheric mole fractions of methane (CH_4) – the second most significant anthropogenic greenhouse gas – have been increasing since the beginning of the industrial era in around 1750. The global mean mole fraction of CH_4 was $1,859 \pm 2$ ppb in 2017, representing an increase of 7 ppb relative to the previous year and 257% of the pre-industrial level of 722 ppb. CH_4 is responsible for around 17% of radiative forcing (relative to the pre-industrial era) caused by long-lived greenhouse gases (WMO, 2018a).

CH_4 has a variety of natural and anthropogenic sources. Natural sources are predominantly wetlands, with various other minor but significant sources including fresh water, wild animals, termites and geological sources. Emissions from ruminant livestock and rice paddies associated with the progress of agriculture are categorized as anthropogenic sources. Other sources are directly related to industrial activity, including gas and oil production, landfills and biomass burning. These anthropogenic sources produce large and comparable amounts of CH_4 . In contrast to the variety of sources, sinks are predominantly attributed to the destruction of CH_4 by reaction with hydroxyl (OH) radical, which is especially abundant over

oceans at low latitudes since it is formed from water vapour exposed to ultraviolet (UV) radiation.

Global mean mole fractions

Figure 2.1 shows global mean CH_4 mole fractions (top) and related growth rate (bottom) in blue dots based on the WDCGG data analysis described in Appendix A. Seasonal cycle is clearly pronounced in CH_4 mole fraction with higher values from boreal winter to spring and lower in summer. The red line in the top panel shows the residual component after removal of seasonal cycle from the globally averaged monthly mean mole fractions (referred to here as the long-term trend).

The seasonal cycle is primarily driven by the destruction of CH_4 via reaction with OH radical. More such radicals are generated in summer due to enhanced UV radiation, resulting in increased CH_4 destruction. Biogenic sources such as wetlands also have individual characteristics of seasonal variability, contributing to variations in observed mole fractions.

The overall profile of the globally averaged mole fraction shows a continuous increase throughout the

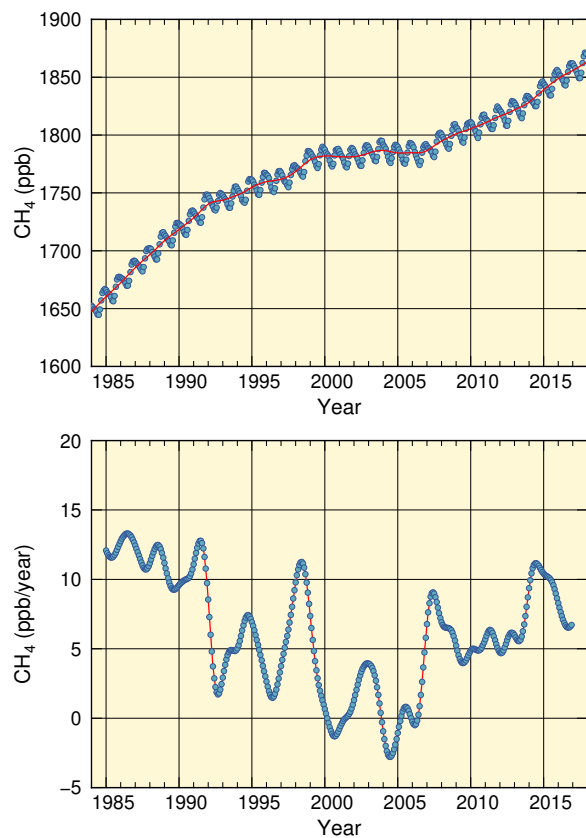


Fig. 2.1 Globally averaged monthly mean mole fraction of CH_4 from 1984 to 2017 and the deseasonalized long-term trend plotted as red line (top), and its growth rate (bottom).

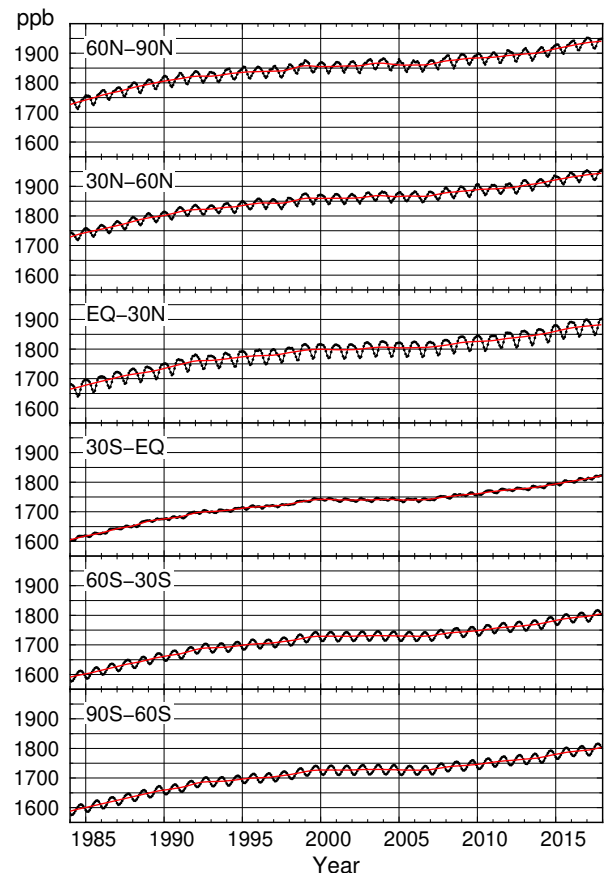


Fig. 2.2 Monthly mean mole fractions of CH_4 from 1984 to 2017 for each 30° latitudinal zone (black) and their deseasonalized long-term trends (red).

period for which observation data are available. Notably, the increase almost stagnated from 1999 to 2006. As shown in the bottom panel, the growth rate actually began to decrease in the late 1990s (in fact approaching zero during this period) for reasons that remain under discussion (IPCC (2013) and references noted therein). Since 2007 mole fractions renewed growing. Recent studies, including work based on CH₄ isotopic composition observations, have suggested that increased emissions from wetlands in the tropics and fossil fuel combustion triggered the resumed increase in global mean mole fractions (WMO, 2018a).

Latitudinal dependence of mole fractions

Figure 2.2 shows CH₄ mole fractions averaged over six 30° latitudinal bands with black lines. The long-term trends are shown by the red lines in each panel. These long-term trends are summarized on the top panel of Figure 2.3. The bottom panel of this figure shows growth rates for the six latitudinal bands, and Figure 2.4 shows average seasonal cycles for each band.

As shown in the top panel of Figure 2.3, the difference in the six long-term trends is especially significant between 30 – 60°N and EQ – 30°N and between EQ – 30°N and 30°S – EQ, indicating that the mole fraction exhibits a large latitudinal gradient in the mid- and low latitudes of the Northern Hemisphere. The gradient is largely attributable to high concentrations of major CH₄ sources in the Northern Hemisphere and to an abundance of OH radicals over oceanic regions extending southward.

The growth rate exhibits broadly similar characteristics in all latitudinal bands, as shown in the bottom panel of Figure 2.3. There are singular peaks and troughs in the growth rate, each of which has an individual complex origin, and collective explanation of two or more peaks is challenging. For example, the peak observed in every band in 1998 is attributed to enhanced CH₄ emissions from tropical wetland areas in association with the strong El Niño event observed the same year, and to forest/peat fires in Siberia and elsewhere (Dlugokencky *et al.*, 2001).

Figure 2.4 shows clear seasonal cycles of CH₄ mole fractions in both hemispheres, while for CO₂ mole fractions it is only pronounced in the Northern Hemisphere (see Figure 1.5). This difference is caused by the difference in the processes that control seasonal cycles of those two species. In the case of CH₄ the seasonal minimum is driven by the availability of OH radicals produced over oceans, which peak in summer in both hemispheres, while the sink of CO₂ in summer is driven by terrestrial biosphere activity, which is limited in the ocean-rich Southern Hemisphere. The cycles have a roughly opposite phase in each hemisphere because the seasons are opposite. The relatively low amplitude of seasonal cycles in the low latitudes of the Southern Hemisphere indicates that the atmosphere in this region tends to be influenced by the northern atmosphere, and the cycles are partially offset. In the low latitudes of the

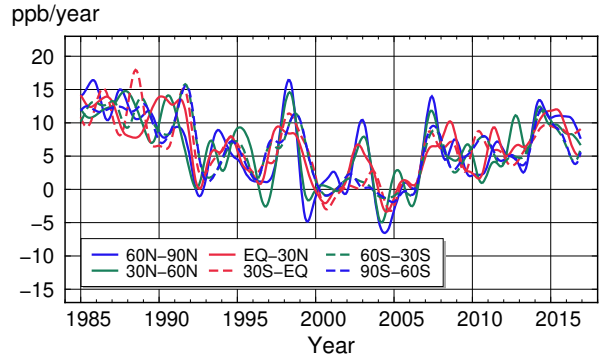
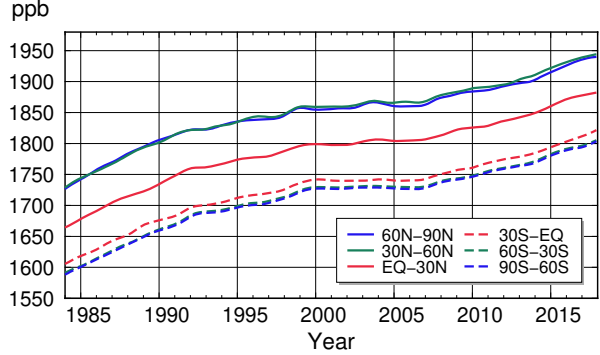


Fig. 2.3 Long-term trends of the CH₄ mole fractions for each 30° latitudinal zone (top) and their growth rates (bottom).

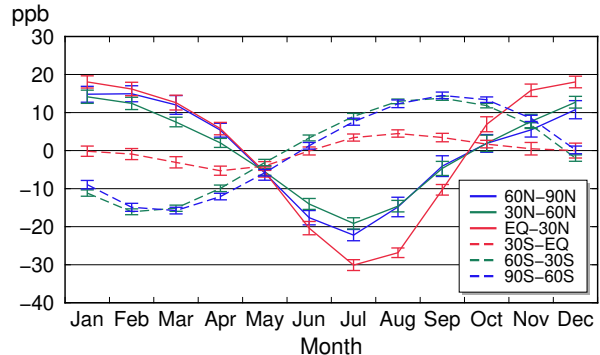


Fig. 2.4 Average seasonal cycles of CH₄ mole fractions for each 30° latitudinal zone obtained by subtracting long-term trends from the zonal mean time series. Vertical error bars represent the range of ±1σ calculated for each month (period 1984 to 2017).

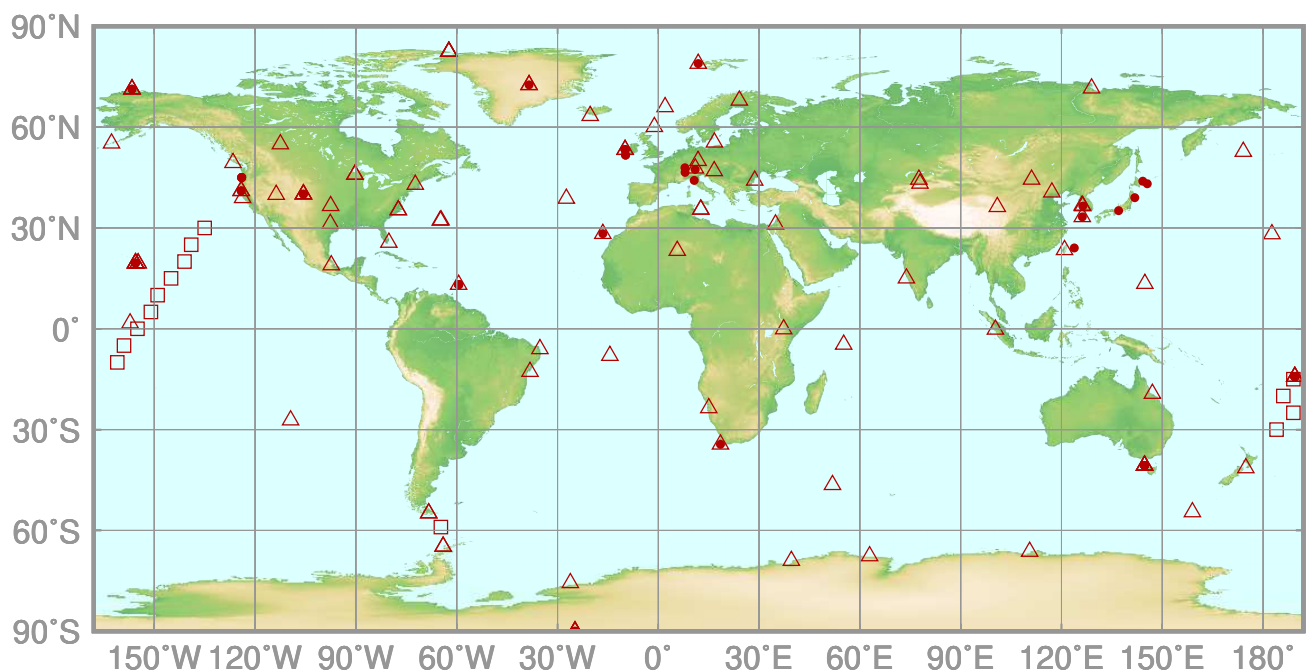
Northern Hemisphere, mole fractions are significantly lower in summer because OH radicals are plentiful over ocean areas due to enhanced UV radiation. As a whole, the amplitudes of seasonal cycles are larger in the Northern Hemisphere, and the global mean mole fraction is therefore at its annual minimum in boreal summer (Figure 2.1).

3.

NITROUS OXIDE

(N₂O)

- : CONTINUOUS STATION
- △ : FLASK STATION
- : FLASK MOBILE (SHIP)



This map shows locations of the stations that have submitted data for monthly mean mole fractions.

N₂O Monthly Data

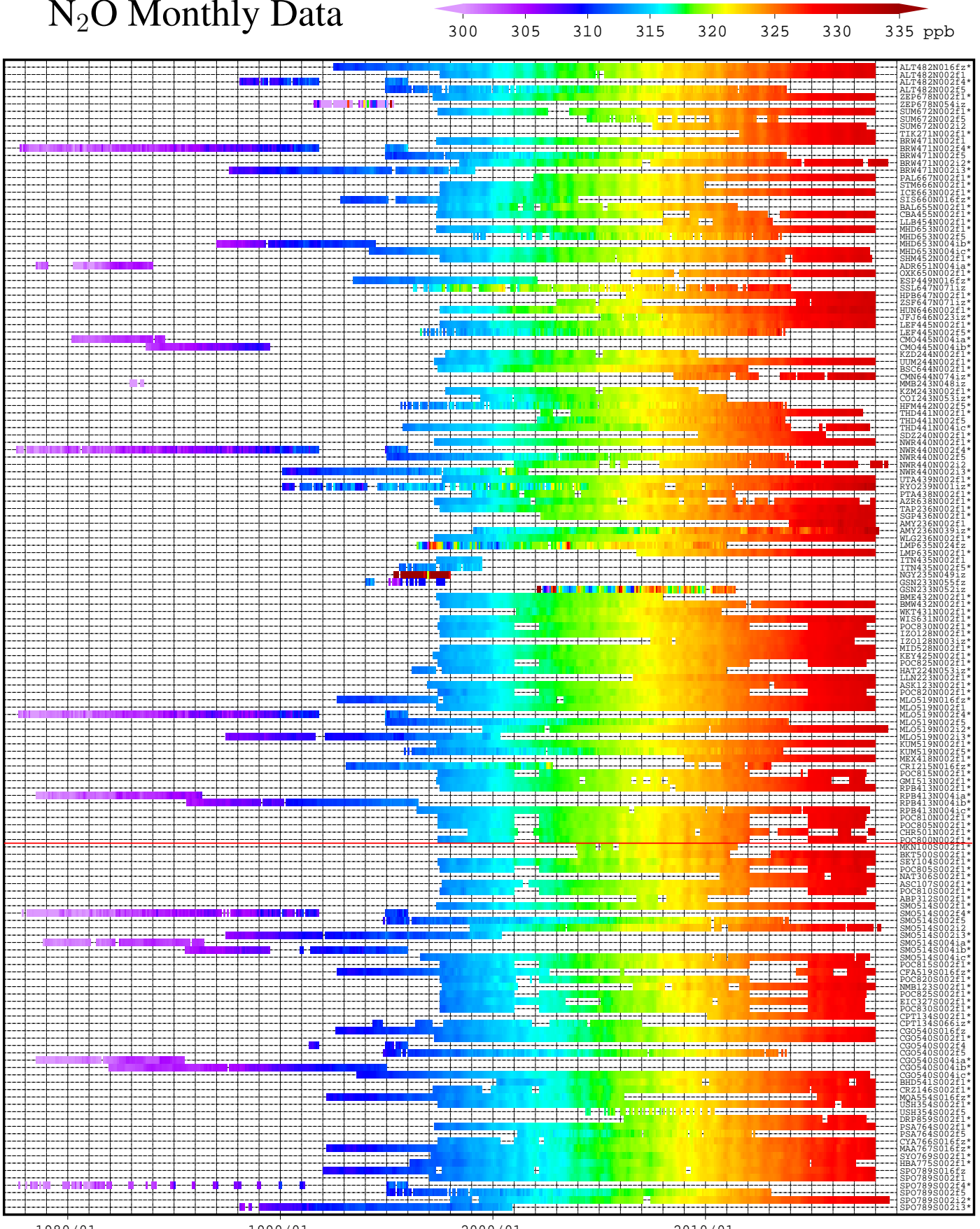
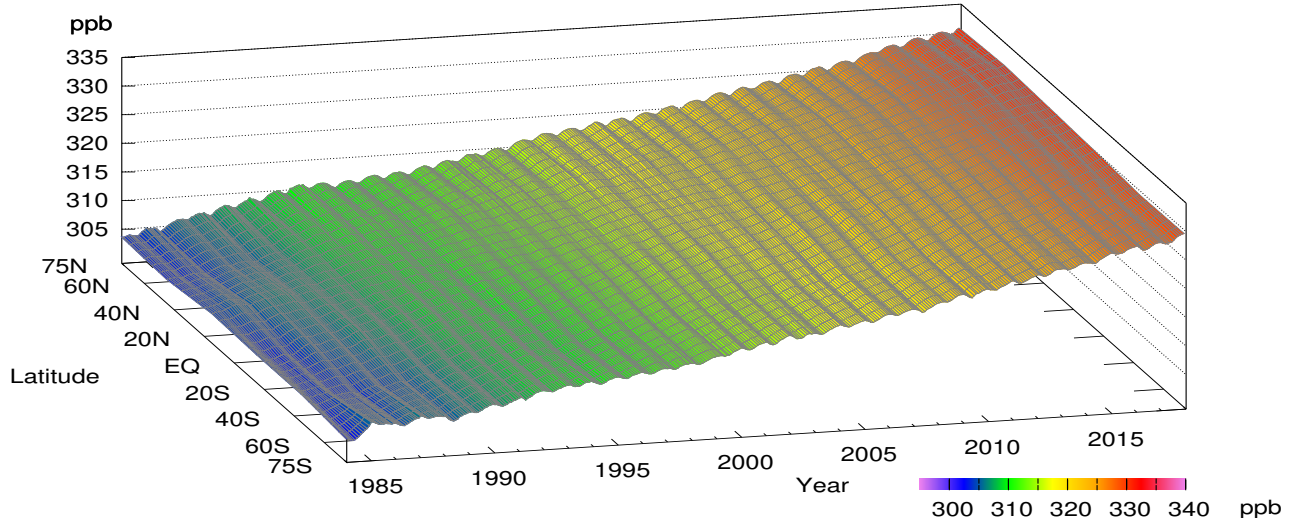


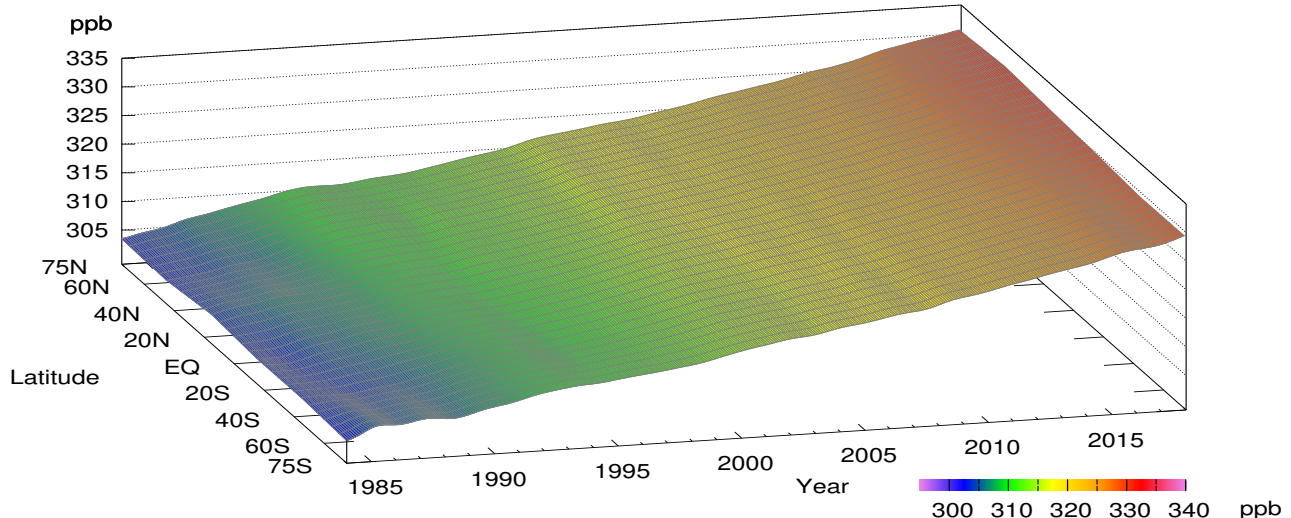
Plate 3.1 Monthly mean N₂O mole fractions that have been reported to the WDCGG. The mole fractions are illustrated in different colors.

The sites are listed in order from north to south. The red line indicates the equator. The data from the sites with an asterisk at the end of the station index were used for the analyses shown in Plate 3.2. (see Appendix A)

N₂O mole fraction



N₂O deseasonalized mole fraction



N₂O growth rate

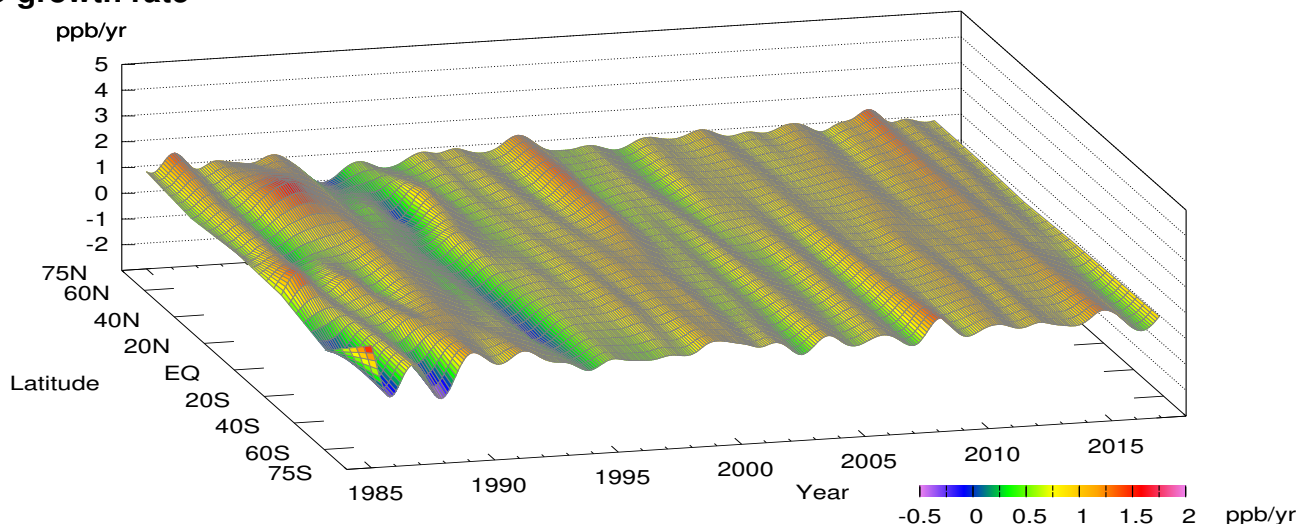


Plate 3.2 Variation of zonally averaged monthly mean N₂O mole fractions (top), deseasonalized long-term trends (middle), and growth rates (bottom). The zonally averaged mole fractions were calculated for each 30° zone. The deseasonalized trends and growth rates were derived as described in Appendix A.

3. NITROUS OXIDE (N_2O)

Atmospheric mole fractions of nitrous oxide (N_2O) – a significant factor in global warming – have been increasing since the beginning of the industrial era in around 1750. The global mean mole fraction in 2017 was 329.9 ± 0.1 ppb, representing an increase of 0.9 ppb relative to the previous year and 122% of the pre-industrial level of 270 ppb. N_2O is responsible for approximately 6% of total radiative forcing (relative to the pre-industrial era) from long-lived greenhouse gases (WMO, 2018a).

N_2O sources include microbial processes (nitrification and denitrification), oceans, nitrogen fertilizers generally used in agriculture, fossil fuel combustion and biomass burning. The gas is relatively stable in the troposphere with a lifetime of around 121 years. Its mole fraction is relatively uniformly distributed in the troposphere and declines in the stratosphere where N_2O is destroyed via ultraviolet (UV) photo-decomposition.

Global and hemispheric average mole fractions

Figure 3.1 shows global mean N_2O mole fraction and the related growth rate. The analysis is described in

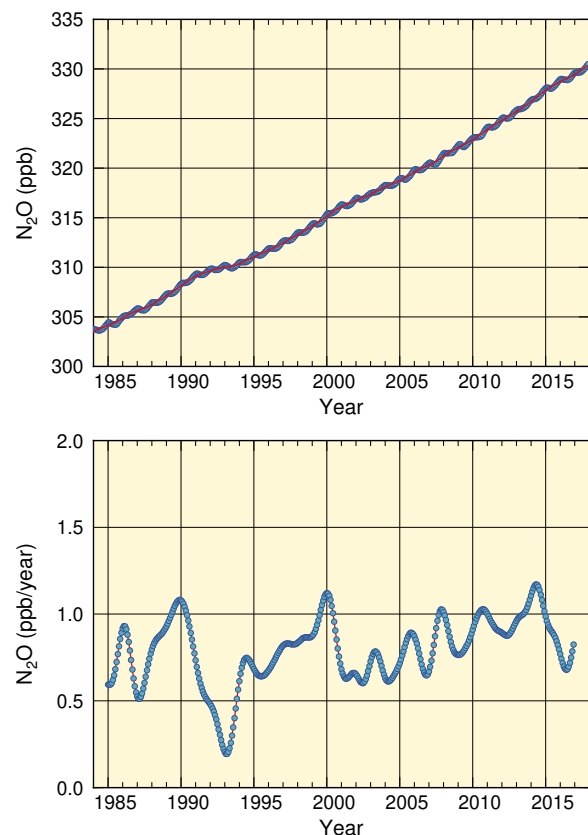


Fig. 3.1 Globally averaged monthly mean mole fraction of N_2O from 1984 to 2017 and the deseasonalized long-term trend shown as a red line (top), and its growth rate (bottom).

Appendix A. Unlike CO_2 and CH_4 global means, these mole fractions exhibit low seasonal variability. Nevertheless, the same procedure for removing seasonal cycles as for CO_2 and CH_4 is performed, and the residual is shown by the red line in the top panel. The values differ only minimally from those of the original mole fractions due to weak seasonal variability. Correspondingly, Figure 3.2 shows mole fractions averaged over the Northern Hemisphere (darker blue) and the Southern Hemisphere (lighter blue) in the top panel, with corresponding growth rates in the bottom panel.

Throughout the period for which observation data are available, the mole fraction has steadily increased in both hemispheres, and therefore over the whole globe. Values tend to be higher in the Northern Hemisphere, mainly due to high concentrations of both anthropogenic and microbial sources in continental areas.

The growth rate is positive over the period as a whole, although significant inter-annual variations are observed. These are partially due to changes in the state of the stratosphere, where N_2O is destroyed, and variability of microbial processes in soil and/or oceanic processes may

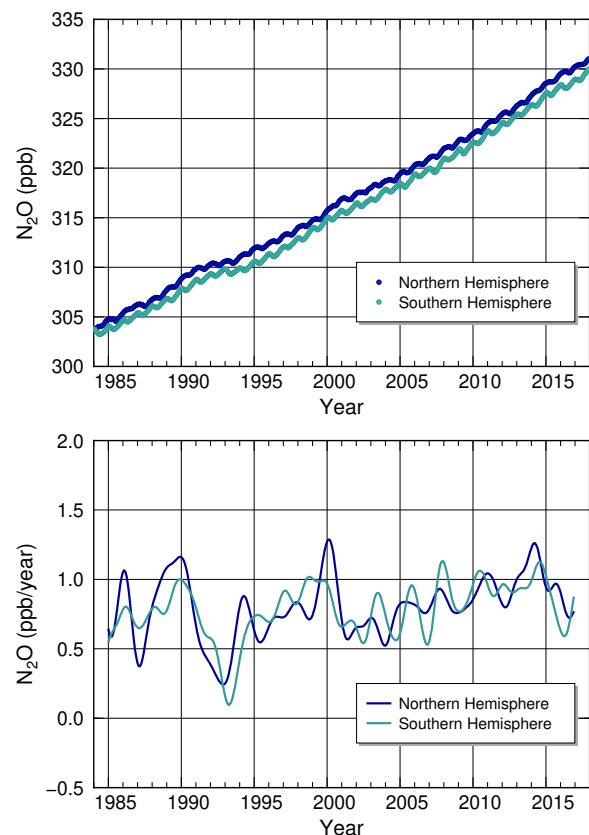
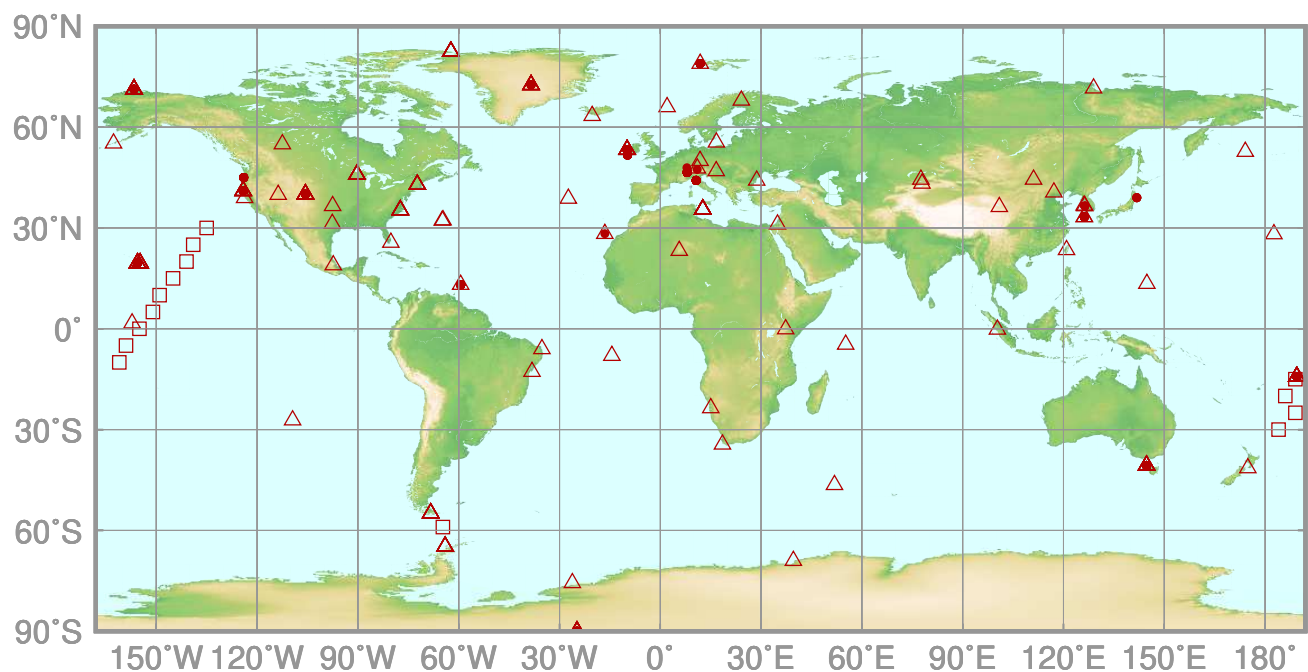


Fig. 3.2 Monthly mean mole fractions of N_2O from 1984 to 2017 (top) and their growth rates (bottom), averaged over the Northern and Southern Hemispheres.

also contribute (IPCC, 2013). However, quantitative verification of specific variability patterns is challenging due to the complexity of related processes and uncertainty over the intensities and locations of N₂O sources. Accordingly, further extension of the global monitoring network is needed.

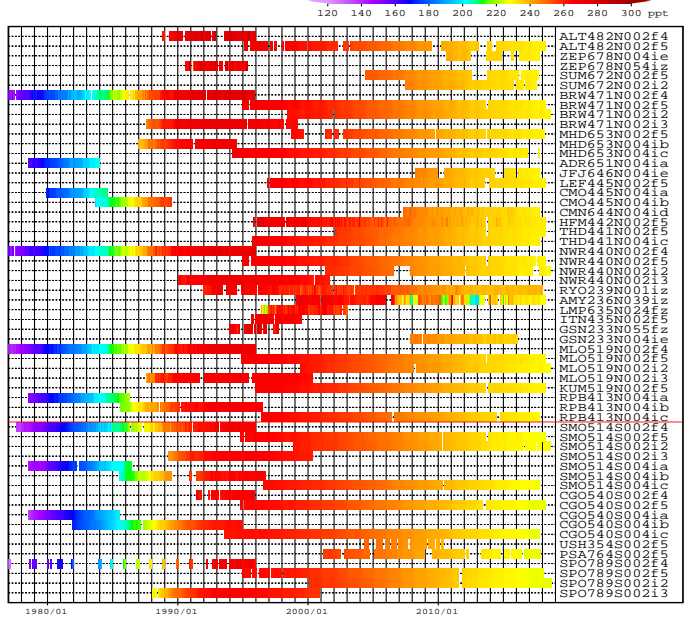
4. HALOCARBONS AND OTHER HALOGENATED SPECIES

- : CONTINUOUS STATION
- △ : FLASK STATION
- : FLASK MOBILE (SHIP)

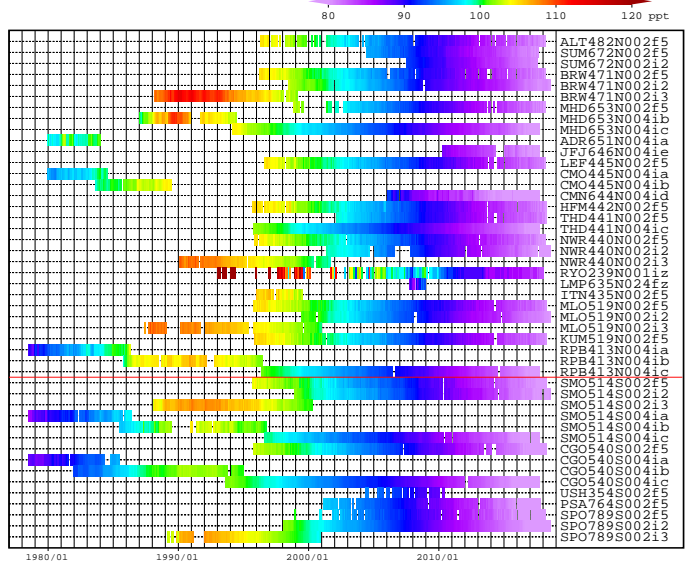


This map shows locations of the stations that have submitted data for monthly mean mole fractions.

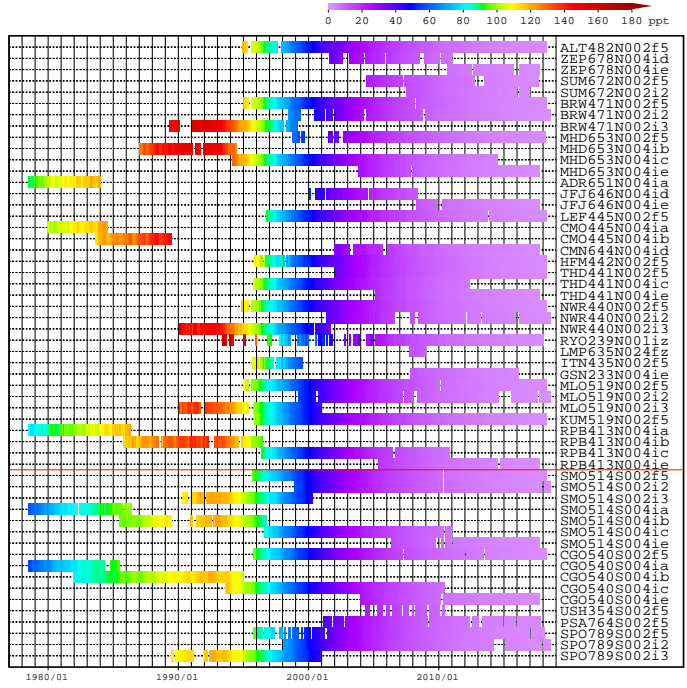
(a) CFC-11 Monthly Data



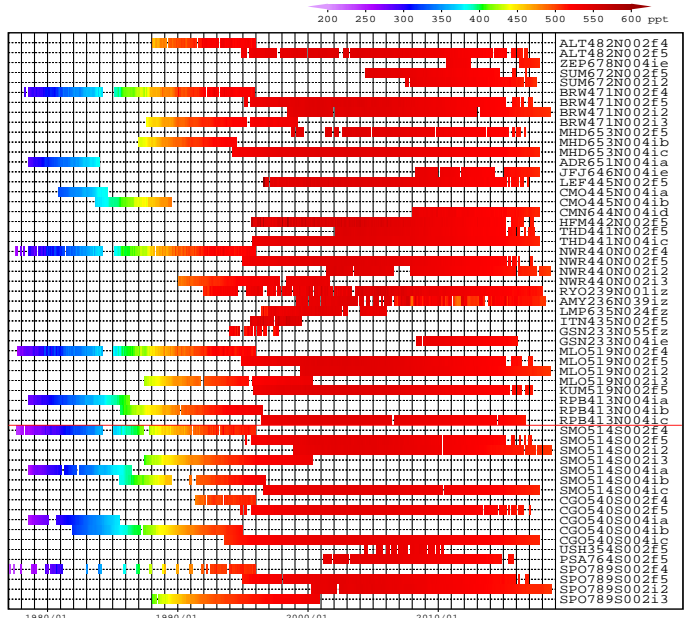
(d) CCl₄ Monthly Data



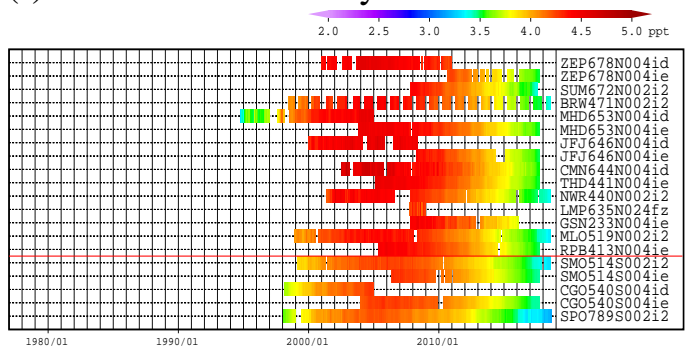
(e) CH₃CCl₃ Monthly Data



(b) CFC-12 Monthly Data



(f) Halon-1211 Monthly Data



(c) CFC-113 Monthly Data

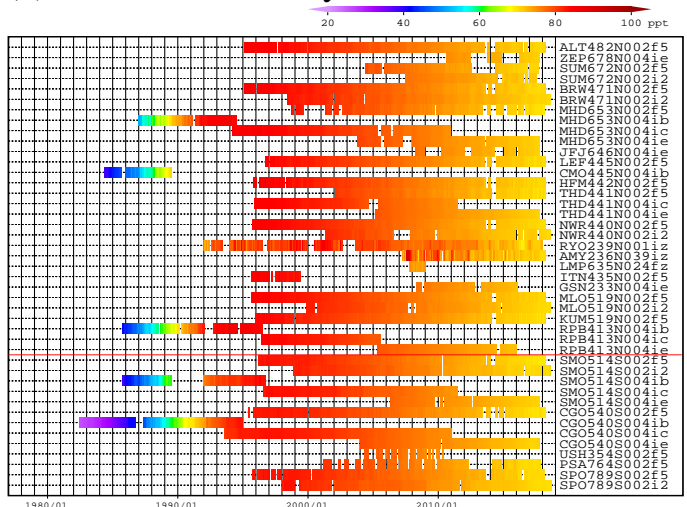
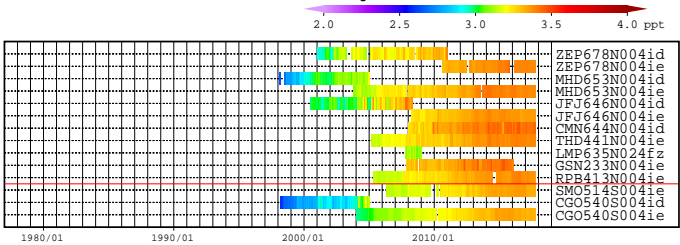
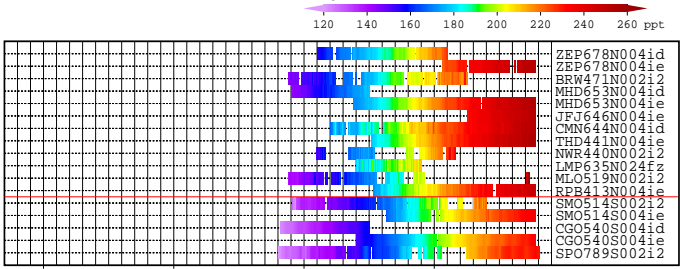


Plate 4.1 Monthly mean (a) CFC-11, (b) CFC-12, (c) CFC-113, (d) CCl₄, (e) CH₃CCl₃, (f) Halon-1211 mole fractions that have been reported to the WDCGG. The mole fractions are illustrated in different colors. The sites are listed in order from north to south. The red line indicates the equator.

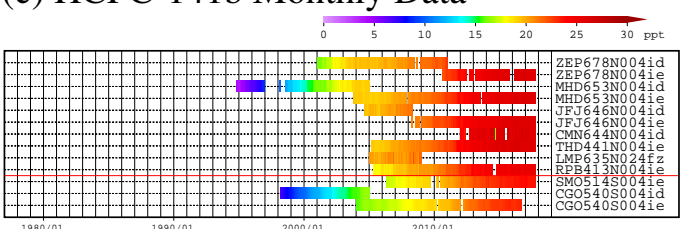
(a) Halon-1301 Monthly Data



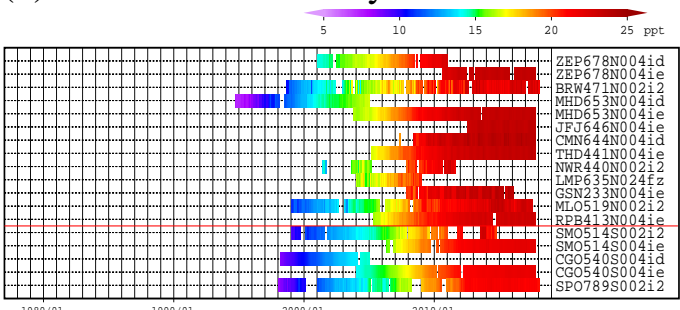
(b) HCFC-22 Monthly Data



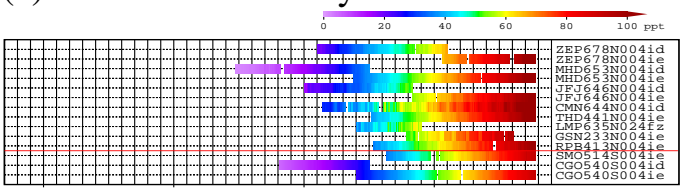
(c) HCFC-141b Monthly Data



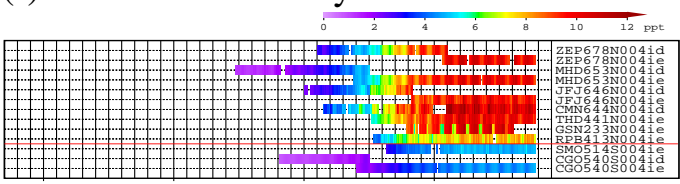
(d) HCFC-142b Monthly Data



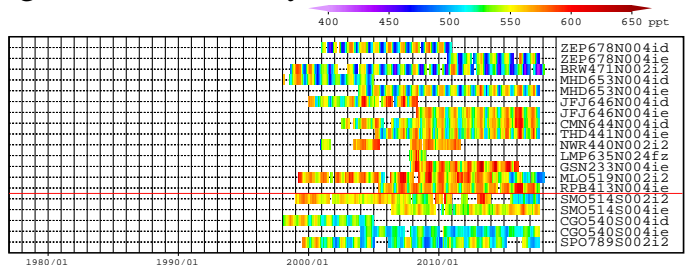
(e) HFC-134a Monthly Data



(f) HFC-152a Monthly Data



(g) CH₃Cl Monthly Data



(h) SF₆ Monthly Data

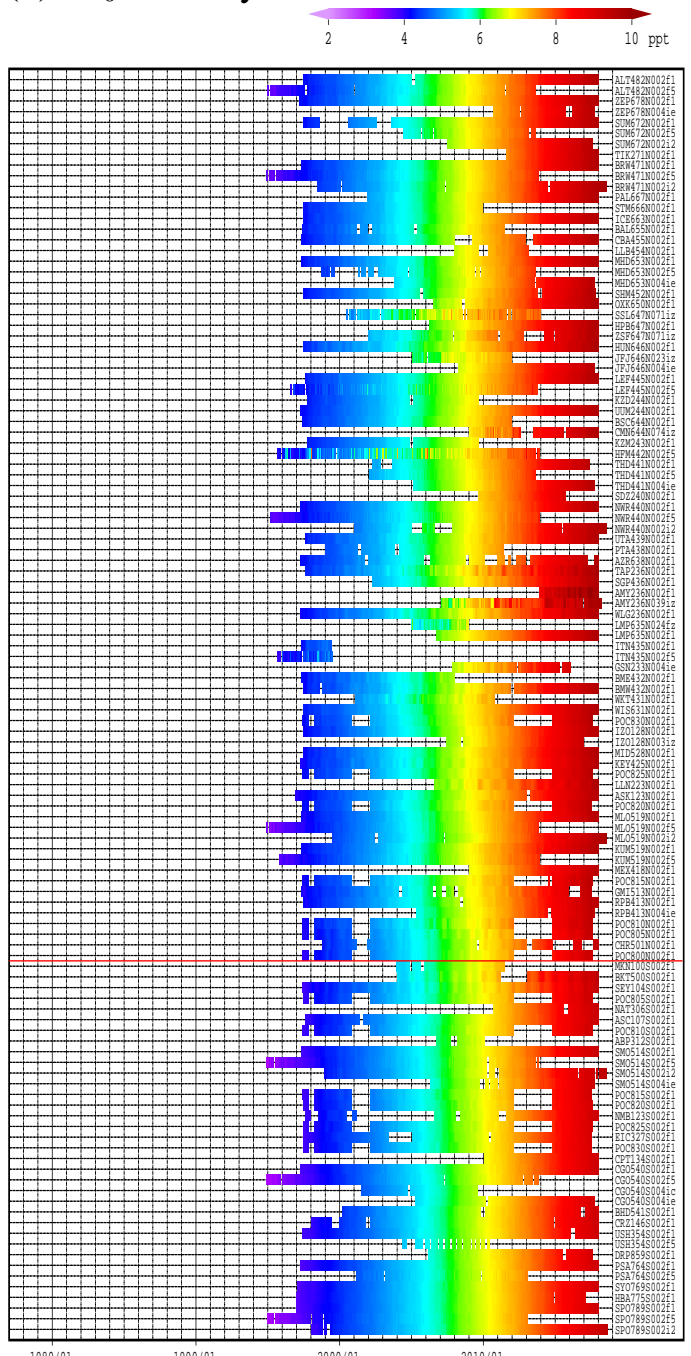


Plate 4.2 Monthly mean (a) Halon-1301, (b) HCFC-22, (c) HCFC-141b, (d) HCFC-142b, (e) HFC-134a, (f) HFC-152a, (g) CH₃Cl, (h)

SF₆ mole fractions that have been reported to the WDCGG. The mole fractions are illustrated in different colors. The sites are listed in order from north to south. The red line indicates the equator.

4. HALOCARBONS AND OTHER HALOGENATED SPECIES

Halocarbons are generally carbon compounds containing halogens. Most are artificially generated and have much lower atmospheric mole fractions than major greenhouse gases, but they contribute significantly to global warming. These gases are responsible for around 11% of the total increase in radiative forcing (relative to the pre-industrial era in around 1750) caused by long-lived greenhouse gases (WMO, 2018a).

Major examples include chlorofluorocarbons (CFCs; carbon compounds containing both fluorine and chlorine), with CFC-11, CFC-12 and CFC-113 having particularly significant impacts on global warming. CFCs used to be mass-produced as refrigerants, propellants, detergents and other functional substances until their connection with stratospheric ozone depletion became evident. Since 1989 when CFC production and consumption were internationally prohibited under the Montreal Protocol, related mole fractions have gradually decreased. Recently, however, a slowing of the decrease in CFC-11 mole fractions has been observed. This is considered to be associated with CFC-11 production in eastern Asia (Montzka *et al.*, 2018).

Carbon tetrachloride (CCl_4), methyl chloroform (1,1,1-trichloroethane, CH_3CCl_3), halons and hydrochlorofluorocarbons (HCFCs) are also considered as ozone-depleting substances, with related production and consumption regulated under the Montreal Protocol and amendments made to it in the 1990s. Halons are carbon compounds containing bromine, with Halon-1211 and Halon-1301 as typical species. HCFCs represent carbon compounds containing hydrogen, in addition to fluorine and chlorine, with HCFC-22, HCFC-141b and HCFC-142b as major examples. Mole fractions of these ozone-depleting substances are either decreasing or increasing more slowly than before.

Hydrofluorocarbons (HFCs; carbon compounds containing hydrogen and fluorine but no chlorine) have no ozone depletion potential, and were developed as substitutes for CFCs and HCFCs. However, due to their significant greenhouse effects, they are regulated under the Kigali amendment to the Montreal Protocol adopted in 2016 (effective as of 2019). Typical species include HFC-134a and HFC-152a.

Unlike other halocarbons, methyl chloride (chloromethane, CH_3Cl) comes from natural sources and exhibits mole fractions with clear seasonal variations. Although it is not regulated under the Montreal Protocol, its current status is monitored at many observation stations.

Although not technically a halocarbon, sulphur hexafluoride (SF_6) is often discussed together with halocarbons and other halogenated gases. It has very significant greenhouse effects considering its low abundance, and is a reduction target under the Kyoto Protocol. Its mole fractions are continuously increasing.

Figure 4 displays mole fractions of 14 gas species, with circles representing monthly mean values at individual stations (rather than average values over stations). Solid and open circles correspond to stations in the Northern Hemisphere and Southern Hemisphere, respectively. Due to more intensive production of artificial halocarbons in the Northern Hemisphere, their mole fractions tend to be higher in this region, especially in their increasing phases.

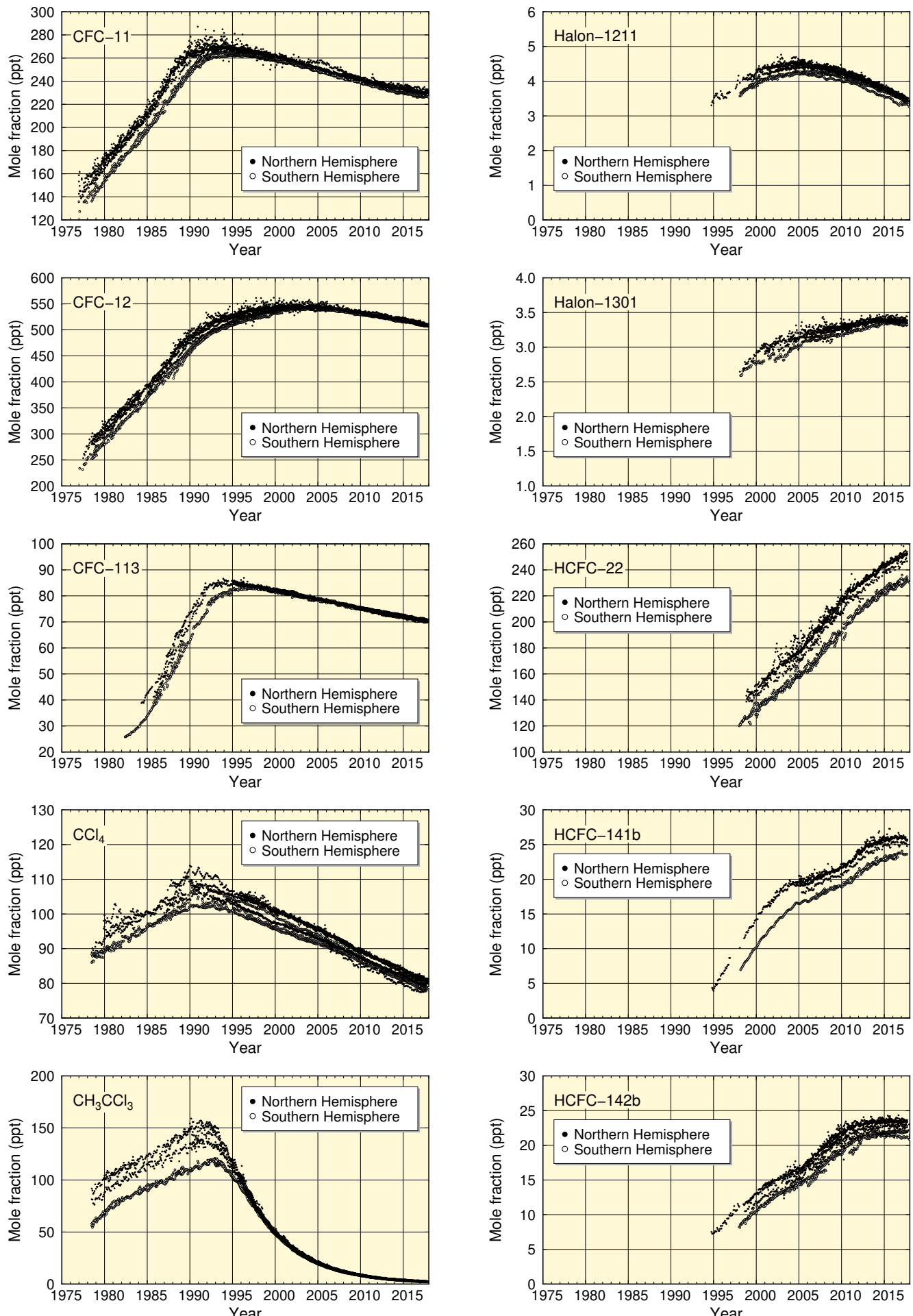


Fig. 4 Time series of the monthly mean mole fractions of halocarbons, other halogenated species and sulphur hexafluoride at individual stations. Solid circles show mole fractions in the Northern Hemisphere and open circles show those measured in the Southern Hemisphere.

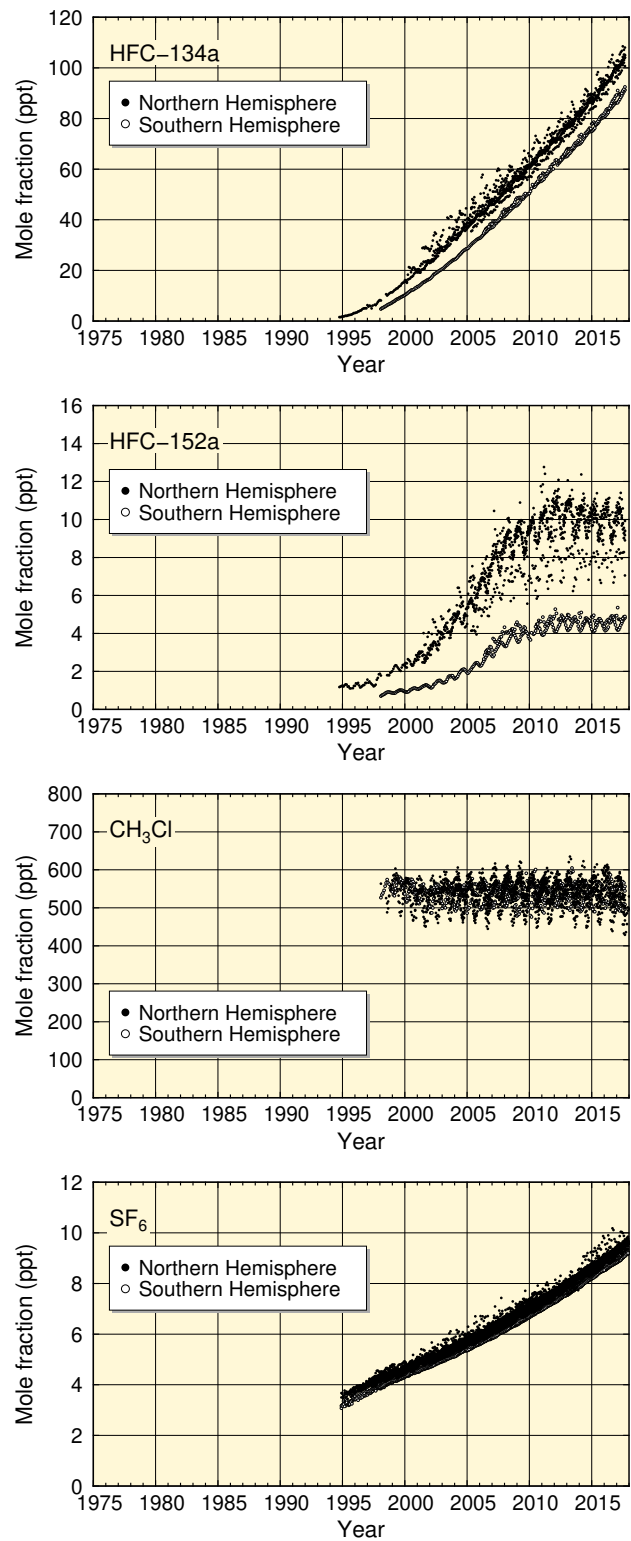


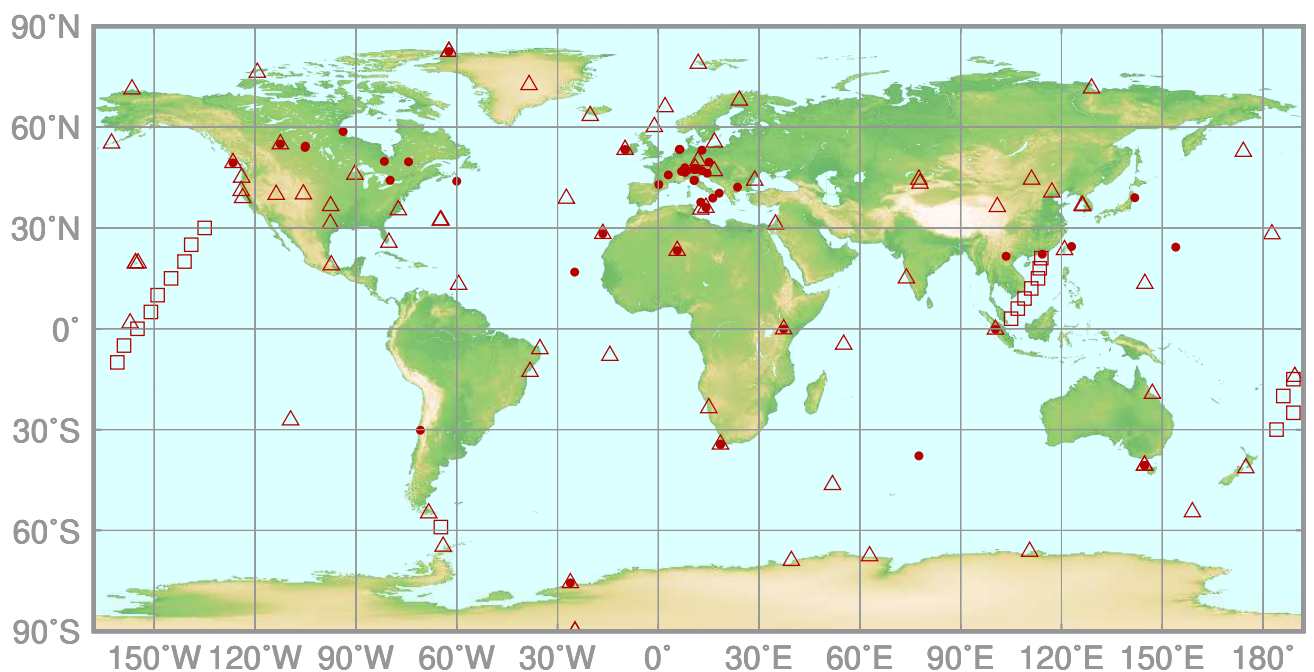
Fig. 4 (Continued)

5.

CARBON MONOXIDE

(CO)

- : CONTINUOUS STATION
- △ : FLASK STATION
- : FLASK MOBILE (SHIP)



This map shows locations of the stations that have submitted data for monthly mean mole fractions.

CO Monthly Data

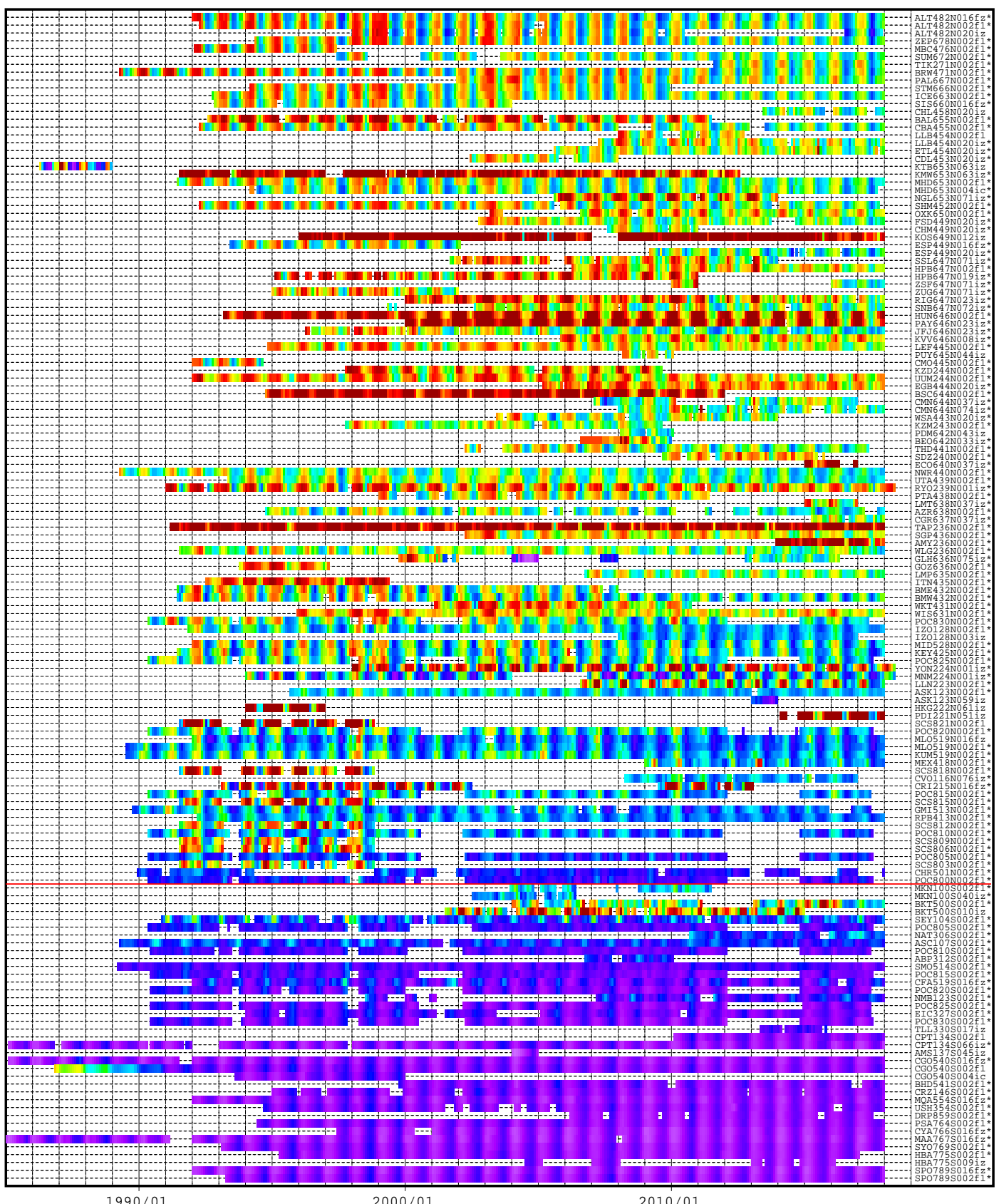
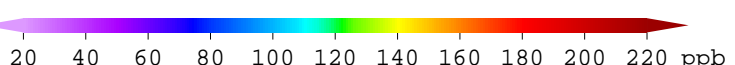
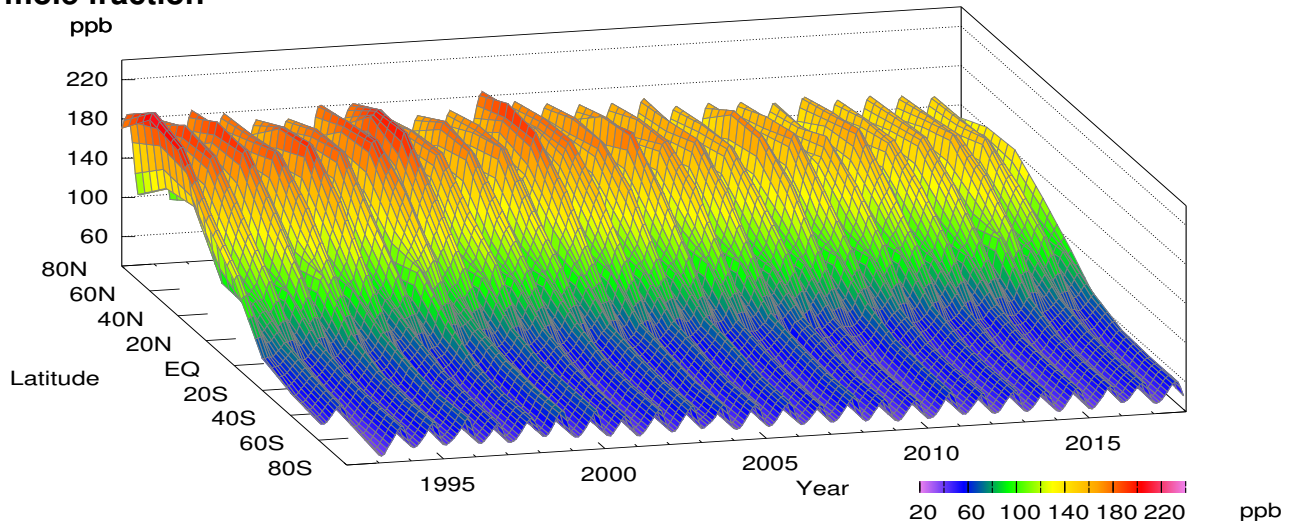


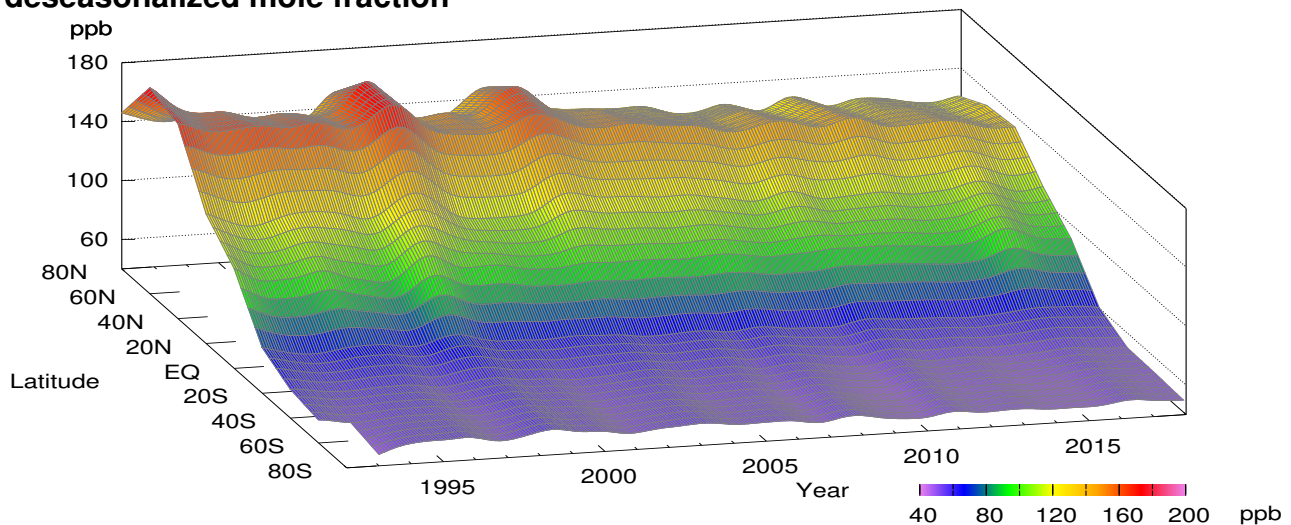
Plate 5.1 Monthly mean CO mole fractions that have been reported to the WDCGG. The mole fractions are illustrated in different colors.

The sites are listed in order from north to south. The red line indicates the equator. The data from the sites with an asterisk at the end of the station index were used for the analyses shown in Plate 5.2. (see Appendix A)

CO mole fraction



CO deseasonalized mole fraction



CO growth rate

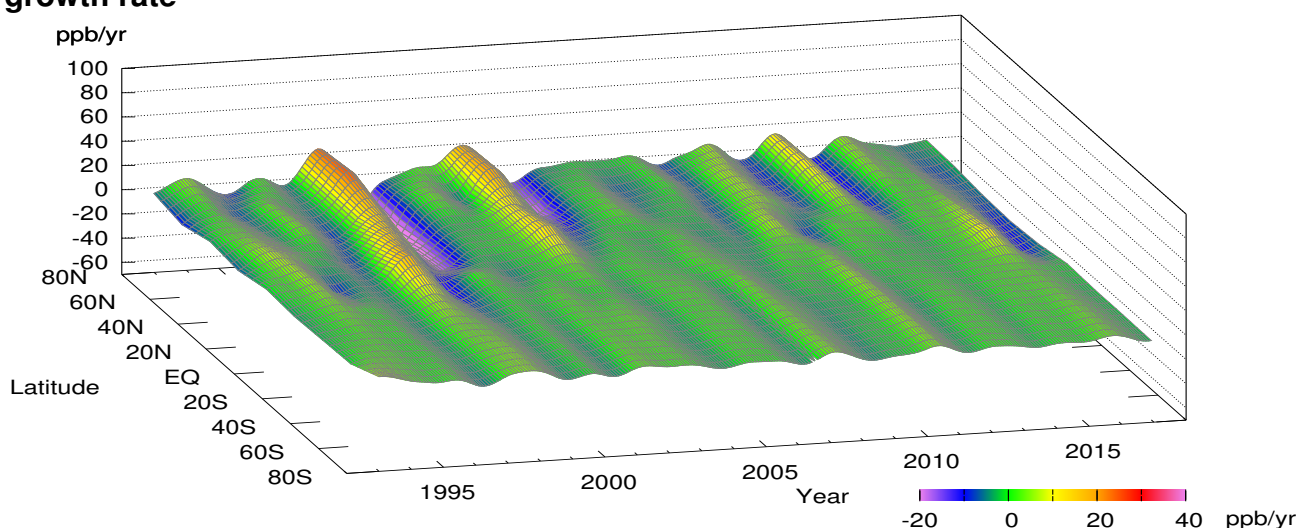


Plate 5.2 Variation of zonally averaged monthly mean CO mole fractions (top), deseasonalized long-term trends (middle), and growth rates (bottom). The zonally averaged mole fractions were calculated for each 20° zone. The deseasonalized trends and growth rates were derived as described in Appendix A.

5. CARBON MONOXIDE (CO)

Carbon monoxide (CO) is not categorized as a greenhouse gas because it absorbs hardly any infrared radiation from the earth. However, it influences major greenhouse gases, particularly through reaction with hydroxyl (OH) radical, and is therefore often addressed in the context of global warming. CO is also part of the global carbon cycle.

In contrast to the situation with major greenhouse gases, CO calibration scales cannot be easily linked to each other (see Appendix B). In this publication analysis was performed irrespective of scale differences, and the resulting global mean CO mole fraction was 90 ± 2 ppb in 2017. Similarly, the analysis results presented in this chapter are based on observations performed on different scales.

CO is emitted into the atmosphere mainly from fossil fuel combustion and biomass burning, and is destroyed predominantly through reaction with OH radical. Due to its chemical reactivity, it has a relatively short lifetime (in the range of tens of days) and large spatial variation. Ice core measurements performed by Haan and Raynaud (1998) revealed that the CO mole fractions of

approximately 90 ppb observed in Greenland in around 1750 had increased to approximately 110 ppb by 1950, indicating an impact of human activity. CO mole fractions have shown a gradual decline since around the beginning of the 21st century, particularly in the Northern Hemisphere (IPCC, 2013).

Global mean mole fractions

Figure 5.1 shows global mean CO mole fraction (top) and the related growth rate (bottom) in blue dots based on the analysis described in Appendix A. Seasonal variability is clearly pronounced in mole fractions, and the long-term trend was estimated after subtraction of the seasonal component (shown by the red line in the top panel of Fig. 5.1). The global mean mole fraction exhibits a gradual decrease, with the growth rate oscillating around zero. The mole fraction exhibits clear seasonal cycles, being lower in boreal summer and higher in winter. This is mainly because OH radicals, which react with and destroy CO, become more abundant in summer due to enhanced ultraviolet (UV) radiation. Seasonally varying sources such as biomass burning also contribute to the seasonal

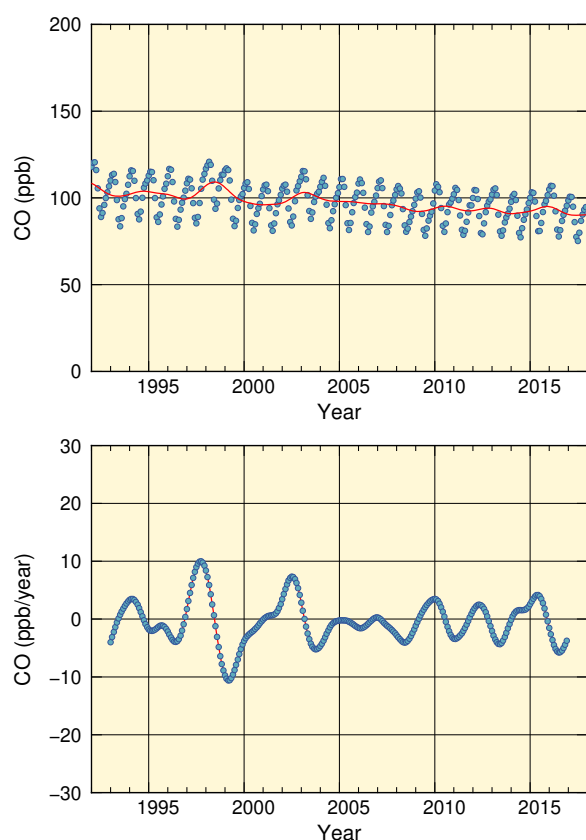


Fig. 5.1 Globally averaged monthly mean mole fraction of CO from 1992 to 2017 and the deseasonalized long-term trend in red line (top), and its growth rate (bottom).

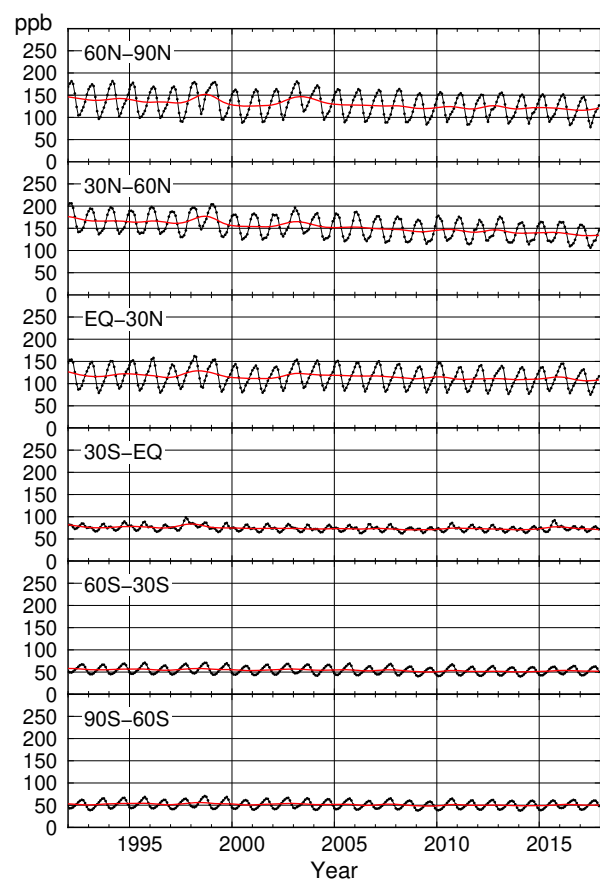


Fig. 5.2 Monthly mean mole fractions of CO from 1992 to 2017 for each 30° latitudinal zone (black) and their deseasonalized long-term trends (red).

cycles of mole fractions.

Latitudinal dependence of mole fractions

Figure 5.2 shows the CO mole fraction averaged over six 30° latitudinal bands with black lines, and the corresponding long-term trends are shown by red lines. The long-term trends are collectively shown in the top panel of Figure 5.3, and the corresponding growth rates are shown in the bottom panel. Average seasonal cycles of mole fractions for every latitudinal band are shown in Figure 5.4.

As shown in Figure 5.3, northern regions tend to have higher mole fractions, indicating the presence of more major CO sources such as fossil fuel combustion and biomass burning. Mole fractions in the Northern Hemisphere have shown slight declines throughout the period for which global averaging is feasible, and have remained almost constant in the Southern Hemisphere. Growth rates also exhibit significant spatial and temporal variability, and tend to be readily influenced by local events with limited time duration. For example, the large growth rate peak of 1997/1998 mainly in the Northern Hemisphere is probably attributable to forest fires in Siberia and tropical areas (Novelli *et al.*, 2003).

The amplitude of seasonal cycles is larger in northern bands than in southern bands, as shown in Figure 5.4. In the Northern Hemisphere, CO emitted from fossil fuel combustion accumulates in the mid- and high latitudes during winter and early spring under low OH radical conditions. In addition, emissions from biomass burning in the low latitudes peak in early spring. In summer, most of the CO accumulated during winter is destroyed by OH radicals. In the Southern Hemisphere, seasonal CO cycles are driven by emissions from biomass burning in the tropics and removal by reaction with OH radicals, which results in a smaller amplitude of seasonal cycles (Novelli *et al.*, 1998). The phase of seasonal cycles in the two hemispheres is opposed due to the reversed seasons. Seasonal variability in the low latitudes of the Southern Hemisphere is slightly more complex, probably influenced by the atmosphere in the Northern Hemisphere.

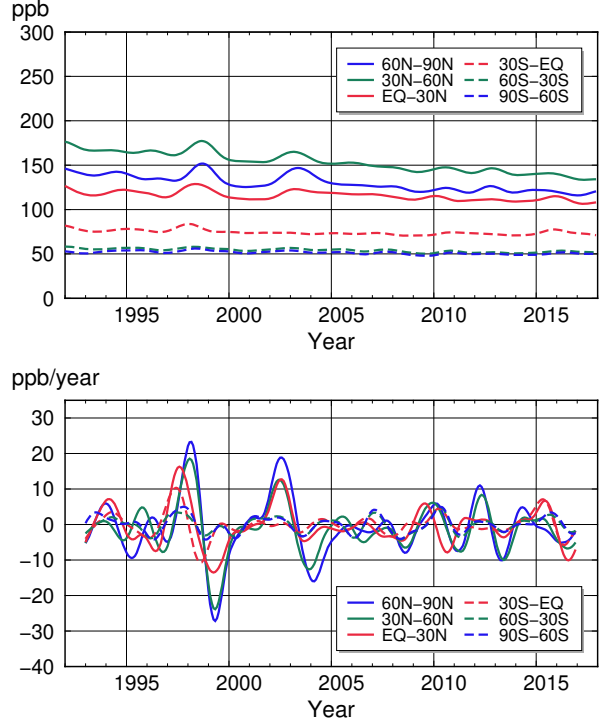


Fig. 5.3 Deseasonalized long-term trends of CO for each 30° latitudinal zone (top) and their growth rates (bottom).

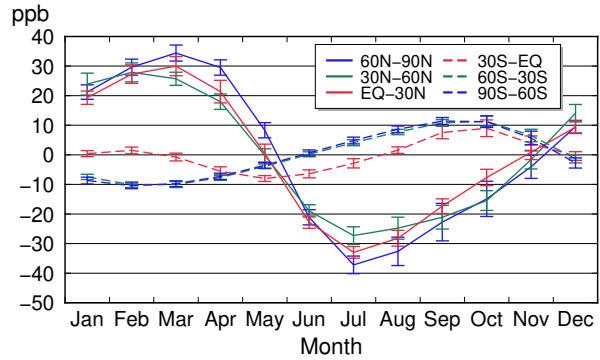


Fig. 5.4 Average seasonal cycles of CO mole fractions for each 30° latitudinal zone obtained by subtracting long-term trends from the zonal mean time series. Error bars represent the range of $\pm 1\sigma$ calculated for each month (period 1992 to 2017).

APPENDICES

APPENDIX A ANALYSIS

This appendix summarizes the method used to calculate global mean mole fractions and related quantities of CO₂, CH₄, N₂O and CO as described by WMO (2009).

The analysis is applied to monthly mean mole fraction data reported to WDCGG by fixed stations and ships with fixed observation points. Where no monthly data are reported, values are calculated from daily or hourly valid data based on simple arithmetic mean with the consent of data contributors. Data from mobile platforms such as ships without fixed observation points and aircraft are not used in this analysis (but they are useful for the other applications). If data for several different altitudes are reported, only those for the highest altitude are used (as they are expected to have a larger footprint).

For halocarbons, only monthly mean mole fractions observed at individual stations are presented. Global averaging is not performed due to the scarcity of reporting sites.

The mole fraction is defined as the number of molecules of a target gas species divided by the number of all molecules of dry air. Values are expressed as parts per million (ppm), parts per billion (ppb) or parts per trillion (ppt), corresponding to the SI units of $\mu\text{mol/mol}$, nmol/mol and pmol/mol, respectively.

(1) Site selection

All observation data are objectively selected for global analysis as described here.

Data with a standard scale traceable to the WMO Mole Fraction Scale (or a compatible standard for conversion) are first selected. CO data are an exception due to the scarcity of standard scales for which accurate conversion to the WMO Scale is possible.

For individual sites, annual mean mole fractions relative to that of the South Pole (averaged over the years for which data are available) are plotted to show latitudinal distribution and fitted to the LOESS model curve (Cleveland and Devlin, 1988). Outlier sites beyond the 3 sigma (residual standard deviation) of the fitted curve are excluded from further analysis, and the process is iterated

until exclusion terminates. The exclusion is not applied to N₂O due to the scarcity of annual mean data from the 1980s.

The numbers of sites that fit for global analysis (before and after this selection procedure) are shown in Table A1.

(2) Extension of observation data to cover the entire analysis period

Time-series data from some sites may contain gaps or not cover the entire analysis period. To ensure the homogeneity of globally averaged values over analysis periods exceeding 30 years, shortfalls in data coverage are filled using interpolation and extrapolation as described below.

Gaps in the time series are first interpolated for each site. The longest period among continuous monthly mean mole fraction data is identified, and the seasonal cycle and long-term trend are determined as detailed in WMO (2009). In short, a time series of mole fractions is approximated based on the sum of a Fourier series up to the third harmonic of the annual cycle and a non-periodic component determined via a Lanczos filter (Duchon, 1979) with a cut-off frequency of 0.48 cycles per year; the former is a seasonal cycle and the latter is a long-term trend. Mole fractions in gaps are then interpolated with a line connecting each end of the deseasonalized monthly values and superposed with the seasonal cycle.

After application of the interpolation, data are extrapolated via a number of statistical procedures. First, a time series of mole fraction growth rates is calculated for each observation site by differentiating the long-term trend that is obtained from the mole fractions whose gaps are interpolated as above. Next, for each of six 30° latitudinal bands (60–90°N, 30°S–EQ, etc.), an average time series of growth rates is calculated as an arithmetic mean over sites located in the band. For individual sites, the long-term trend is then extended to cover the entire analysis period based on growth rates for the latitudinal band where the site is located, and it is finally superposed with the seasonal cycle for the site determined after

Table A1. Numbers of sites before/after the selection procedure outlined in Section (1) for CO₂, CH₄, N₂O and CO

	CO ₂	CH ₄	N ₂ O	CO
Pre-selection ^(a)	163	140	100	132
Post-selection ^(b)	129	126	96	122

(a) Figures are derived from the number of the first seven characters of the Filename Code (e.g., RYO239N) in Plate 1.1, 2.1, 3.1 and 5.1 (or Table B3 to B6), excluding duplicates.

(b) As per (a), but with Filename Codes marked with asterisks.

interpolation.

(3) Calculation of global and hemispheric mean mole fractions

With the extension procedure described above, all sites selected as described in Section (1) have a time series of mole fractions covering the entire analysis period with no data gaps. From these data, latitudinal mean mole fractions are calculated for the six bands, and global and hemispheric mean mole fractions are then determined by averaging the mole fractions of six and three latitudinal bands, respectively, with weighting for surface area. The seasonal cycle, long-term trend and growth rate are then determined for every averaged time series. As long-term trend calculation is less precise at either end of mole fraction time-series representations (see WMO 2009 for details), growth rates originating from the related derivative function are characterized by larger uncertainty. Accordingly, growth rates for a year each from either end of the analysis period are not shown in the figures here.

(4) Uncertainty estimation

In this analysis, uncertainty in global mean mole fractions (at a 68% confidence level) is calculated using bootstrap analysis as described in Conway *et al.* (1994). From the dataset of mole fractions obtained after the site selection and data extension procedure described above, n sites are randomly selected, with duplication of the same sites allowed on condition that at least one site is selected from each of the six latitudinal bands, and a global mean mole fraction is calculated using the data from the n sites. The procedure is repeated m times to determine m different global mean mole fractions. Uncertainty is defined as the standard deviation of these mole fractions. In this analysis, the number of sites selected as described in Section (1) and 200 are chosen as n and m , respectively, for maximum stability in the standard deviation thus determined.

APPENDIX B CALIBRATION AND STANDARD SCALES

1. Calibration System in the GAW Programme

Under the Global Atmosphere Watch (GAW) Programme, the Central Calibration Laboratories (CCLs) are assigned to host a Primary (Reference) Standard/scale, while the World Calibration Centres (WCCs) and Regional Calibration Centres (RCC) are responsible for the scale propagation to the stations via distribution of calibration standards for certain compounds, conducting instrument calibrations, comparison campaigns, station

audits and providing training to the station personnel. A Reference Standard/scale is designated for each variable to be used for all GAW measurements of that variable. Table B1 lists the organizations that serve as WCCs and CCLs for GAW (WMO, 2017). For CFCs, no central facilities or quality control systems have so far been established within the GAW Programme.

Table B1. Overview of the GAW Central Calibration Laboratories (GAW-CCL, Reference Standard) and World Calibration Centres for greenhouse and other related gases. The World Calibration Centres have assumed global responsibilities, except where indicated (Am, Americas; E/A, Europe and Africa; A/O, Asia and the South-West Pacific)

Compounds	Central Calibration Laboratory (Host of Primary Standard)	World Calibration Centre
Carbon Dioxide (CO ₂)	NOAA/ESRL	NOAA/ESRL (Round Robin) Empa (audits)
Carbon Dioxide (CO ₂) isotopes	MPI-BGC	
Methane (CH ₄)	NOAA/ESRL	Empa (Am, E/A) JMA (A/O)
Nitrous Oxide (N ₂ O)	NOAA/ESRL	KIT/IMK-IFU
Chlorofluorocarbons (CFCs)		
Sulphur Hexafluoride (SF ₆)	NOAA/ESRL	KMA
Molecular Hydrogen (H ₂)	MPI-BGC	
Carbon Monoxide (CO)	NOAA/ESRL	Empa

2. Carbon Dioxide (CO₂)

In 1995, the National Oceanic and Atmospheric Administration's Earth System Research Laboratory (NOAA/ESRL, formerly CMDL; Climate Monitoring and Diagnostics Laboratory) in Boulder, Colorado, USA, took over the role of the CCL from the Scripps Institution of Oceanography (SIO) in San Diego, California, USA. Since then, NOAA/ESRL has served as the CCL responsible for the maintenance of the GAW Primary Standard for CO₂. As CCL for CO₂, NOAA/ESRL maintains a high-precision manometric system for absolute calibration of CO₂ as the reference for GAW measurements throughout the world (Zhao *et al.*, 1997), as well as carrying out Round Robin in the function of WCC. It has been recommended that the standards of the GAW measurement laboratories be calibrated at least every three years at the CCL (WMO, 2018b).

Under the WMO calibration system, there have been several calibration scales for CO₂, *e.g.*, SIO-based X74,

X85, X87, X93 and X2002 scales and the NOAA/ESRL-based WMO Mole Fraction Scale partially based on previous SIO scales. The CCL adopted the WMO X2005 scale, reflecting historical manometric calibrations of the CCL's set of cylinders and the possible small differences between SIO and NOAA/ESRL calibrations. The most current WMO Mole Fraction Scale is the WMO X2007 scale.

To assess the differences in standard scales among measuring laboratories, about every three years NOAA/ESRL organizes intercomparisons or Round Robin experiments endorsed by WMO. Many laboratories participated in the experiments organized in 1991–1992, 1995–1997, 1999–2000, 2002–2006, 2009–2012 and 2014–2015. Table B2 shows the results of the experiments performed in 2014–2015, in which the mole fractions measured by various laboratories are compared with the mole fractions measured by NOAA/ESRL

(http://www.esrl.noaa.gov/gmd/ccgg/wmorr/wmorr_results.php).

Table B3 lists organizations and sites that contributed to

the present issue of the Data Summary with standard scales of reported data and history of participation in WMO intercomparison experiments.

Table B2. Round Robin results for the mole fraction of carbon dioxide. Differences between the mole fractions measured by various laboratories and the mole fractions measured by NOAA (Laboratory minus NOAA, ppm).

Laboratory	Measurement Date	Mole Fraction Difference (ppm)	
		Low 375-380 ppm	High 400-415 ppm
NCAR	Mar-14 & Jun-15	-0.01 ~ 0.02	-0.05
NOAA-CSD	Apr-14	0.06	0.03
NEON	May-14	0.01	0.02
NIST	Jul-14	-0.37	-0.49
HU	Jul & Dec-14	0.05	0.01
PSU	Aug-14	0.03	-0.02
CALTECH	Sep-14	-0.02	-0.04
BLG	Oct-14	0.06	-0.09
AMERIFLUX	Nov-14	-0.01	-0.02
ECCC	Dec-14	0.09	0.06
HMS	Jun-15	0.03	0.02
AEMET	Aug-15	-0.01	-0.01
CSIRO	May-14	0.04	0.00
NIWA	Jun-14	0.08	-0.08
SAWS	Aug-14	0.16	0.14
CMA	Oct-14	0.02	-0.02
KMA	Jan-15	0.03	0.04
MGO	Aug-15	0.00	-0.03
LSCE	May-14	-0.05	-0.00
WCC-Empa	Jun-14	-0.10	-0.06
Empa	Jul-14	-0.07	-0.06
FMI	Sep-14 & Jul-15	0.01	-0.10
RUG	Dec-14	0.03	0.06
ECN	Jan-15	0.31	0.51
UEA	Mar-15	-0.31	-0.25
RHUL	Apr-15	-0.10	-0.02
UHEI-IUP	Jun-14	-0.03	-0.06
UBAG-SCHAU	Jul-14	0.05	-0.04
UBAG/ZUG	Sep-14	0.03	0.02
MPI-BGC	Nov-14	-0.01	-0.02
RSE	Jan-15	0.07	-0.08
IAFMC	Feb-15	-1.63	-1.62
ENEA	May-15	-0.01	-0.05
ICOS	Jul-15	-0.01	-0.03
JMA	Oct-13	-0.04	-0.04
MRI	Nov-13	-0.15	-0.14
AIST	Jan-14	0.13	0.18
NIES	Jan-14	-0.09	-0.04
TU	Feb-14	0.16	0.25

Table B3. Status of standard scales and calibration/intercomparison for CO₂.

Organization	WDCGG Filename	Filename Code in Plate 1.1	Calibration Scale	WMO Inter-comparison
AEMET	co2_izo_surface-insitu_3_9999-9999_monthly.txt	IZO128N003iz*	WMO	91/92, 96/97, 99/00, 09/12, 14/15
AICH	co2_mkw_surface-insitu_5_9999-9999_monthly.txt	MKW234N005iz	WMO	
AIST	co2_tky_tower-insitu_6_6028-9999_monthly.txt	TKY236N006it		96/97, 99/00, 02/06, 09/12, 14/15
BMKG	co2_bkt_surface-insitu_10_9999-9999_monthly.txt	BKT500S010iz	WMO	
CMA	co2_wlg_surface-insitu_13_9999-9999_monthly.txt	WLG236N013iz*	WMO	96/97, 99/00, 02/06, 09/12, 14/15
CSIRO	co2_alt_surface-flask_16_9999-9999_monthly.txt co2_cfa_surface-flask_16_9999-9999_monthly.txt co2_cgo_surface-flask_16_9999-9999_monthly.txt co2_cgo_surface-insitu_16_9998-9999_monthly.txt co2_cgo_surface-insitu_16_9999-9999_monthly.txt co2_cri_surface-flask_16_9999-9999_monthly.txt co2_cya_surface-flask_16_9999-9999_monthly.txt co2_esp_surface-flask_16_9999-9999_monthly.txt co2_maa_surface-flask_16_9999-9999_monthly.txt co2_mlo_surface-flask_16_9999-9999_monthly.txt co2_mqa_surface-flask_16_9999-9999_monthly.txt co2_sis_surface-flask_16_9999-9999_monthly.txt co2_spo_surface-flask_16_9999-9999_monthly.txt	ALT482N016fz CFA519S016fz* CGO540S016fz CGO540S016iy* CGO540S016iz* CRI215N016fz* CYA766S016fz* ESP449N016fz* MAA767S016fz* MLO519N016fz MQA554S016fz* SIS660N016fz* SPO789S016fz	WMO	91/92, 96/97, 99/00, 02/06, 09/12, 14/15
DMC	co2_tll_surface-insitu_17_9999-9999_monthly.txt	TLL330S017iz	WMO	
ECCC	co2_alt_surface-insitu_20_9999-9999_monthly.txt co2_cdl_surface-insitu_20_9999-9999_monthly.txt co2_chl_surface-insitu_20_9999-9999_monthly.txt co2_chm_surface-insitu_20_9999-9999_monthly.txt co2_egb_surface-insitu_20_9999-9999_monthly.txt co2_esp_surface-insitu_20_9999-9999_monthly.txt co2_etl_surface-insitu_20_9999-9999_monthly.txt co2_fsd_surface-insitu_20_9999-9999_monthly.txt co2_llb_surface-insitu_20_9999-9999_monthly.txt co2_wsa_surface-insitu_20_9999-9999_monthly.txt	ALT482N020iz CDL453N020iz* CHL458N020iz* CHM449N020iz* EGB444N020iz* ESP449N020iz* ETL454N020iz* FSD449N020iz* LLB454N020iz* WSA443N020iz*	WMO	91/92, 96/97, 99/00, 02/06, 09/12, 14/15
Empa	co2_jfj_surface-insitu_23_9999-9999_monthly.txt	JFJ646N023iz*	WMO	09/12, 14/15
ENEA	co2_lmp_surface-flask_24_9999-9999_monthly.txt	LMP635N024fz*	WMO	91/92, 96/97, 99/00, 02/06, 09/12, 14/15
FMI	co2_pal_surface-insitu_25_9999-9999_monthly.txt	PAL667N025iz*	WMO	02/06, 09/12 14/15
GERC	co2_gsn_surface-insitu_52_9999-9999_monthly.txt	GSN233N052iz	WMO	
HKO	co2_hkg_surface-insitu_27_9999-9999_monthly.txt	HKG222N027iz*	WMO	
	co2_hko_surface-insitu_27_9999-9999_monthly.txt	HKO222N027iz	WMO NIST	
HMS	co2_hun_tower-insitu_28_6116-9999_monthly.txt co2_kps_surface-insitu_28_9999-9999_monthly.txt	HUN646N028it KPS646N028iz*	WMO	91/92, 96/97, 99/00, 02/06, 09/12, 14/15
IAA	co2_jbn_surface-insitu_18_9999-9999_monthly.txt	JBN762S018iz*	WMO	

IAFMS	co2_cmn_surface-insitu_29_9999-9999_monthly.txt	CMN644N029iz*	WMO	91/92, 96/97, 02/06, 14/15
IGP	co2_hua_surface-insitu_30_9999-9999_monthly.txt	HUA312S030iz	WMO	
IMKIFU	co2_wnk_surface-insitu_31_9999-9999_monthly.txt co2_zug_surface-insitu_31_9999-9999_monthly.txt	WNK647N031iz ZUG647N031iz	WMO	99/00
INMH	co2_fdt_surface-insitu_58_9999-9999_monthly.txt	FDT645N058iz		
INRNE	co2_beo_surface-insitu_33_9999-9999_monthly.txt	BEO642N033iz	WMO	
IOEP	co2_dig_surface-insitu_35_9999-9999_monthly.txt	DIG654N035iz		
ISAC	co2_cgr_surface-insitu_37_9999-9999_monthly.txt co2_lmt_surface-insitu_37_9999-9999_monthly.txt	CGR637N037iz* LMT638N037iz	WMO	
	co2_eco_surface-insitu_37_9999-9999_monthly.txt	ECO640N037iz		
ITM	co2_zep_surface-insitu_38_9999-9999_monthly.txt	ZEP678N038iz	WMO	96/97, 99/00, 09/12
JMA	co2_mnm_surface-insitu_1_9999-9999_monthly.txt co2_ryo_surface-insitu_1_9999-9999_monthly.txt co2_yon_surface-insitu_1_9999-9999_monthly.txt	MNM224N001iz* RYO239N001iz* YON224N001iz*	WMO	91/92, 96/97, 99/00, 02/06, 09/12, 14/15
KMA	co2_amy_surface-insitu_39_9999-9999_monthly.txt co2_jgs_surface-insitu_39_9999-9999_monthly.txt	AMY236N039iz* JGS233N039iz	WMO	02/06, 09/12 14/15
	co2_ksg_surface-insitu_39_9999-9999_monthly.txt	KSG762S039iz	KRISS	
KSNU	co2_isk_surface-remote_41_9999-9999_monthly.txt	ISK242N041rz		
KUP	co2_jfj_surface-insitu_42_9999-9999_monthly.txt	JFJ646N042iz*	WMO	09/12
LSCE	co2_ams_surface-insitu_45_9998-9999_monthly.txt co2_bgu_surface-flask_45_9999-9999_monthly.txt co2_lpo_surface-flask_45_9999-9999_monthly.txt co2_mhd_surface-insitu_45_9999-9999_monthly.txt co2_pdm_surface-flask_45_9999-9999_monthly.txt co2_puy_surface-insitu_45_9999-9999_monthly.txt	AMS137S045iy* BGU641N045fz* LPO648N045fz MHD653N045iz PDM642N045fz* PUY645N045iz*	WMO	91/92, 96/97, 99/00, 02/06, 09/12, 14/15
	co2_fik_surface-flask_45_9999-9999_monthly.txt	FIK635N045fz		
METRI	co2_gsn_surface-flask_55_9999-9999_monthly.txt	GSN233N055fz*		
MGO	co2_ber_surface-flask_46_9999-9999_monthly.txt co2_kot_surface-flask_46_9999-9999_monthly.txt co2_kyz_surface-flask_46_9999-9999_monthly.txt co2_stc_surface-flask_46_9999-9999_monthly.txt co2_ter_surface-flask_46_9999-9999_monthly.txt co2_tik_surface-flask_46_9999-9999_monthly.txt	BER255N046fz* KOT276N046fz* KYZ240N046fz* STC654N046fz* TER669N046fz* TIK271N046fz*		
MMD	co2_dmv_surface-insitu_47_9999-9999_monthly.txt	DMV504N047iz		
MRI	co2_tkb_tower-insitu_48_6201-9999_monthly.txt	TKB236N048it	MRI-87	91/92, 96/97, 99/00, 02/06, 09/12, 14/15
NIES	co2_coi_surface-insitu_53_9999-9999_monthly.txt co2_hat_surface-insitu_53_9999-9999_monthly.txt	COI243N053iz* HAT224N053iz*	NIES 95**	96/97, 99/00, 02/06, 09/12, 14/15
NIWA	co2_bhd_surface-insitu_57_9999-9999_monthly.txt	BHD541S057iz*	WMO	91/92, 96/97, 99/00, 02/06, 09/12, 14/15
NOAA	co2_abp_surface-flask_2_3001-9999_monthly.txt co2_alt_surface-flask_2_3001-9999_monthly.txt co2_ams_surface-flask_2_3001-9999_monthly.txt co2_amy_surface-flask_2_3001-9999_monthly.txt co2_asc_surface-flask_2_3001-9999_monthly.txt co2_ask_surface-flask_2_3001-9999_monthly.txt co2_avi_surface-flask_2_3001-9999_monthly.txt co2_azr_surface-flask_2_3001-9999_monthly.txt	ABP312S002f1* ALT482N002f1* AMS137S002f1 AMY236N002f1 ASC107S002f1* ASK123N002f1* AVI417N002f1* AZR638N002f1*	WMO	91/92, 96/97, 99/00, 02/06, 09/12, 14/15

co2_bal_surface-flask_2_3001-9999_monthly.txt	BAL655N002f1*
co2_bhd_surface-flask_2_3001-9999_monthly.txt	BHD541S002f1*
co2_bkt_surface-flask_2_3001-9999_monthly.txt	BKT500S002f1
co2_bme_surface-flask_2_3001-9999_monthly.txt	BME432N002f1*
co2_bmw_surface-flask_2_3001-9999_monthly.txt	BMW432N002f1*
co2_brw_surface-flask_2_3001-9999_monthly.txt	BRW471N002f1*
co2_brw_surface-insitu_2_3001-9999_monthly.txt	BRW471N002i1*
co2_bsc_surface-flask_2_3001-9999_monthly.txt	BSC644N002f1
co2_cba_surface-flask_2_3001-9999_monthly.txt	CBA455N002f1*
co2_cgo_surface-flask_2_3001-9999_monthly.txt	CGO540S002f1*
co2_chr_surface-flask_2_3001-9999_monthly.txt	CHR501N002f1*
co2_cmo_surface-flask_2_3001-9999_monthly.txt	CMO445N002f1*
co2_cpt_surface-flask_2_3001-9999_monthly.txt	CPT134S002f1
co2_crz_surface-flask_2_3001-9999_monthly.txt	CRZ146S002f1*
co2_drp_ship-flask_2_3001-9999_monthly.txt	DRP859S002f1*
co2_eic_surface-flask_2_3001-9999_monthly.txt	EIC327S002f1*
co2_gmi_surface-flask_2_3001-9999_monthly.txt	GMI513N002f1*
co2_goz_surface-flask_2_3001-9999_monthly.txt	GOZ636N002f1*
co2_hba_surface-flask_2_3001-9999_monthly.txt	HBA775S002f1*
co2_hpb_surface-flask_2_3001-9999_monthly.txt	HPB647N002f1*
co2_hun_surface-flask_2_3001-9999_monthly.txt	HUN646N002f1*
co2_ice_surface-flask_2_3001-9999_monthly.txt	ICE663N002f1*
co2_izo_surface-flask_2_3001-9999_monthly.txt	IZO128N002f1
co2_key_surface-flask_2_3001-9999_monthly.txt	KEY425N002f1*
co2_kum_surface-flask_2_3001-9999_monthly.txt	KUM519N002f1*
co2_kzd_surface-flask_2_3001-9999_monthly.txt	KZD244N002f1*
co2_kzm_surface-flask_2_3001-9999_monthly.txt	KZM243N002f1*
co2_lef_surface-flask_2_3001-9999_monthly.txt	LEF445N002f1*
co2_llb_surface-flask_2_3001-9999_monthly.txt	LLB454N002f1
co2_lln_surface-flask_2_3001-9999_monthly.txt	LLN223N002f1*
co2_lmp_surface-flask_2_3001-9999_monthly.txt	LMP635N002f1*
co2_mbc_surface-flask_2_3001-9999_monthly.txt	MBC476N002f1*
co2_mex_surface-flask_2_3001-9999_monthly.txt	MEX418N002f1*
co2_mhd_surface-flask_2_3001-9999_monthly.txt	MHD653N002f1*
co2_mid_surface-flask_2_3001-9999_monthly.txt	MID528N002f1*
co2_mkn_surface-flask_2_3001-9999_monthly.txt	MKN100S002f1*
co2_mlo_surface-flask_2_3001-9999_monthly.txt	MLO519N002f1*
co2_mlo_surface-insitu_2_3001-9999_monthly.txt	MLO519N002i1*
co2_nat_surface-flask_2_3001-9999_monthly.txt	NAT306S002f1*
co2_nmb_surface-flask_2_3001-9999_monthly.txt	NMB123S002f1*
co2_nwr_surface-flask_2_3001-9999_monthly.txt	NWR440N002f1*
co2_opw_surface-flask_2_3001-9999_monthly.txt	OPW448N002f1*
co2_oxk_surface-flask_2_3001-9999_monthly.txt	OXK650N002f1*
co2_pal_surface-flask_2_3001-9999_monthly.txt	PAL667N002f1
co2_poc_ship-flask_2_3001-3001_monthly.txt	POC800N002f1*
co2_poc_ship-flask_2_3001-3002_monthly.txt	POC805N002f1*
co2_poc_ship-flask_2_3001-3003_monthly.txt	POC810N002f1*
co2_poc_ship-flask_2_3001-3004_monthly.txt	POC815N002f1*
co2_poc_ship-flask_2_3001-3005_monthly.txt	POC820N002f1*
co2_poc_ship-flask_2_3001-3006_monthly.txt	POC825N002f1*
co2_poc_ship-flask_2_3001-3007_monthly.txt	POC830N002f1*
co2_poc_ship-flask_2_3001-3012_monthly.txt	POC805S002f1*
co2_poc_ship-flask_2_3001-3013_monthly.txt	POC810S002f1*
co2_poc_ship-flask_2_3001-3014_monthly.txt	POC815S002f1*
co2_poc_ship-flask_2_3001-3015_monthly.txt	POC820S002f1*
co2_poc_ship-flask_2_3001-3016_monthly.txt	POC825S002f1*

	co2_poc_ship-flask_2_3001-3017_monthly.txt co2_poc_ship-flask_2_3001-3018_monthly.txt co2_psa_surface-flask_2_3001-9999_monthly.txt co2_pta_surface-flask_2_3001-9999_monthly.txt co2_rpb_surface-flask_2_3001-9999_monthly.txt co2_scs_ship-flask_2_3001-3101_monthly.txt co2_scs_ship-flask_2_3001-3102_monthly.txt co2_scs_ship-flask_2_3001-3103_monthly.txt co2_scs_ship-flask_2_3001-3104_monthly.txt co2_scs_ship-flask_2_3001-3105_monthly.txt co2_scs_ship-flask_2_3001-3106_monthly.txt co2_scs_ship-flask_2_3001-3107_monthly.txt co2_sdz_surface-flask_2_3001-9999_monthly.txt co2_sey_surface-flask_2_3001-9999_monthly.txt co2_sgp_surface-flask_2_3001-9999_monthly.txt co2_shm_surface-flask_2_3001-9999_monthly.txt co2_smo_surface-flask_2_3001-9999_monthly.txt co2_smo_surface-insitu_2_3001-9999_monthly.txt co2_spo_surface-flask_2_3001-9999_monthly.txt co2_spo_surface-insitu_2_3001-9999_monthly.txt co2_stc_surface-flask_2_3001-9999_monthly.txt co2_stm_surface-flask_2_3001-9999_monthly.txt co2_sum_surface-flask_2_3001-9999_monthly.txt co2_syo_surface-flask_2_3001-9999_monthly.txt co2_tap_surface-flask_2_3001-9999_monthly.txt co2_thd_surface-flask_2_3001-9999_monthly.txt co2_tik_surface-flask_2_3001-9999_monthly.txt co2_ush_surface-flask_2_3001-9999_monthly.txt co2_uta_surface-flask_2_3001-9999_monthly.txt co2_uum_surface-flask_2_3001-9999_monthly.txt co2_wis_surface-flask_2_3001-9999_monthly.txt co2_wlg_surface-flask_2_3001-9999_monthly.txt co2_zep_surface-flask_2_3001-9999_monthly.txt	POC830S002f1* POC835S002f1* PSA764S002f1* PTA438N002f1* RPB413N002f1* SCS803N002f1* SCS806N002f1* SCS809N002f1* SCS812N002f1* SCS815N002f1* SCS818N002f1* SCS821N002f1* SDZ240N002f1 SEY104S002f1* SGP436N002f1* SHM452N002f1* SMO514S002f1* SMO514S002i1* SPO789S002f1* SPO789S002i1* STC654N002f1 STM666N002f1* SUM672N002f1* SYO769S002f1* TAP236N002f1 THD441N002f1* TIK271N002f1* USH354S002f1* UTA439N002f1* UUM244N002f1* WIS631N002f1* WLG236N002f1* ZEP678N002f1*		
OSAKAU	co2_sui_surface-insitu_60_9999-9999_monthly.txt	SUI234N060iz		
RIVM	co2_kmw_surface-insitu_63_9999-9999_monthly.txt	KMW653N063iz	NIST	
RSE	co2_prs_surface-insitu_64_9999-9999_monthly.txt	PRS645N064iz*	WMO	99/00, 02/06 14/15
SAIPF	co2_ddr_surface-insitu_65_9999-9999_monthly.txt co2_kis_surface-insitu_65_9999-9999_monthly.txt co2_urw_surface-insitu_65_9999-9999_monthly.txt	DDR236N065iz* KIS236N065iz URW235N065iz	WMO	
SAWS	co2_cpt_surface-insitu_66_9999-1001_monthly.txt	CPT134S066iz*	WMO	99/00, 02/06, 09/12, 14/15
SHIZU	co2_hmm_surface-insitu_67_9999-9999_monthly.txt	HMM234N067iz		
TU	co2_syo_surface-insitu_70_9999-9999_monthly.txt	SYO769S070iz	Tohoku Univ. 2010	91/92, 96/97, 99/00, 02/06, 09/12
UBAA	co2_snb_surface-insitu_72_9999-9999_monthly.txt	SNB647N072iz*	WMO	
UBAG	co2_brt_surface-insitu_71_9999-9999_monthly.txt co2_deu_surface-insitu_71_9999-9999_monthly.txt co2_lgb_surface-insitu_71_9999-9999_monthly.txt co2_ngl_surface-insitu_71_9999-9999_monthly.txt co2_ssl_surface-insitu_71_9998-9999_monthly.txt co2_ssl_surface-insitu_71_9999-9999_monthly.txt co2_wes_surface-insitu_71_9999-9999_monthly.txt co2_zgt_surface-insitu_71_9999-9999_monthly.txt	BRT648N071iz* DEU649N071iz LGB652N071iz NGL653N071iz SSL647N071iy SSL647N071iz* WES654N071iz ZGT654N071iz	WMO	91/92, 96/97, 99/00, 02/06, 09/12, 14/15

	co2_zsf_surface-insitu_71_9999-9999_monthly.txt co2_zug_surface-insitu_71_9999-9999_monthly.txt	ZSF647N071iz* ZUG647N071iz*		
UMLT	co2_glh_surface-insitu_75_9999-9999_monthly.txt	GLH636N075iz		
VNMHA	co2_pdi_surface-insitu_51_9999-9999_monthly.txt	PDI221N051iz	WMO	

* Stations marked with an asterisk are used for the calculation of global mean mole fractions and related quantities. The site selection procedure is described in Appendix A.

** NIES 95 CO₂ scale is 0.10 to 0.14 ppm lower than that of WMO in the range 355 to 385 ppm.

(Machida *et al.*, WMO/GAW Report No. 186, 26-29, 2009.)

3. Methane (CH₄)

The GAW Programme has a CCL for CH₄ at NOAA/ESRL (Dlugokencky *et al.*, 2005; WMO, 2017). Two WCCs for CH₄ are also run by the Swiss Federal Laboratory for Materials Testing and Research (Empa; Dübendorf, Switzerland) and the Japan Meteorological Agency (JMA; Tokyo, Japan) (WMO, 2017).

The current WMO Mole Fraction Scale is X2004A, which consists of 16 existing standards covering the range of the previous WMO X2004 scale and 6 new standards to expand the range of the scale. Table B4 summarizes the CH₄ standard scales used by stations contributing to the WDCGG and lists provisional multiplying conversion factors applied for analysis in the Data Summary. In this issue, the factor for conversion between the X2004A and X2004 scales is taken as 1 because the difference between

them is minor.

Mole fractions on the WMO X2004 scale are 1.0124 times higher than those on the NOAA 1983 scale (Dlugokencky *et al.*, 2005). Values on the NOAA 1983 scale are up to around 1.5% lower than those of the Tohoku University gravimetric scale (Aoki *et al.*, 1992; Dlugokencky *et al.*, 1994) and 1.0151 times lower than those on the scale of the Atmospheric Environment Service (AES, now known as Environment and Climate Change Canada (ECCC)) (Worthy *et al.*, 1998). The NOAA 1983 scale can be converted to the Tohoku University standard by multiplying by 1.0121 (Dlugokencky *et al.*, 2005). The conversion factors 1.0124 / 1.0151 = 0.9973 and 1.0124 / 1.0121 = 1.0003 are adopted for comparison with the WMO X2004 scale.

Table B4. Status of the standard scales of CH₄ with conversion factors.

Organization	WDCGG Filename	Filename Code in Plate 2.1	Calibration Scale	Conversion Factor
AEMET	ch4_izo_surface-insitu_3_9999-9999_monthly.txt	IZO128N003iz*	WMO X2004A	1
AGAGE	ch4_cgo_surface-insitu_4_2011-2016_monthly.txt ch4_cgo_surface-insitu_4_2021-2021_monthly.txt ch4_cmo_surface-insitu_4_2011-2016_monthly.txt ch4_mhd_surface-insitu_4_2011-2016_monthly.txt ch4_mhd_surface-insitu_4_2021-2021_monthly.txt ch4_rpb_surface-insitu_4_2021-2021_monthly.txt ch4_smo_surface-insitu_4_2011-2016_monthly.txt ch4_smo_surface-insitu_4_2021-2021_monthly.txt ch4_thd_surface-insitu_4_2021-2021_monthly.txt	CGO540S004ib CGO540S004ic* CMO445N004ib MHD653N004ib* MHD653N004ic* RPB413N004ic* SMO514S004ib SMO514S004ic* THD441N004ic*	Tohoku Univ.	1.0003
BMKG	ch4_bkt_surface-insitu_10_9999-9999_monthly.txt	BKT500S010iz	WMO X2004	1
CHMI	ch4_kos_surface-insitu_12_9999-9999_monthly.txt	KOS649N012iz		
CMA	ch4_wlg_surface-insitu_13_9999-9999_monthly.txt	WLG236N013iz	WMO X2004	1
CSIRO	ch4_alt_surface-flask_16_9999-9999_monthly.txt ch4_cfa_surface-flask_16_9999-9999_monthly.txt ch4_cgo_surface-flask_16_9999-9999_monthly.txt ch4_cri_surface-flask_16_9999-9999_monthly.txt ch4_cya_surface-flask_16_9999-9999_monthly.txt ch4_esp_surface-flask_16_9999-9999_monthly.txt ch4_maa_surface-flask_16_9999-9999_monthly.txt ch4_mlo_surface-flask_16_9999-9999_monthly.txt ch4_mqa_surface-flask_16_9999-9999_monthly.txt ch4_sis_surface-flask_16_9999-9999_monthly.txt ch4_spo_surface-flask_16_9999-9999_monthly.txt	ALT482N016fz CFA519S016fz* CGO540S016fz CRI215N016fz* CYA766S016fz* ESP449N016fz* MAA767S016fz* MLO519N016fz MQA554S016fz* SIS660N016fz* SPO789S016fz	WMO X2004A	1

DMC	ch4_tll_surface-insitu_17_9999-9999_monthly.txt	TLL330S017iz	WMO X2004	1
ECCC	ch4_alt_surface-insitu_20_9999-9999_monthly.txt ch4_cdl_surface-insitu_20_9999-9999_monthly.txt ch4_chl_surface-insitu_20_9999-9999_monthly.txt ch4_chm_surface-insitu_20_9999-9999_monthly.txt ch4_egb_surface-insitu_20_9999-9999_monthly.txt ch4_esp_surface-insitu_20_9999-9999_monthly.txt ch4_etl_surface-insitu_20_9999-9999_monthly.txt ch4_fsd_surface-insitu_20_9999-9999_monthly.txt ch4_llb_surface-insitu_20_9999-9999_monthly.txt ch4_wsa_surface-insitu_20_9999-9999_monthly.txt	ALT482N020iz CDL453N020iz* CHL458N020iz* CHM449N020iz* EGB444N020iz* ESP449N020iz* ETL454N020iz* FSD449N020iz* LLB454N020iz* WSA443N020iz*	WMO X2004A	1
Empa	ch4_jfj_surface-insitu_23_9999-9999_monthly.txt	JFJ646N023iz*	WMO X2004A	1
ENEA	ch4_lmp_surface-flask_24_9999-9999_monthly.txt	LMP635N024fz*	WMO X2004	1
FMI	ch4_pal_surface-insitu_25_9999-9999_monthly.txt	PAL667N025iz	WMO X2004A	1
GERC	ch4_gsn_surface-insitu_52_9999-9999_monthly.txt	GSN233N052iz*	WMO X2004	1
IAFMS	ch4_cmn_surface-insitu_29_9999-9999_monthly.txt	CMN644N029iz	WMO X2004	1
INSTAAR	ch4_sum_surface-insitu_34_9999-9999_monthly.txt	SUM672N034iz		
ISAC	ch4_lmt_surface-insitu_37_9999-9999_monthly.txt	LMT638N037iz	WMO X2004A	1
	ch4_cgr_surface-insitu_37_9999-9999_monthly.txt ch4_eco_surface-insitu_37_9999-9999_monthly.txt	CGR637N037iz ECO640N037iz		
JMA	ch4_mnm_surface-insitu_1_9999-9999_monthly.txt ch4_ryo_surface-insitu_1_9999-9999_monthly.txt ch4_yon_surface-insitu_1_9999-9999_monthly.txt	MNM224N001iz* RYO239N001iz* YON224N001iz*	WMO X2004A	1
KMA	ch4_amy_surface-insitu_39_9999-9999_monthly.txt	AMY236N039iz*	WMO X2004 WMO X2004A KRISS	1 1
KSNU	ch4_isk_surface-remote_41_9999-9999_monthly.txt	ISK242N041rz		
LSCE	ch4_ams_surface-flask_45_9999-9999_monthly.txt ch4_bgu_surface-flask_45_9999-9999_monthly.txt ch4_lpo_surface-flask_45_9999-9999_monthly.txt ch4_pdm_surface-flask_45_9999-9999_monthly.txt ch4_puy_surface-flask_45_9999-9999_monthly.txt	AMS137S045fz* BGU641N045fz* LPO648N045fz PDM642N045fz PUY645N045fz*	NOAA 1983	1.0124
	ch4_fik_surface-flask_45_9999-9999_monthly.txt ch4_mhd_surface-flask_45_9999-9999_monthly.txt	FIK635N045fz MHD653N045fz		
METRI	ch4_gsn_surface-flask_55_9999-9999_monthly.txt	GSN233N055fz	SIO-97	
MGO	ch4_ter_surface-flask_46_9999-9999_monthly.txt ch4_tik_surface-flask_46_9999-9999_monthly.txt	TER669N046fz* TIK271N046fz*	WMO X2004A	1
MRI	ch4_tkb_surface-insitu_48_9999-9999_monthly.txt	TKB236N048iz*	MRI	0.9973
NIES	ch4_coi_surface-insitu_53_9999-9999_monthly.txt ch4_hat_surface-insitu_53_9999-9999_monthly.txt	COI243N053iz* HAT224N053iz*	NIES	0.9973
NOAA	ch4_abp_surface-flask_2_3001-9999_monthly.txt ch4_alt_surface-flask_2_3001-9999_monthly.txt ch4_ams_surface-flask_2_3001-9999_monthly.txt ch4_amy_surface-flask_2_3001-9999_monthly.txt ch4_asc_surface-flask_2_3001-9999_monthly.txt ch4_ask_surface-flask_2_3001-9999_monthly.txt ch4_avi_surface-flask_2_3001-9999_monthly.txt ch4_azr_surface-flask_2_3001-9999_monthly.txt ch4_bal_surface-flask_2_3001-9999_monthly.txt ch4_bhd_surface-flask_2_3001-9999_monthly.txt ch4_bkt_surface-flask_2_3001-9999_monthly.txt ch4_bme_surface-flask_2_3001-9999_monthly.txt ch4_bmw_surface-flask_2_3001-9999_monthly.txt	ABP312S002f1* ALT482N002f1* AMS137S002f1* AMY236N002f1 ASC107S002f1* ASK123N002f1* AVI417N002f1* AZR638N002f1* BAL655N002f1* BHD541S002f1* BKT500S002f1 BME432N002f1* BMW432N002f1*	WMO X2004A	1

ch4_brw_surface-flask_2_3001-9999_monthly.txt	BRW471N002f1*
ch4_brw_surface-insitu_2_3001-9999_monthly.txt	BRW471N002i1*
ch4_bsc_surface-flask_2_3001-9999_monthly.txt	BSC644N002f1
ch4_cba_surface-flask_2_3001-9999_monthly.txt	CBA455N002f1*
ch4_cgo_surface-flask_2_3001-9999_monthly.txt	CGO540S002f1*
ch4_chr_surface-flask_2_3001-9999_monthly.txt	CHR501N002f1*
ch4_cmo_surface-flask_2_3001-9999_monthly.txt	CMO445N002f1*
ch4_cpt_surface-flask_2_3001-9999_monthly.txt	CPT134S002f1
ch4_crz_surface-flask_2_3001-9999_monthly.txt	CRZ146S002f1*
ch4_drp_ship-flask_2_3001-9999_monthly.txt	DRP859S002f1*
ch4_eic_surface-flask_2_3001-9999_monthly.txt	EIC327S002f1*
ch4_gmi_surface-flask_2_3001-9999_monthly.txt	GMI513N002f1*
ch4_goz_surface-flask_2_3001-9999_monthly.txt	GOZ636N002f1*
ch4_hba_surface-flask_2_3001-9999_monthly.txt	HBA775S002f1*
ch4_hpb_surface-flask_2_3001-9999_monthly.txt	HPB647N002f1*
ch4_hun_surface-flask_2_3001-9999_monthly.txt	HUN646N002f1*
ch4_ice_surface-flask_2_3001-9999_monthly.txt	ICE663N002f1*
ch4_itn_surface-flask_2_3001-9999_monthly.txt	ITN435N002f1*
ch4_izo_surface-flask_2_3001-9999_monthly.txt	IZO128N002f1*
ch4_key_surface-flask_2_3001-9999_monthly.txt	KEY425N002f1*
ch4_kum_surface-flask_2_3001-9999_monthly.txt	KUM519N002f1*
ch4_kzd_surface-flask_2_3001-9999_monthly.txt	KZD244N002f1*
ch4_kzm_surface-flask_2_3001-9999_monthly.txt	KZM243N002f1*
ch4_lef_surface-flask_2_3001-9999_monthly.txt	LEF445N002f1*
ch4_llb_surface-flask_2_3001-9999_monthly.txt	LLB454N002f1
ch4_lln_surface-flask_2_3001-9999_monthly.txt	LLN223N002f1*
ch4_lmp_surface-flask_2_3001-9999_monthly.txt	LMP635N002f1*
ch4_mbc_surface-flask_2_3001-9999_monthly.txt	MBC476N002f1*
ch4_mex_surface-flask_2_3001-9999_monthly.txt	MEX418N002f1*
ch4_mhd_surface-flask_2_3001-9999_monthly.txt	MHD653N002f1*
ch4_mid_surface-flask_2_3001-9999_monthly.txt	MID528N002f1*
ch4_mkn_surface-flask_2_3001-9999_monthly.txt	MKN100S002f1*
ch4_mlo_surface-flask_2_3001-9999_monthly.txt	MLO519N002f1*
ch4_mlo_surface-insitu_2_3001-9999_monthly.txt	MLO519N002i1*
ch4_nat_surface-flask_2_3001-9999_monthly.txt	NAT306S002f1*
ch4_nmb_surface-flask_2_3001-9999_monthly.txt	NMB123S002f1*
ch4_nwr_surface-flask_2_3001-9999_monthly.txt	NWR440N002f1*
ch4_opw_surface-flask_2_3001-9999_monthly.txt	OPW448N002f1*
ch4_oxk_surface-flask_2_3001-9999_monthly.txt	OXK650N002f1*
ch4_pal_surface-flask_2_3001-9999_monthly.txt	PAL667N002f1*
ch4_poc_ship-flask_2_3001-3001_monthly.txt	POC800N002f1*
ch4_poc_ship-flask_2_3001-3002_monthly.txt	POC805N002f1*
ch4_poc_ship-flask_2_3001-3003_monthly.txt	POC810N002f1*
ch4_poc_ship-flask_2_3001-3004_monthly.txt	POC815N002f1*
ch4_poc_ship-flask_2_3001-3005_monthly.txt	POC820N002f1*
ch4_poc_ship-flask_2_3001-3006_monthly.txt	POC825N002f1*
ch4_poc_ship-flask_2_3001-3007_monthly.txt	POC830N002f1*
ch4_poc_ship-flask_2_3001-3012_monthly.txt	POC805S002f1*
ch4_poc_ship-flask_2_3001-3013_monthly.txt	POC810S002f1*
ch4_poc_ship-flask_2_3001-3014_monthly.txt	POC815S002f1*
ch4_poc_ship-flask_2_3001-3015_monthly.txt	POC820S002f1*
ch4_poc_ship-flask_2_3001-3016_monthly.txt	POC825S002f1*
ch4_poc_ship-flask_2_3001-3017_monthly.txt	POC830S002f1*
ch4_poc_ship-flask_2_3001-3018_monthly.txt	POC835S002f1*
ch4_psa_surface-flask_2_3001-9999_monthly.txt	PSA764S002f1*
ch4_pta_surface-flask_2_3001-9999_monthly.txt	PTA438N002f1*

	ch4_rpb_surface-flask_2_3001-9999_monthly.txt ch4_scs_ship-flask_2_3001-3101_monthly.txt ch4_scs_ship-flask_2_3001-3102_monthly.txt ch4_scs_ship-flask_2_3001-3103_monthly.txt ch4_scs_ship-flask_2_3001-3104_monthly.txt ch4_scs_ship-flask_2_3001-3105_monthly.txt ch4_scs_ship-flask_2_3001-3106_monthly.txt ch4_scs_ship-flask_2_3001-3107_monthly.txt ch4_sdz_surface-flask_2_3001-9999_monthly.txt ch4_sey_surface-flask_2_3001-9999_monthly.txt ch4_sgp_surface-flask_2_3001-9999_monthly.txt ch4_shm_surface-flask_2_3001-9999_monthly.txt ch4_smo_surface-flask_2_3001-9999_monthly.txt ch4_spo_surface-flask_2_3001-9999_monthly.txt ch4_stm_surface-flask_2_3001-9999_monthly.txt ch4_sum_surface-flask_2_3001-9999_monthly.txt ch4_syo_surface-flask_2_3001-9999_monthly.txt ch4_tap_surface-flask_2_3001-9999_monthly.txt ch4_thd_surface-flask_2_3001-9999_monthly.txt ch4_tik_surface-flask_2_3001-9999_monthly.txt ch4_ush_surface-flask_2_3001-9999_monthly.txt ch4_uta_surface-flask_2_3001-9999_monthly.txt ch4_uum_surface-flask_2_3001-9999_monthly.txt ch4_wis_surface-flask_2_3001-9999_monthly.txt ch4_wkt_surface-flask_2_3001-9999_monthly.txt ch4_wlg_surface-flask_2_3001-9999_monthly.txt ch4_zep_surface-flask_2_3001-9999_monthly.txt	RPB413N002f1* SCS803N002f1* SCS806N002f1* SCS809N002f1* SCS812N002f1* SCS815N002f1* SCS818N002f1* SCS821N002f1* SDZ240N002f1* SEY104S002f1* SGP436N002f1* SHM452N002f1* SMO514S002f1* SPO789S002f1* STM666N002f1* SUM672N002f1* SYO769S002f1* TAP236N002f1* THD441N002f1 TIK271N002f1* USH354S002f1* UTA439N002f1* UUM244N002f1* WIS631N002f1* WKT431N002f1* WLG236N002f1* ZEP678N002f1*		
RIVM	ch4_kmw_surface-insitu_63_9999-9999_monthly.txt	KMW653N063iz	NIST	0.9973
RSE	ch4_prs_surface-insitu_64_9999-9999_monthly.txt	PRS645N064iz*	WMO X2004	1
SAWS	ch4_cpt_surface-insitu_66_9999-1001_monthly.txt	CPT134S066iz*	WMO X2004 WMO X2004A	1 1
UBAA	ch4_snb_surface-insitu_72_9999-9999_monthly.txt	SNB647N072iz*	WMO X2004	1
UBAG	ch4_deu_surface-insitu_71_9999-9999_monthly.txt ch4_ngl_surface-insitu_71_9999-9999_monthly.txt ch4_ssl_surface-insitu_71_9999-9999_monthly.txt ch4_zgt_surface-insitu_71_9999-9999_monthly.txt ch4_zsf_surface-insitu_71_9999-9999_monthly.txt ch4 zug_surface-insitu_71_9999-9999_monthly.txt	DEU649N071iz* NGL653N071iz* SSL647N071iz* ZGT654N071iz* ZSF647N071iz* ZUG647N071iz*	WMO X2004	1
UMLT	ch4_glh_surface-insitu_75_9999-9999_monthly.txt	GLH636N075iz		
UNIURB	ch4_cmn_surface-insitu_74_9999-9999_monthly.txt	CMN644N074iz*	WMO X2004A	1
VNMHA	ch4_pdi_surface-insitu_51_9999-9999_monthly.txt	PDI221N051iz	WMO X2004	1

* Stations with an asterisk are used for the calculation of the global mean mole fractions and related quantities. The site selection procedure is described in Appendix A.

4. Nitrous Oxide (N_2O)

The Halocarbons and other Atmospheric Trace Species (HATS) Group of NOAA/ESRL maintains a set of standards for N_2O (Hall *et al.*, 2001) and serves as a CCL for N_2O . The WMO X2006 scale (Hall *et al.*, 2007), revised and updated to WMO X2006A in 2011 to deal with drifting in secondary standards, has been designated as the Primary scale for the GAW Programme. CCL compares its standards with the ones of other laboratories, including those of ECCC and the Australian Commonwealth Scientific and Industrial Research

Organisation (CSIRO). Karlsruhe Institute of Technology, Institute for Meteorology and Climate Research (KIT/IMK-IFU), Germany, serves as the GAW WCC for N_2O .

The SIO-98 scale is approximately equivalent to the WMO X2006 scale, with an average difference of 0.01% over the range of 299–319 ppb. SIO-16 scale can be converted to WMO X2006A via multiplication by a factor of 0.9983 (Prinn *et al.*, 2018). The WMO X2000 scale can be converted to the WMO X2006 scale by using the factor

0.999402 (Hall *et al.*, 2007).

Table B5. Status of the standard scales of N₂O with conversion factors.

Organization	WDCGG Filename	Filename Code in Plate 3.1	Calibration Scale	Conversion Factor
AEMET	n2o_izo_surface-insitu_3_9999-9999_monthly.txt	IZO128N003iz*	WMO X2006A	1
AGAGE	n2o_cgo_surface-insitu_4_2021-2021_monthly.txt n2o_mhd_surface-insitu_4_2021-2021_monthly.txt n2o_rpb_surface-insitu_4_2021-2021_monthly.txt n2o_smo_surface-insitu_4_2021-2021_monthly.txt n2o_thd_surface-insitu_4_2021-2021_monthly.txt	CGO540S004ic* MHD653N004ic* RPB413N004ic* SMO514S004ic* THD441N004ic*	SIO-16	0.9983
	n2o_adr_surface-insitu_4_2001-2004_monthly.txt n2o_cgo_surface-insitu_4_2001-2004_monthly.txt n2o_cgo_surface-insitu_4_2011-2015_monthly.txt n2o_cmo_surface-insitu_4_2001-2004_monthly.txt n2o_cmo_surface-insitu_4_2011-2015_monthly.txt n2o_mhd_surface-insitu_4_2011-2015_monthly.txt n2o_rpb_surface-insitu_4_2001-2004_monthly.txt n2o_rpb_surface-insitu_4_2011-2015_monthly.txt n2o_smo_surface-insitu_4_2001-2004_monthly.txt n2o_smo_surface-insitu_4_2011-2015_monthly.txt	ADR651N004ia* CGO540S004ia* CGO540S004ib* CMO445N004ia* CMO445N004ib* MHD653N004ib* RPB413N004ia* RPB413N004ib* SMO514S004ia* SMO514S004ib*		
CSIRO	n2o_alt_surface-flask_16_9999-9999_monthly.txt n2o_cfa_surface-flask_16_9999-9999_monthly.txt n2o_cgo_surface-flask_16_9999-9999_monthly.txt n2o_cri_surface-flask_16_9999-9999_monthly.txt n2o_cya_surface-flask_16_9999-9999_monthly.txt n2o_esp_surface-flask_16_9999-9999_monthly.txt n2o_maa_surface-flask_16_9999-9999_monthly.txt n2o_mlo_surface-flask_16_9999-9999_monthly.txt n2o_mqa_surface-flask_16_9999-9999_monthly.txt n2o_sis_surface-flask_16_9999-9999_monthly.txt n2o_spo_surface-flask_16_9999-9999_monthly.txt	ALT482N016fz* CFA519S016fz* CGO540S016fz CRI215N016fz* CYA766S016fz* ESP449N016fz* MAA767S016fz* MLO519N016fz* MQA554S016fz* SIS660N016fz* SPO789S016fz	WMO X2006A	1
	n2o_jfj_surface-insitu_23_9999-9999_monthly.txt	JFJ646N023iz*		
Empa	n2o_jfj_surface-insitu_23_9999-9999_monthly.txt	JFJ646N023iz*	WMO X2006A SIO-98	1 1
ENEA	n2o_lmp_surface-flask_24_9999-9999_monthly.txt	LMP635N024fz	WMO X2006	1
GERC	n2o_gsn_surface-insitu_52_9999-9999_monthly.txt	GSN233N052iz	WMO X2006	1
JMA	n2o_ryo_surface-insitu_1_9999-9999_monthly.txt	RYO239N001iz*	WMO X2006A	1
KMA	n2o_amy_surface-insitu_39_9999-9999_monthly.txt	AMY236N039iz*	WMO X2006 KRISS	1
METRI	n2o_gsn_surface-flask_55_9999-9999_monthly.txt	GSN233N055fz	WMO X1997	
MRI	n2o_mmb_surface-insitu_48_9999-9999_monthly.txt	MMB243N048iz		
NAGOU	n2o_ngy_surface-insitu_49_9999-9999_monthly.txt	NGY235N049iz		
NIES	n2o_coi_surface-insitu_53_9999-9999_monthly.txt n2o_hat_surface-insitu_53_9999-9999_monthly.txt	COI243N053iz* HAT224N053iz*	NIES 96**	1
NILU	n2o_zep_surface-insitu_54_9999-9999_monthly.txt	ZEP678N054iz		
NOAA	n2o_brw_surface-insitu_2_3003-9999_monthly.txt n2o_mlo_surface-insitu_2_3003-9999_monthly.txt n2o_nwr_surface-insitu_2_3003-9999_monthly.txt n2o_smo_surface-insitu_2_3003-9999_monthly.txt n2o_spo_surface-insitu_2_3003-9999_monthly.txt	BRW471N002i3* MLO519N002i3* NWR440N002i3* SMO514S002i3* SPO789S002i3*	WMO X2006	1
	n2o_abp_surface-flask_2_3001-9999_monthly.txt n2o_alt_surface-flask_2_3001-9999_monthly.txt	ABP312S002f1* ALT482N002f1		
			WMO X2006A	1

n2o_alt_surface-flask_2_3004-9999_monthly.txt	ALT482N002f4*
n2o_alt_surface-flask_2_3005-9999_monthly.txt	ALT482N002f5
n2o_amy_surface-flask_2_3001-9999_monthly.txt	AMY236N002f1
n2o_asc_surface-flask_2_3001-9999_monthly.txt	ASC107S002f1*
n2o_ask_surface-flask_2_3001-9999_monthly.txt	ASK123N002f1*
n2o_azr_surface-flask_2_3001-9999_monthly.txt	AZR638N002f1*
n2o_bal_surface-flask_2_3001-9999_monthly.txt	BAL655N002f1*
n2o_bhd_surface-flask_2_3001-9999_monthly.txt	BHD541S002f1*
n2o_bkt_surface-flask_2_3001-9999_monthly.txt	BKT500S002f1*
n2o_bme_surface-flask_2_3001-9999_monthly.txt	BME432N002f1*
n2o_bmw_surface-flask_2_3001-9999_monthly.txt	BMW432N002f1*
n2o_brw_surface-flask_2_3001-9999_monthly.txt	BRW471N002f1
n2o_brw_surface-flask_2_3004-9999_monthly.txt	BRW471N002f4*
n2o_brw_surface-flask_2_3005-9999_monthly.txt	BRW471N002f5
n2o_brw_surface-insitu_2_3002-9999_monthly.txt	BRW471N002i2*
n2o_bsc_surface-flask_2_3001-9999_monthly.txt	BSC644N002f1*
n2o_cba_surface-flask_2_3001-9999_monthly.txt	CBA455N002f1*
n2o_cgo_surface-flask_2_3001-9999_monthly.txt	CGO540S002f1*
n2o_cgo_surface-flask_2_3004-9999_monthly.txt	CGO540S002f4
n2o_cgo_surface-flask_2_3005-9999_monthly.txt	CGO540S002f5
n2o_chr_surface-flask_2_3001-9999_monthly.txt	CHR501N002f1*
n2o_cpt_surface-flask_2_3001-9999_monthly.txt	CPT134S002f1*
n2o_crz_surface-flask_2_3001-9999_monthly.txt	CRZ146S002f1*
n2o_drp_ship-flask_2_3001-9999_monthly.txt	DRP859S002f1*
n2o_eic_surface-flask_2_3001-9999_monthly.txt	EIC327S002f1*
n2o_gmi_surface-flask_2_3001-9999_monthly.txt	GMI513N002f1*
n2o_hba_surface-flask_2_3001-9999_monthly.txt	HBA775S002f1*
n2o_hfm_surface-flask_2_3005-9999_monthly.txt	HFM442N002f5*
n2o_hpb_surface-flask_2_3001-9999_monthly.txt	HPB647N002f1*
n2o_hun_surface-flask_2_3001-9999_monthly.txt	HUN646N002f1*
n2o_ice_surface-flask_2_3001-9999_monthly.txt	ICE663N002f1*
n2o_itn_surface-flask_2_3001-9999_monthly.txt	ITN435N002f1
n2o_itn_surface-flask_2_3005-9999_monthly.txt	ITN435N002f5*
n2o_izo_surface-flask_2_3001-9999_monthly.txt	IZO128N002f1*
n2o_key_surface-flask_2_3001-9999_monthly.txt	KEY425N002f1*
n2o_kum_surface-flask_2_3001-9999_monthly.txt	KUM519N002f1*
n2o_kum_surface-flask_2_3005-9999_monthly.txt	KUM519N002f5*
n2o_kzd_surface-flask_2_3001-9999_monthly.txt	KZD244N002f1*
n2o_kzm_surface-flask_2_3001-9999_monthly.txt	KZM243N002f1*
n2o_lef_surface-flask_2_3001-9999_monthly.txt	LEF445N002f1*
n2o_lef_surface-flask_2_3005-9999_monthly.txt	LEF445N002f5*
n2o_llb_surface-flask_2_3001-9999_monthly.txt	LLB454N002f1*
n2o_lln_surface-flask_2_3001-9999_monthly.txt	LLN223N002f1*
n2o_lmp_surface-flask_2_3001-9999_monthly.txt	LMP635N002f1*
n2o_mex_surface-flask_2_3001-9999_monthly.txt	MEX418N002f1*
n2o_mhd_surface-flask_2_3001-9999_monthly.txt	MHD653N002f1*
n2o_mhd_surface-flask_2_3005-9999_monthly.txt	MHD653N002f5
n2o_mid_surface-flask_2_3001-9999_monthly.txt	MID528N002f1*
n2o_mkn_surface-flask_2_3001-9999_monthly.txt	MKN100S002f1*
n2o_mlo_surface-flask_2_3001-9999_monthly.txt	MLO519N002f1
n2o_mlo_surface-flask_2_3004-9999_monthly.txt	MLO519N002f4*
n2o_mlo_surface-flask_2_3005-9999_monthly.txt	MLO519N002f5
n2o_mlo_surface-insitu_2_3002-9999_monthly.txt	MLO519N002i2*
n2o_nat_surface-flask_2_3001-9999_monthly.txt	NAT306S002f1*
n2o_nmb_surface-flask_2_3001-9999_monthly.txt	NMB123S002f1*
n2o_nwr_surface-flask_2_3001-9999_monthly.txt	NWR440N002f1*

	n2o_nwr_surface-flask_2_3004-9999_monthly.txt n2o_nwr_surface-flask_2_3005-9999_monthly.txt n2o_nwr_surface-insitu_2_3002-9999_monthly.txt n2o_oxk_surface-flask_2_3001-9999_monthly.txt n2o_pal_surface-flask_2_3001-9999_monthly.txt n2o_poc_ship-flask_2_3001-3001_monthly.txt n2o_poc_ship-flask_2_3001-3002_monthly.txt n2o_poc_ship-flask_2_3001-3003_monthly.txt n2o_poc_ship-flask_2_3001-3004_monthly.txt n2o_poc_ship-flask_2_3001-3005_monthly.txt n2o_poc_ship-flask_2_3001-3006_monthly.txt n2o_poc_ship-flask_2_3001-3007_monthly.txt n2o_poc_ship-flask_2_3001-3012_monthly.txt n2o_poc_ship-flask_2_3001-3013_monthly.txt n2o_poc_ship-flask_2_3001-3014_monthly.txt n2o_poc_ship-flask_2_3001-3015_monthly.txt n2o_poc_ship-flask_2_3001-3016_monthly.txt n2o_poc_ship-flask_2_3001-3017_monthly.txt n2o_psa_surface-flask_2_3001-9999_monthly.txt n2o_psa_surface-flask_2_3005-9999_monthly.txt n2o_pta_surface-flask_2_3001-9999_monthly.txt n2o_rpb_surface-flask_2_3001-9999_monthly.txt n2o_sdz_surface-flask_2_3001-9999_monthly.txt n2o_sey_surface-flask_2_3001-9999_monthly.txt n2o_sgp_surface-flask_2_3001-9999_monthly.txt n2o_shm_surface-flask_2_3001-9999_monthly.txt n2o_smo_surface-flask_2_3001-9999_monthly.txt n2o_smo_surface-flask_2_3004-9999_monthly.txt n2o_smo_surface-flask_2_3005-9999_monthly.txt n2o_smo_surface-insitu_2_3002-9999_monthly.txt n2o_spo_surface-flask_2_3001-9999_monthly.txt n2o_spo_surface-flask_2_3004-9999_monthly.txt n2o_spo_surface-flask_2_3005-9999_monthly.txt n2o_spo_surface-insitu_2_3002-9999_monthly.txt n2o_stm_surface-flask_2_3001-9999_monthly.txt n2o_sum_surface-flask_2_3001-9999_monthly.txt n2o_sum_surface-flask_2_3005-9999_monthly.txt n2o_sum_surface-insitu_2_3002-9999_monthly.txt n2o_syo_surface-flask_2_3001-9999_monthly.txt n2o_tap_surface-flask_2_3001-9999_monthly.txt n2o_thd_surface-flask_2_3001-9999_monthly.txt n2o_thd_surface-flask_2_3005-9999_monthly.txt n2o_tik_surface-flask_2_3001-9999_monthly.txt n2o_ush_surface-flask_2_3001-9999_monthly.txt n2o_ush_surface-flask_2_3005-9999_monthly.txt n2o_uta_surface-flask_2_3001-9999_monthly.txt n2o_uum_surface-flask_2_3001-9999_monthly.txt n2o_wis_surface-flask_2_3001-9999_monthly.txt n2o_wkt_surface-flask_2_3001-9999_monthly.txt n2o_wlg_surface-flask_2_3001-9999_monthly.txt n2o_zep_surface-flask_2_3001-9999_monthly.txt	NWR440N002f4* NWR440N002f5 NWR440N002i2 OXK650N002f1* PAL667N002f1* POC800N002f1* POC805N002f1* POC810N002f1* POC815N002f1* POC820N002f1* POC825N002f1* POC830N002f1* POC805S002f1* POC810S002f1* POC815S002f1* POC820S002f1* POC825S002f1* POC830S002f1* PSA764S002f1* PSA764S002f5 PTA438N002f1* RPB413N002f1* SDZ240N002f1* SEY104S002f1* SGP436N002f1* SHM452N002f1* SMO514S002f1* SMO514S002f4* SMO514S002f5 SMO514S002i2 SPO789S002f1 SPO789S002f4* SPO789S002f5 SPO789S002i2* STM666N002f1* SUM672N002f1* SUM672N002f5 SUM672N002i2 SYO769S002f1* TAP236N002f1* THD441N002f1* THD441N002f5 TIK271N002f1* USH354S002f1* USH354S002f5 UTA439N002f1* UUM244N002f1* WIS631N002f1* WKT431N002f1* WLG236N002f1* ZEP678N002f1*		
SAWS	n2o_cpt_surface-insitu_66_9999-1001_monthly.txt	CPT134S066iz*	NOAA	0.999402
UBAG	n2o_zsf_surface-insitu_71_9999-9999_monthly.txt	ZSF647N071iz*	WMO X2006A	1
	n2o_ssl_surface-insitu_71_9999-9999_monthly.txt	SSL647N071iz	SIO-98	1
UNIURB	n2o_cmn_surface-insitu_74_9999-9999_monthly.txt	CMN644N074iz*	WMO X2006A	1

* Stations with an asterisk are used for the calculation of the global mean mole fractions and related quantities. The site selection procedure is described in Appendix A.

** NIES 96 N₂O scale is approximately 0.7 ppb lower than that of WMO X2006A in the range 325 to 326 ppb.
http://www.esrl.noaa.gov/gmd/ccgg/wmorr/wmorr_results.php?rr=rr6¶m=n2o

5. Carbon Monoxide (CO)

NOAA/ESRL is the WMO/GAW CCL for carbon monoxide. Due to lack of stability of CO in high pressure cylinders, the CO scale has historically been defined by repeated sets of gravimetric standards made in 1996/1997, 1999/2000, 2006 and 2011. The CCL make revisions in the CO scale whenever new gravimetric standard sets indicate a significant drift in the scale. Scale revisions are indicated with date codes (WMO X2000, WMO X2004, WMO X2014) with the most recent made in December 2015 being WMO X2014A (WMO, 2018b).

Empa serves as the WCC under GAW based on its secondary standards calibrated against the standard at NOAA/ESRL designated as the Primary Standard for GAW. Empa, as WCC for CO, has developed an audit system for CO measurements at GAW stations.

A small fraction of the data is reported in units of $\mu\text{g}/\text{m}^3$ or mg/m^3 . In WDCGG analysis, these units are converted

to ppb using the following formulas:

$$X_p [\text{ppb}] = (R \times T / M / P_0) \times 10 \times X_g [\mu\text{g}/\text{m}^3]$$

and

$$X_p [\text{ppb}] = (R \times T / M / P_0) \times 10^4 \times X_g [\text{mg}/\text{m}^3],$$

where

R is the molar gas constant (8.31451 [J/K/mol]),

T is the reported temperature for conversion (293.15 [K] or 298.15 [K]),

M is the molecular weight of CO (28.0101) and

P_0 is the standard pressure (1013.25 [hPa]).

It is highly desirable to report CO concentration data in mole fractions (mostly in ppb) traceable to the WMO Mole Fraction Scale.

Table B6. Status of CO standard scales.

Organization	WDCGG Filename	Filename Code in Plate 5.1	Calibration Scale / Units except for using ppb	Audit Empa-WCC
AEMET	co_izo_surface-insitu_3_9999-9999_monthly.txt	IZO128N003iz	WMO X2014A	00, 04, 09, 13
AGAGE	co_cgo_surface-insitu_4_2021-2021_monthly.txt co_mhd_surface-insitu_4_2021-2021_monthly.txt	CGO540S004ic MHD653N004ic*	CSIRO-94	
ARSO	co_kvv_surface-insitu_8_9999-9999_monthly.txt	KVV646N008iz*		
BAS	co_hba_surface-insitu_9_9999-9999_monthly.txt	HBA775S009iz	WMO X2014A	
BMKG	co_bkt_surface-insitu_10_9999-9999_monthly.txt	BKT500S010iz	WMO X2000	01, 04, 07, 08, 11, 14, 19
CHMI	co_kos_surface-insitu_12_9999-9999_monthly.txt	KOS649N012iz	$\mu\text{g}/\text{m}^3$ -20°C	
CSIRO	co_alt_surface-flask_16_9999-9999_monthly.txt co_cfa_surface-flask_16_9999-9999_monthly.txt co_cgo_surface-flask_16_9999-9999_monthly.txt co_cri_surface-flask_16_9999-9999_monthly.txt co_cya_surface-flask_16_9999-9999_monthly.txt co_esp_surface-flask_16_9999-9999_monthly.txt co_maa_surface-flask_16_9999-9999_monthly.txt co_mlo_surface-flask_16_9999-9999_monthly.txt co_mqa_surface-flask_16_9999-9999_monthly.txt co_sis_surface-flask_16_9999-9999_monthly.txt co_spo_surface-flask_16_9999-9999_monthly.txt	ALT482N016fz* CFA519S016fz* CGO540S016fz* CRI215N016fz* CYA766S016fz* ESP449N016fz* MAA767S016fz* MLO519N016fz MQA554S016fz* SIS660N016fz* SPO789S016fz*	CSIRO-94	Cape Grim: 02, 16
DMC	co_tll_surface-insitu_17_9999-9999_monthly.txt	TLL330S017iz	WMO X2004	
DWD	co_hpib_surface-insitu_19_9999-9999_monthly.txt	HPB647N019iz*	WMO X2004	97, 06, 11

ECCC	co_alt_surface-insitu_20_9999-9999_monthly.txt co_cdl_surface-insitu_20_9999-9999_monthly.txt co_chl_surface-insitu_20_9999-9999_monthly.txt co_chm_surface-insitu_20_9999-9999_monthly.txt co_egb_surface-insitu_20_9999-9999_monthly.txt co_esp_surface-insitu_20_9999-9999_monthly.txt co_etl_surface-insitu_20_9999-9999_monthly.txt co_fsd_surface-insitu_20_9999-9999_monthly.txt co_llb_surface-insitu_20_9999-9999_monthly.txt co_wsa_surface-insitu_20_9999-9999_monthly.txt	ALT482N020iz CDL453N020iz* CHL458N020iz CHM449N020iz* EGB444N020iz* ESP449N020iz* ETL454N020iz* FSD449N020iz* LLB454N020iz* WSA443N020iz*	WMO X2014A	Alert: 04
Empa	co_jfj_surface-insitu_23_9999-9999_monthly.txt	JFJ646N023iz*	WMO	99, 06, 15
	co_pay_surface-insitu_23_9999-9999_monthly.txt co_rig_surface-insitu_23_9999-9999_monthly.txt	PAY646N023iz* RIG647N023iz*	NPL	
INRNE	co_beo_surface-insitu_33_9999-9999_monthly.txt	BEO642N033iz*		
ISAC	co_cmn_surface-insitu_37_9999-9999_monthly.txt	CMN644N037iz*	WMO X2004 WMO X2014A	12, 18
	co_lmt_surface-insitu_37_9999-9999_monthly.txt	LMT638N037iz*	WMO X2014A	
	co_cgr_surface-insitu_37_9999-9999_monthly.txt co_eco_surface-insitu_37_9999-9999_monthly.txt	CGR637N037iz* ECO640N037iz*		
JMA	co_mnm_surface-insitu_1_9999-9999_monthly.txt co_ryo_surface-insitu_1_9999-9999_monthly.txt co_yon_surface-insitu_1_9999-9999_monthly.txt	MNM224N001iz* RYO239N001iz* YON224N001iz*	WMO X2014A	
KMD	co_mkn_surface-insitu_40_9999-9999_monthly.txt	MKN100S040iz*	WMO X2000	05, 06, 08, 10, 15
LA	co_pdm_surface-insitu_43_9999-9999_monthly.txt	PDM642N043iz		
LAMP	co_puy_surface-insitu_44_9999-9999_monthly.txt	PUY645N044iz		16
LSCE	co_ams_surface-insitu_45_9999-9999_monthly.txt	AMS137S045iz		08
NOAA	co_abp_surface-flask_2_3001-9999_monthly.txt co_alt_surface-flask_2_3001-9999_monthly.txt co_amy_surface-flask_2_3001-9999_monthly.txt co_asc_surface-flask_2_3001-9999_monthly.txt co_ask_surface-flask_2_3001-9999_monthly.txt co_azr_surface-flask_2_3001-9999_monthly.txt co_bal_surface-flask_2_3001-9999_monthly.txt co_bhd_surface-flask_2_3001-9999_monthly.txt co_bkt_surface-flask_2_3001-9999_monthly.txt co_bme_surface-flask_2_3001-9999_monthly.txt co_bmw_surface-flask_2_3001-9999_monthly.txt co_brw_surface-flask_2_3001-9999_monthly.txt co_bsc_surface-flask_2_3001-9999_monthly.txt co_cba_surface-flask_2_3001-9999_monthly.txt co_cgo_surface-flask_2_3001-9999_monthly.txt co_chr_surface-flask_2_3001-9999_monthly.txt co_cmo_surface-flask_2_3001-9999_monthly.txt co_cpt_surface-flask_2_3001-9999_monthly.txt co_crz_surface-flask_2_3001-9999_monthly.txt co_drp_ship-flask_2_3001-9999_monthly.txt co_eic_surface-flask_2_3001-9999_monthly.txt co_gmi_surface-flask_2_3001-9999_monthly.txt co_goz_surface-flask_2_3001-9999_monthly.txt co_hba_surface-flask_2_3001-9999_monthly.txt co_hpb_surface-flask_2_3001-9999_monthly.txt	ABP312S002f1* ALT482N002f1* AMY236N002f1* ASC107S002f1* ASK123N002f1* AZR638N002f1* BAL655N002f1* BHD541S002f1* BKT500S002f1* BME432N002f1* BMW432N002f1* BRW471N002f1* BSC644N002f1* CBA455N002f1* CGO540S002f1 CHR501N002f1* CMO445N002f1* CPT134S002f1 CRZ146S002f1* DRP859S002f1* EIC327S002f1* GMI513N002f1* GOZ636N002f1* HBA775S002f1* HPB647N002f1*	WMO X2014A	

co_hun_surface-flask_2_3001-9999_monthly.txt	HUN646N002f1*
co_ice_surface-flask_2_3001-9999_monthly.txt	ICE663N002f1*
co_itn_surface-flask_2_3001-9999_monthly.txt	ITN435N002f1*
co_izo_surface-flask_2_3001-9999_monthly.txt	IZO128N002f1*
co_key_surface-flask_2_3001-9999_monthly.txt	KEY425N002f1*
co_kum_surface-flask_2_3001-9999_monthly.txt	KUM519N002f1*
co_kzd_surface-flask_2_3001-9999_monthly.txt	KZD244N002f1*
co_kzm_surface-flask_2_3001-9999_monthly.txt	KZM243N002f1*
co_lef_surface-flask_2_3001-9999_monthly.txt	LEF445N002f1*
co_llb_surface-flask_2_3001-9999_monthly.txt	LLB454N002f1
co_lln_surface-flask_2_3001-9999_monthly.txt	LLN223N002f1*
co_lmp_surface-flask_2_3001-9999_monthly.txt	LMP635N002f1*
co_mbc_surface-flask_2_3001-9999_monthly.txt	MBC476N002f1*
co_mex_surface-flask_2_3001-9999_monthly.txt	MEX418N002f1*
co_mhd_surface-flask_2_3001-9999_monthly.txt	MHD653N002f1*
co_mid_surface-flask_2_3001-9999_monthly.txt	MID528N002f1*
co_mkn_surface-flask_2_3001-9999_monthly.txt	MKN100S002f1*
co_mlo_surface-flask_2_3001-9999_monthly.txt	MLO519N002f1*
co_nat_surface-flask_2_3001-9999_monthly.txt	NAT306S002f1*
co_nmb_surface-flask_2_3001-9999_monthly.txt	NMB123S002f1*
co_nwr_surface-flask_2_3001-9999_monthly.txt	NWR440N002f1*
co_oxk_surface-flask_2_3001-9999_monthly.txt	OXK650N002f1*
co_pal_surface-flask_2_3001-9999_monthly.txt	PAL667N002f1*
co_poc_ship-flask_2_3001-3001_monthly.txt	POC800N002f1*
co_poc_ship-flask_2_3001-3002_monthly.txt	POC805N002f1*
co_poc_ship-flask_2_3001-3003_monthly.txt	POC810N002f1*
co_poc_ship-flask_2_3001-3004_monthly.txt	POC815N002f1*
co_poc_ship-flask_2_3001-3005_monthly.txt	POC820N002f1*
co_poc_ship-flask_2_3001-3006_monthly.txt	POC825N002f1*
co_poc_ship-flask_2_3001-3007_monthly.txt	POC830N002f1*
co_poc_ship-flask_2_3001-3012_monthly.txt	POC805S002f1*
co_poc_ship-flask_2_3001-3013_monthly.txt	POC810S002f1*
co_poc_ship-flask_2_3001-3014_monthly.txt	POC815S002f1*
co_poc_ship-flask_2_3001-3015_monthly.txt	POC820S002f1*
co_poc_ship-flask_2_3001-3016_monthly.txt	POC825S002f1*
co_poc_ship-flask_2_3001-3017_monthly.txt	POC830S002f1*
co_psa_surface-flask_2_3001-9999_monthly.txt	PSA764S002f1*
co_pta_surface-flask_2_3001-9999_monthly.txt	PTA438N002f1*
co_rpb_surface-flask_2_3001-9999_monthly.txt	RPB413N002f1*
co_scs_ship-flask_2_3001-3101_monthly.txt	SCS803N002f1*
co_scs_ship-flask_2_3001-3102_monthly.txt	SCS806N002f1*
co_scs_ship-flask_2_3001-3103_monthly.txt	SCS809N002f1*
co_scs_ship-flask_2_3001-3104_monthly.txt	SCS812N002f1*
co_scs_ship-flask_2_3001-3105_monthly.txt	SCS815N002f1*
co_scs_ship-flask_2_3001-3106_monthly.txt	SCS818N002f1*
co_scs_ship-flask_2_3001-3107_monthly.txt	SCS821N002f1
co_sdz_surface-flask_2_3001-9999_monthly.txt	SDZ240N002f1*
co_sey_surface-flask_2_3001-9999_monthly.txt	SEY104S002f1*
co_sgp_surface-flask_2_3001-9999_monthly.txt	SGP436N002f1*
co_shm_surface-flask_2_3001-9999_monthly.txt	SHM452N002f1*
co_smo_surface-flask_2_3001-9999_monthly.txt	SMO514S002f1*
co_spo_surface-flask_2_3001-9999_monthly.txt	SPO789S002f1*
co_stm_surface-flask_2_3001-9999_monthly.txt	STM666N002f1*
co_sum_surface-flask_2_3001-9999_monthly.txt	SUM672N002f1*
co_syo_surface-flask_2_3001-9999_monthly.txt	SYO769S002f1*
co_tap_surface-flask_2_3001-9999_monthly.txt	TAP236N002f1*

	co_thd_surface-flask_2_3001-9999_monthly.txt co_tik_surface-flask_2_3001-9999_monthly.txt co_ush_surface-flask_2_3001-9999_monthly.txt co_uta_surface-flask_2_3001-9999_monthly.txt co_uum_surface-flask_2_3001-9999_monthly.txt co_wis_surface-flask_2_3001-9999_monthly.txt co_wkt_surface-flask_2_3001-9999_monthly.txt co_wlg_surface-flask_2_3001-9999_monthly.txt co_zep_surface-flask_2_3001-9999_monthly.txt	THD441N002f1* TIK271N002f1* USH354S002f1* UTA439N002f1* UUM244N002f1* WIS631N002f1* WKT431N002f1* WLG236N002f1* ZEP678N002f1*		
ONM	co_ask_surface-insitu_59_9999-9999_monthly.txt	ASK123N059iz		07, 15
PolyU	co_hkg_surface-insitu_61_9999-9999_monthly.txt	HKG222N061iz		
RIVM	co_kmw_surface-insitu_63_9999-9999_monthly.txt	KMW653N063iz*		
	co_ktb_surface-insitu_63_9999-9999_monthly.txt	KTB653N063iz	µg/m³-25°C	
SAWS	co_cpt_surface-insitu_66_9999-1001_monthly.txt	CPT134S066iz*	WMO X2004 WMO X2014A CPT	98, 02, 06, 11, 15
UBAA	co_snb_surface-insitu_72_9999-9999_monthly.txt	SNB647N072iz*	NIST	98
UBAG	co_zsf_surface-insitu_71_9999-9999_monthly.txt	ZSF647N071iz*	WMO X2014 WMO X2014A	01, 06, 11
	co_ngl_surface-insitu_71_9999-9999_monthly.txt co_ssl_surface-insitu_71_9999-9999_monthly.txt	NGL653N071iz* SSL647N071iz*		
	co zug_surface-insitu_71_9999-9999_monthly.txt	ZUG647N071iz*	mg/m³-25°C	97, 01
UMLT	co_glh_surface-insitu_75_9999-9999_monthly.txt	GLH636N075iz*		
UNIURB	co_cmn_surface-insitu_74_9999-9999_monthly.txt	CMN644N074iz*	WMO X2014	
UYRK	co_cvo_surface-insitu_76_9999-9999_monthly.txt	CVO116N076iz*	WMO X2014	12
VNMHA	co_pdi_surface-insitu_51_9999-9999_monthly.txt	PDI221N051iz	WMO X2004	

* Stations with an asterisk are used for the calculation of the global mean mole fractions and related quantities. The site selection procedure is described in Appendix A.

APPENDIX C LIST OF OBSERVATIONAL STATIONS

Station	Country/Territory	GAW ID	Organization	Latitude (°)	Longitude (°)	Altitude (m)	Parameter
REGION I (Africa)							
Amsterdam Island	France	AMS	NOAA	37.80 S	77.54 E	70	CO ₂ , CH ₄
Amsterdam Island	France	AMS	LSCE	37.80 S	77.54 E	70	CO ₂ , CH ₄ , CO
Ascension Island	United Kingdom of Great Britain and Northern Ireland	ASC	NOAA	7.97 S	14.40 W	91	CO ₂ , CH ₄ , N ₂ O, SF ₆ , ¹³ CH ₄ , ¹³ CO ₂ , C ¹⁸ O ₂ , CO, H ₂
Assekrem	Algeria	ASK	NOAA	23.27 N	5.63 E	2710	CO ₂ , CH ₄ , N ₂ O, SF ₆ , ¹³ CO ₂ , C ¹⁸ O ₂ , CO, H ₂
Assekrem	Algeria	ASK	ONM	23.27 N	5.63 E	2710	CO
Cape Point	South Africa	CPT	NOAA	34.35 S	18.49 E	230	CO ₂ , CH ₄ , N ₂ O, SF ₆ , ¹³ CO ₂ , C ¹⁸ O ₂ , CO
Cape Point	South Africa	CPT	ANSTO	34.35 S	18.49 E	230	CO ₂ , CH ₄ , N ₂ O, CO
Cape Verde Atmospheric Observatory	Cabo Verde	CVO	UYRK	16.86 N	24.87 W	10	CO
Crozet	France	CRZ	NOAA	46.43 S	51.83 E	120	CO ₂ , CH ₄ , N ₂ O, SF ₆ , ¹³ CO ₂ , C ¹⁸ O ₂ , CO, H ₂
Gobabeb	Namibia	NMB	NOAA	23.57 S	15.03 E	408	CO ₂ , CH ₄ , N ₂ O, SF ₆ , ¹³ CO ₂ , C ¹⁸ O ₂ , CO
Izaña (Tenerife)	Spain	IZO	NOAA	28.31 N	16.50 W	2373	CO ₂ , CH ₄ , N ₂ O, SF ₆ , ¹³ CO ₂ , C ¹⁸ O ₂ , CO, H ₂
Izaña (Tenerife)	Spain	IZO	AEMET	28.31 N	16.50 W	2373	CO ₂ , CH ₄ , N ₂ O, SF ₆ , CO
Mahé	Seychelles	SEY	NOAA	4.67 S	55.17 E	3	CO ₂ , CH ₄ , N ₂ O, SF ₆ , ¹³ CO ₂ , C ¹⁸ O ₂ , CO, H ₂
Mt. Kenya	Kenya	MKN	NOAA	0.06 S	37.30 E	3678	CO ₂ , CH ₄ , N ₂ O, SF ₆ , ¹³ CO ₂ , C ¹⁸ O ₂ , CO
Mt. Kenya	Kenya	MKN	KMD	0.06 S	37.30 E	3678	CO
REGION II (Asia)							
Anmyeon-do	Republic of Korea	AMY	NOAA	36.54 N	126.33 E	46	CO ₂ , CH ₄ , N ₂ O, SF ₆ , ¹³ CH ₄ , CO
Anmyeon-do	Republic of Korea	AMY	KMA	36.54 N	126.33 E	46	CO ₂ , CH ₄ , N ₂ O, SF ₆ , CFCs, CO
Bering Island	Russian Federation	BER	MGO	55.20 N	165.98 E	13	CO ₂
Cape Ochiishi	Japan	COI	NIES	43.17 N	145.50 E	49	CO ₂ , CH ₄ , N ₂ O, SF ₆ , CFCs, HCFCs, HFCs
Cape Rama	India	CRI	CSIRO	15.08 N	73.83 E	60	CO ₂ , CH ₄ , N ₂ O, ¹³ CO ₂ , CO, H ₂
Gosan	Republic of Korea	GSN	AGAGE	33.28 N	126.17 E	72	SF ₆ , CH ₃ CCl ₃ , CFCs, HCFCs, HFCs, PFCs, CBrClF ₂ , CBrF ₃ , C ₂ Br ₂ F ₄ , CHCl ₃ , CH ₃ Cl
Gosan	Republic of Korea	GSN	GERC	33.28 N	126.17 E	72	CO ₂ , CH ₄ , N ₂ O
Gosan	Republic of Korea	GSN	METRI	33.28 N	126.17 E	72	CO ₂ , CH ₄ , N ₂ O, CFCs
Hamamatsu	Japan	HMM	SHIZU	34.72 N	137.72 E	29	CO ₂
Hateruma Island	Japan	HAT	NIES	24.05 N	123.81 E	10	CO ₂ , CH ₄ , N ₂ O, SF ₆ , CFCs, HCFCs, HFCs
Hok Tsui / Cape d Aguilar	Hong Kong, China	HKG	HKO	22.21 N	114.26 E	60	CO ₂

LIST OF OBSERVATIONAL STATIONS (continued)

Station	Country/Territory	GAW ID	Organization	Latitude (°)	Longitude (°)	Location Altitude (m)	Parameter
Hok Tsui / Cape d Aguilar	Hong Kong, China	HKG	PolyU	22.21 N	114.26 E	60	CO
Issyk-Kul	Kyrgyzstan	ISK	KSNU	42.62 N	76.98 E	1640	CO ₂ , CH ₄
Jeju Gosan	Republic of Korea	JGS	KMA	33.18 N	126.12 E	52	CO ₂
Kaashidhoo (Male Atoll)	Maldives	KCO	NOAA	4.97 N	73.47 E	1	CO ₂ , CH ₄ , N ₂ O, SF ₆ , CO
King's Park	Hong Kong, China	HKO	HKO	22.31 N	114.17 E	65	CO ₂
Kisai	Japan	KIS	SAIPF	36.08 N	139.55 E	13	CO ₂
Kotelnyj Island	Russian Federation	KOT	MGO	76.00 N	137.87 E	5	CO ₂
Kyzylcha	Uzbekistan	KYZ	MGO	40.87 N	66.15 E	340	CO ₂
Lulin	Taiwan, Province of China	LLN	NOAA	23.47 N	120.87 E	2862	CO ₂ , CH ₄ , N ₂ O, SF ₆ , ¹³ CO ₂ , C ¹⁸ O ₂ , CO
Memanbetsu	Japan	MMB	MRI	43.92 N	144.20 E	33	N ₂ O
Mikawa-Ichinomiya	Japan	MKW	AICH	34.85 N	137.43 E	50	CO ₂
Minamitorishima	Japan	MNM	JMA	24.29 N	153.98 E	7.1	CO ₂ , CH ₄ , CO
Mt. Dodaira	Japan	DDR	SAIPF	36.00 N	139.20 E	840	CO ₂
Mt. Waliguan	China	WLG	NOAA	36.29 N	100.90 E	3810	CO ₂ , CH ₄ , N ₂ O, SF ₆ , ¹³ CH ₄ , ¹³ CO ₂ , C ¹⁸ O ₂ , CO, H ₂
Mt. Waliguan	China	WLG	CMA	36.29 N	100.90 E	3810	CO ₂ , CH ₄
Nagoya	Japan	NGY	NAGOU	35.15 N	136.97 E	35	N ₂ O
Nepal Climate Observatory - Pyramid	Nepal	PYR	UNIURB	27.96 N	86.81 E	5079	SO ₂ F ₂ , COS, CCl ₄ , CH ₃ CCl ₃ , CFCs, HCFCs, HFCs, PFCs, CBrClF ₂ , CBrF ₃ , CHCl ₃ , CH ₃ Cl, CH ₂ Cl ₂ , CH ₃ I, CH ₃ Br, CH ₂ Br ₂ , C ₂ HCl ₃ , C ₂ Cl ₄ , CHBr ₃
Pha Din Plateau Assy	Viet Nam Kazakhstan	PDI KZM	VNMHA NOAA	21.57 N 43.25 N	103.52 E 77.88 E	1466 2519	CO ₂ , CH ₄ , CO CO ₂ , CH ₄ , N ₂ O, SF ₆ , ¹³ CO ₂ , C ¹⁸ O ₂ , CO, H ₂
Ryori	Japan	RYO	JMA	39.03 N	141.82 E	260	CO ₂ , CH ₄ , N ₂ O, CCl ₄ , CH ₃ CCl ₃ , CFCs, CO
Sary Taukum	Kazakhstan	KZD	NOAA	44.45 N	77.57 E	412	CO ₂ , CH ₄ , N ₂ O, SF ₆ , ¹³ CO ₂ , C ¹⁸ O ₂ , CO, H ₂
Shangdianzi	China	SDZ	NOAA	40.65 N	117.12 E	287	CO ₂ , CH ₄ , N ₂ O, SF ₆ , ¹³ CO ₂ , C ¹⁸ O ₂ , CO
Suita Tae-ahn Peninsula	Japan Republic of Korea	SUI TAP	OSAKAU NOAA	34.82 N 36.73 N	135.52 E 126.13 E	63 20	CO ₂ CO ₂ , CH ₄ , N ₂ O, SF ₆ , ¹³ CH ₄ , ¹³ CO ₂ , C ¹⁸ O ₂ , CO, H ₂
Takayama Tateno (Tsukuba)	Japan	TKY TKB	AIST MRI	36.15 N 36.06 N	137.42 E 140.13 E	1420 25.2	CO ₂ CO ₂ , CH ₄
Tiksi	Russian Federation	TIK	NOAA	71.59 N	128.92 E	8	CO ₂ , CH ₄ , N ₂ O, SF ₆ , ¹³ CO ₂ , C ¹⁸ O ₂ , CO
Tiksi Ulaan Uul	Russian Federation Mongolia	TIK UUM	MGO NOAA	71.59 N 44.44 N	128.92 E 111.09 E	8 992	CO ₂ , CH ₄ CO ₂ , CH ₄ , N ₂ O, SF ₆ , ¹³ CO ₂ , C ¹⁸ O ₂ , CO, H ₂
Urawa Yonagunijima	Japan	URW YON	SAIPF JMA	35.87 N 24.47 N	139.62 E 123.01 E	10 30	CO ₂ CO ₂ , CH ₄ , CO

REGION III (South America)

LIST OF OBSERVATIONAL STATIONS (continued)

Station	Country/Territory	GAW ID	Organization	Latitude (°)	Longitude (°)	Location Altitude (m)	Parameter
Arembepe	Brazil	ABP	NOAA	12.77 S	38.17 W	0	CO ₂ , CH ₄ , N ₂ O, SF ₆ , ¹³CO ₂ , C ¹⁸ O ₂ , CO
Arembepe	Brazil	ABP	INPE	12.77 S	38.17 W	0	CO ₂ , CH ₄ , N ₂ O, CO
Bird Island (South Georgia)	United Kingdom of Great Britain and Northern Ireland	SGI	NOAA	54.01 S	38.05 W	30	CO ₂ , CH ₄
Easter Island	Chile	EIC	NOAA	27.17 S	109.42 W	41	CO ₂ , CH ₄ , N ₂ O, SF ₆ , ¹³CO ₂ , C ¹⁸ O ₂ , CO, H ₂
El Tololo	Chile	TLL	DMC	30.17 S	70.80 W	2154	CO ₂ , CH ₄ , CO
Huancayo	Peru	HUA	IGP	12.15 S	75.57 W	4575	CO ₂
Natal	Brazil	NAT	NOAA	6.00 S	35.20 W	0	CO ₂ , CH ₄ , N ₂ O, SF ₆ , ¹³CO ₂ , C ¹⁸ O ₂ , CO
Ushuaia	Argentina	USH	NOAA	54.85 S	68.31 W	18	CO ₂ , CH ₄ , N ₂ O, SF ₆ , ¹³CO ₂ , C ¹⁸ O ₂ , CCl ₄ , CH ₃ CCl ₃ , CFCs, CO

REGION IV (North and Central America)

Alert	Canada	ALT	NOAA	82.50 N	62.34 W	210	CO ₂ , CH ₄ , N ₂ O, SF ₆ , ¹³CH ₄ , ¹³ CO ₂ , C ¹⁸ O ₂ , CCl ₄ , CH ₃ CCl ₃ , CFCs, HCFCs, HFCs, CBrClF ₂ , CO, CH ₃ Cl, CH ₂ Cl ₂ , CH ₃ Br, C ₂ Cl ₄ , H ₂
Alert	Canada	ALT	CSIRO	82.50 N	62.34 W	210	CO ₂ , CH ₄ , N ₂ O, ¹³ CO ₂ , CO, H ₂
Alert	Canada	ALT	ECCC	82.50 N	62.34 W	210	CO ₂ , CH ₄ , N ₂ O, ¹³ CO ₂ , C ¹⁸ O ₂ , CO
Argyle (ME)	United States of America	AMT	NOAA	45.03 N	68.68 W	50	CH ₄ , N ₂ O, SF ₆ , ¹³ CO ₂ , C ¹⁸ O ₂ , CO
Barrow (AK)	United States of America	BRW	NOAA	71.32 N	156.61 W	11	CO ₂ , CH ₄ , N ₂ O, SF ₆ , ¹³CH ₄ , ¹³ CO ₂ , C ¹⁸ O ₂ , CCl ₄ , CH ₃ CCl ₃ , CFCs, HCFCs, HFCs, CBrClF ₂ , CBrF ₃ , CO, CH ₃ Cl, CH ₂ Cl ₂ , CH ₃ Br, C ₂ Cl ₄ , H ₂
Candle Lake	Canada	CDL	ECCC	53.99 N	105.12 W	591	CO ₂ , CH ₄ , CO
Cape Meares (OR)	United States of America	CMO	NOAA	45.00 N	124.00 W	30	CO ₂ , CH ₄ , ¹³ CO ₂ , C ¹⁸ O ₂ , CO, H ₂
Cape Meares (OR)	United States of America	CMO	AGAGE	45.00 N	124.00 W	30	CH ₄ , N ₂ O, CCl ₄ , CH ₃ CCl ₃ , CFCs
Chibougamau	Canada	CHM	ECCC	49.69 N	74.34 W	383	CO ₂ , CH ₄ , CO
Churchill	Canada	CHL	ECCC	58.74 N	93.82 W	16	CO ₂ , CH ₄ , N ₂ O, ¹³ CO ₂ , C ¹⁸ O ₂ , CO
Cold Bay (AK)	United States of America	CBA	NOAA	55.20 N	162.72 W	25	CO ₂ , CH ₄ , N ₂ O, SF ₆ , ¹³CH ₄ , ¹³ CO ₂ , C ¹⁸ O ₂ , CO, H ₂
East Trout Lake	Canada	ETL	ECCC	54.35 N	104.99 W	500	CO ₂ , CH ₄ , ¹³ CO ₂ , C ¹⁸ O ₂ , CO
Egbert	Canada	EGB	ECCC	44.23 N	79.78 W	255	CO ₂ , CH ₄ , CO
Estevan Point	Canada	ESP	CSIRO	49.38 N	126.54 W	7	CO ₂ , CH ₄ , N ₂ O, ¹³ CO ₂ , CO, H ₂

LIST OF OBSERVATIONAL STATIONS (continued)

Station	Country/Territory	GAW ID	Organization	Latitude (°)	Longitude (°)	Location Altitude (m)	Parameter
Estevan Point	Canada	ESP	ECCC	49.38 N	126.54 W	7	CO ₂ , CH ₄ , N ₂ O, ¹³ CO ₂ , C ¹⁸ O ₂ , CO
Fraserdale	Canada	FSD	ECCC	49.84 N	81.52 W	210	CO ₂ , CH ₄ , ¹³ CO ₂ , C ¹⁸ O ₂ , CO
Grifton - Georgia Station (NC)	United States of America	ITN	NOAA	35.35 N	77.38 W	505	CH ₄ , N ₂ O, SF ₆ , ¹³ CO ₂ , C ¹⁸ O ₂ , CCl ₄ , CH ₃ CCl ₃ , CFCs, CO, H ₂
Harvard Forest (MA)	United States of America	HFM	NOAA	42.90 N	72.30 W	340	N ₂ O, SF ₆ , CCl ₄ , CH ₃ CCl ₃ , CFCs, HCFCs, HFCs, CBrClF ₂ , CH ₃ Cl, CH ₂ Cl ₂ , CH ₃ Br, C ₂ Cl ₄
Key Biscane (FL)	United States of America	KEY	NOAA	25.67 N	80.20 W	3	CO ₂ , CH ₄ , N ₂ O, SF ₆ , ¹³ CO ₂ , C ¹⁸ O ₂ , CO, H ₂
Kitt Peak (AZ)	United States of America	KPA	NOAA	31.97 N	111.60 W	2083	CH ₄
La Jolla (CA)	United States of America	SIO	NOAA	32.83 N	117.27 W	14	CH ₄
Lac La Biche (Alberta)	Canada	LLB	NOAA	54.95 N	112.47 W	548	CO ₂ , CH ₄ , N ₂ O, SF ₆ , ¹³ CH ₄ , ¹³ CO ₂ , C ¹⁸ O ₂ , CO
Lac La Biche (Alberta)	Canada	LLB	ECCC	54.95 N	112.47 W	548	CO ₂ , CH ₄ , CO
Mex High Altitude Global Climate Observation Center	Mexico	MEX	NOAA	18.99 N	97.31 W	4560	CO ₂ , CH ₄ , N ₂ O, SF ₆ , ¹³ CH ₄ , ¹³ CO ₂ , C ¹⁸ O ₂ , CO
Moody (TX)	United States of America	WKT	NOAA	31.32 N	97.62 W	723	CH ₄ , N ₂ O, SF ₆ , ¹³ CO ₂ , C ¹⁸ O ₂ , CO
Mould Bay	Canada	MBC	NOAA	76.25 N	119.35 W	58	CO ₂ , CH ₄ , ¹³ CO ₂ , C ¹⁸ O ₂ , CO, H ₂
Niwot Ridge - T-van (CO)	United States of America	NWR	NOAA	40.05 N	105.59 W	3523	CO ₂ , CH ₄ , N ₂ O, SF ₆ , ¹³ CH ₄ , ¹³ CO ₂ , C ¹⁸ O ₂ , CCl ₄ , CH ₃ CCl ₃ , CFCs, HCFCs, HFCs, CBrClF ₂ , CO, CH ₃ Cl, CH ₂ Cl ₂ , CH ₃ Br, C ₂ Cl ₄ , H ₂ , ¹⁴ CO ₂
Olympic Peninsula (WA)	United States of America	OPW	NOAA	48.25 N	124.42 W	488	CO ₂ , CH ₄
Park Falls (WI)	United States of America	LEF	NOAA	45.93 N	90.27 W	868	CO ₂ , CH ₄ , N ₂ O, SF ₆ , ¹³ CO ₂ , C ¹⁸ O ₂ , CCl ₄ , CH ₃ CCl ₃ , CFCs, HCFCs, HFCs, CBrClF ₂ , CO, CH ₃ Cl, CH ₂ Cl ₂ , CH ₃ Br, C ₂ Cl ₄ , H ₂
Point Arena (CA)	United States of America	PTA	NOAA	38.95 N	123.73 W	17	CO ₂ , CH ₄ , N ₂ O, SF ₆ , ¹³ CO ₂ , C ¹⁸ O ₂ , CO
Ragged Point	Barbados	RPB	NOAA	13.17 N	59.43 W	45	CO ₂ , CH ₄ , N ₂ O, SF ₆ , ¹³ CO ₂ , C ¹⁸ O ₂ , CO, H ₂
Ragged Point	Barbados	RPB	AGAGE	13.17 N	59.43 W	45	CH ₄ , N ₂ O, SF ₆ , SO ₂ F ₂ , NF ₃ , CCl ₄ , CH ₃ CCl ₃ , CFCs, HCFCs, HFCs, PFCs, CBrClF ₂ , CBrF ₃ , C ₂ Br ₂ F ₄ , CHCl ₃ , CH ₃ Cl, CH ₂ Cl ₂ , CH ₃ Br, C ₂ Cl ₄
Sable Island	Canada	WSA	ECCC	43.93 N	60.01 W	2	CO ₂ , CH ₄ , N ₂ O, ¹³ CO ₂ , C ¹⁸ O ₂ , CO

LIST OF OBSERVATIONAL STATIONS (continued)

Station	Country/Territory	GAW ID	Organization	Latitude (°)	Longitude (°)	Location Altitude (m)	Parameter
Shemya Island	United States of America	SHM	NOAA	52.72 N	174.10 E	40	CO ₂ , CH ₄ , N ₂ O, SF ₆ , ¹³ CO ₂ , C ¹⁸ O ₂ , CO, H ₂
Southern Great Plains E13 (OK)	United States of America	SGP	NOAA	36.60 N	97.50 W	318	CO ₂ , CH ₄ , N ₂ O, SF ₆ , ¹³ CO ₂ , C ¹⁸ O ₂ , CO
St. Croix	United States of America	AVI	NOAA	17.75 N	64.75 W	3	CO ₂ , CH ₄
St. David's Head	United Kingdom of Great Britain and Northern Ireland	BME	NOAA	32.37 N	64.65 W	30	CO ₂ , CH ₄ , N ₂ O, SF ₆ , ¹³ CO ₂ , C ¹⁸ O ₂ , CO, H ₂
Trinidad Head (CA)	United States of America	THD	NOAA	41.05 N	124.15 W	107	CO ₂ , CH ₄ , N ₂ O, SF ₆ , ¹³ CO ₂ , C ¹⁸ O ₂ , CCl ₄ , CH ₃ CCl ₃ , CFCs, HCFCs, HFCs, CBrClF ₂ , CBrF ₃ , CO, CH ₃ Cl, CH ₂ Cl ₂ , CH ₃ Br, C ₂ Cl ₄
Trinidad Head (CA)	United States of America	THD	AGAGE	41.05 N	124.15 W	107	CH ₄ , N ₂ O, SF ₆ , SO ₂ F ₂ , NF ₃ , CCl ₄ , CH ₃ CCl ₃ , CFCs, HCFCs, HFCs, PFCs, CBrClF ₂ , CBrF ₃ , C ₂ Br ₂ F ₄ , CHCl ₃ , CH ₃ Cl, CH ₂ Cl ₂ , CH ₃ Br, C ₂ Cl ₄
Tudor Hill (Bermuda)	United Kingdom of Great Britain and Northern Ireland	BMW	NOAA	32.27 N	64.88 W	30	CO ₂ , CH ₄ , N ₂ O, SF ₆ , ¹³ CO ₂ , C ¹⁸ O ₂ , CO, H ₂
Wendover (UT)	United States of America	UTA	NOAA	39.90 N	113.72 W	1320	CO ₂ , CH ₄ , N ₂ O, SF ₆ , ¹³ CO ₂ , C ¹⁸ O ₂ , CO, H ₂
West Branch (Iowa)	United States of America	WBI	NOAA	41.72 N	91.35 W	242	C ¹⁸ O ₂

REGION V (South-West Pacific)

Baring Head	New Zealand	BHD	NOAA	41.41 S	174.87 E	85	CO ₂ , CH ₄ , N ₂ O, SF ₆ , ¹³ CH ₄ , ¹³ CO ₂ , C ¹⁸ O ₂ , CO
Baring Head	New Zealand	BHD	NIWA	41.41 S	174.87 E	85	CO ₂ , CH ₄ , N ₂ O, ¹³ CH ₄ , CO, ¹⁴ CO ₂
Bukit Kototabang	Indonesia	BKT	NOAA	0.20 S	100.32 E	864	CO ₂ , CH ₄ , N ₂ O, SF ₆ , ¹³ CO ₂ , C ¹⁸ O ₂ , CO
Bukit Kototabang	Indonesia	BKT	BMKG	0.20 S	100.32 E	864	CO ₂ , CH ₄ , CO
Cape Ferguson	Australia	CFA	CSIRO	19.28 S	147.06 E	2	CO ₂ , CH ₄ , N ₂ O, ¹³ CO ₂ , CO, H ₂
Cape Grim	Australia	CGO	NOAA	40.68 S	144.69 E	94	CO ₂ , CH ₄ , N ₂ O, SF ₆ , ¹³ CH ₄ , ¹³ CO ₂ , C ¹⁸ O ₂ , CCl ₄ , CH ₃ CCl ₃ , CFCs, HCFCs, HFCs, CBrClF ₂ , CBrF ₃ , CO, CH ₃ Cl, CH ₂ Cl ₂ , CH ₃ Br, C ₂ Cl ₄ , H ₂
Cape Grim	Australia	CGO	AGAGE	40.68 S	144.69 E	94	CH ₄ , N ₂ O, SF ₆ , SO ₂ F ₂ , NF ₃ , CCl ₄ , CH ₃ CCl ₃ , CFCs, HCFCs, HFCs, PFCs, CBrClF ₂ , CBrF ₃ , C ₂ Br ₂ F ₄ , CO, CHCl ₃ , CH ₃ Cl, CH ₂ Cl ₂ , CH ₃ Br, C ₂ Cl ₄ , H ₂
Cape Grim	Australia	CGO	ANSTO	40.68 S	144.69 E	94	²²² Rn

LIST OF OBSERVATIONAL STATIONS (continued)

Station	Country/Territory	GAW ID	Organization	Latitude (°)	Longitude (°)	Location Altitude (m)	Parameter
Cape Grim	Australia	CGO	CSIRO	40.68 S	144.69 E	94	CO ₂ , CH ₄ , N ₂ O, ¹³ CO ₂ , CO, H ₂
Cape Kumukahi (HI)	United States of America	KUM	NOAA	19.52 N	154.82 W	3	CO ₂ , CH ₄ , N ₂ O, SF ₆ , ¹³ CH ₄ , ¹³ CO ₂ , C ¹⁸ O ₂ , CCl ₄ , CH ₃ CCl ₃ , CFCs, HCFCs, HFCs, CBrClF ₂ , CBrF ₃ , CO, CH ₃ Cl, CH ₂ Cl ₂ , CH ₃ Br, C ₂ Cl ₄ , H ₂
Christmas Island	Kiribati	CHR	NOAA	1.70 N	157.17 W	3	CO ₂ , CH ₄ , N ₂ O, SF ₆ , ¹³ CO ₂ , C ¹⁸ O ₂ , CO, H ₂
Danum Valley	Malaysia	DMV	MMD	4.98 N	117.84 E	426	CO ₂
Guam (Mariana Island)	United States of America	GMI	NOAA	13.43 N	144.78 E	2	CO ₂ , CH ₄ , N ₂ O, SF ₆ , ¹³ CO ₂ , C ¹⁸ O ₂ , CO, H ₂
Gunn Point	Australia	GPA	CSIRO	12.25 S	131.05 E	25	CO ₂ , CH ₄ , N ₂ O, ¹³ CO ₂ , CO, H ₂
Kaitorete Spit	New Zealand	NZL	NOAA	43.83 S	172.63 E	3	CH ₄
Lauder	New Zealand	LAU	NIWA	45.04 S	169.68 E	370	CH ₄
Macquarie Island	Australia	MQA	CSIRO	54.50 S	158.94 E	6	CO ₂ , CH ₄ , N ₂ O, ¹³ CO ₂ , CO, H ₂
Mauna Loa (HI)	United States of America	MLO	NOAA	19.54 N	155.58 W	3397	CO ₂ , CH ₄ , N ₂ O, SF ₆ , ¹³ CH ₄ , ¹³ CO ₂ , C ¹⁸ O ₂ , CCl ₄ , CH ₃ CCl ₃ , CFCs, HCFCs, HFCs, CBrClF ₂ , CBrF ₃ , CO, CH ₃ Cl, CH ₂ Cl ₂ , CH ₃ Br, C ₂ Cl ₄ , H ₂
Mauna Loa (HI)	United States of America	MLO	CSIRO	19.54 N	155.58 W	3397	CO ₂ , CH ₄ , N ₂ O, ¹³ CO ₂ , CO, H ₂
Samoa (Cape Matatula)	United States of America	SMO	NOAA	14.25 S	170.56 W	77	CO ₂ , CH ₄ , N ₂ O, SF ₆ , ¹³ CH ₄ , ¹³ CO ₂ , C ¹⁸ O ₂ , CCl ₄ , CH ₃ CCl ₃ , CFCs, HCFCs, HFCs, CBrClF ₂ , CBrF ₃ , CO, CH ₃ Cl, CH ₂ Cl ₂ , CH ₃ Br, C ₂ Cl ₄ , H ₂
Samoa (Cape Matatula)	United States of America	SMO	AGAGE	14.25 S	170.56 W	77	CH ₄ , N ₂ O, SF ₆ , SO ₂ F ₂ , NF ₃ , CCl ₄ , CH ₃ CCl ₃ , CFCs, HCFCs, HFCs, PFCs, CBrClF ₂ , CBrF ₃ , C ₂ Br ₂ F ₄ , CHCl ₃ , CH ₃ Cl, CH ₂ Cl ₂ , CH ₃ Br, C ₂ Cl ₄
Sand Island	United States of America	MID	NOAA	28.22 N	177.37 W	4	CO ₂ , CH ₄ , N ₂ O, SF ₆ , ¹³ CO ₂ , C ¹⁸ O ₂ , CO, H ₂

REGION VI (Europe)

Adrigole	Ireland	ADR	AGAGE	51.68 N	9.73 W	50	N ₂ O, CCl ₄ , CH ₃ CCl ₃ , CFCs
BEO Moussala Baltic Sea	Bulgaria Poland	BEO BAL	INRNE NOAA	42.18 N 55.50 N	23.59 E 16.67 E	2925 7	CO ₂ , CO CO ₂ , CH ₄ , N ₂ O, SF ₆ , ¹³ CH ₄ , ¹³ CO ₂ , C ¹⁸ O ₂ , CO, H ₂
Begur Brotjacklriegel	Spain Germany	BGU BRT	LSCE UBAG	41.97 N 48.82 N	3.23 E 13.22 E	13 1016	CO ₂ , CH ₄ CO ₂

LIST OF OBSERVATIONAL STATIONS (continued)

Station	Country/Territory	GAW ID	Organization	Latitude (°)	Longitude (°)	Location Altitude (m)	Parameter
Capo Granitola	Italy	CGR	ISAC	37.67 N	12.65 E	5	CO ₂ , CH ₄ , CO
Constanta (Black Sea)	Romania	BSC	NOAA	44.17 N	28.68 E	3	CO ₂ , CH ₄ , N ₂ O, SF ₆ , ¹³ CO ₂ , C ¹⁸ O ₂ , CO, H ₂
Deuselbach	Germany	DEU	UBAG	49.77 N	7.05 E	480	CO ₂ , CH ₄
Diabla Gora / Puszczna Borecka	Poland	DIG	IOEP	54.15 N	22.07 E	157	CO ₂
Dwejra Point	Malta	GOZ	NOAA	36.05 N	14.18 E	30	CO ₂ , CH ₄ , ¹³ CO ₂ , C ¹⁸ O ₂ , CO, H ₂
Finokalia	Greece	FIK	LSCE	35.34 N	25.67 E	150	CO ₂ , CH ₄
Fundata	Romania	FDT	INMH	45.43 N	25.27 E	1384	CO ₂
Gartow	Germany	GAT	DWD	53.07 N	11.44 E	69	CO ₂ , CH ₄ , CO
Giordan Lighthouse	Malta	GLH	UMLT	36.07 N	14.22 E	167	CO ₂ , CH ₄ , CO, ²²² Rn
Hegyhatsal	Hungary	HUN	NOAA	46.95 N	16.65 E	248	CO ₂ , CH ₄ , N ₂ O, SF ₆ , ¹³ CO ₂ , C ¹⁸ O ₂ , CO, H ₂
Hegyhatsal	Hungary	HUN	HMS	46.95 N	16.65 E	248	CO ₂
Hohenpeissenberg	Germany	HPB	NOAA	47.80 N	11.01 E	985	CO ₂ , CH ₄ , N ₂ O, SF ₆ , ¹³ CO ₂ , C ¹⁸ O ₂ , CO
Hohenpeissenberg	Germany	HPB	DWD	47.80 N	11.01 E	985	CO ₂ , CH ₄ , CO, ²²² Rn
Ile Grande	France	LPO	LSCE	48.80 N	3.58 W	20	CO ₂ , CH ₄
Jungfraujoch	Switzerland	JFJ	AGAGE	46.55 N	7.99 E	3580	SF ₆ , SO ₂ F ₂ , NF ₃ , CCl ₄ , CH ₃ CCl ₃ , CFCs, HCFCs, HFCs, PFCs, CBrClF ₂ , CBrF ₃ , C ₂ Br ₂ F ₄ , CHCl ₃ , CH ₃ Cl, CH ₂ Cl ₂ , CH ₃ Br, C ₂ HCl ₃ , C ₂ Cl ₄
Jungfraujoch	Switzerland	JFJ	Empa	46.55 N	7.99 E	3580	CO ₂ , CH ₄ , N ₂ O, SF ₆ , CO
Jungfraujoch	Switzerland	JFJ	KUP	46.55 N	7.99 E	3580	CO ₂
K-Puszta	Hungary	KPS	HMS	46.97 N	19.58 E	125	CO ₂
Kloosterburen	Netherlands	KTB	RIVM	53.40 N	6.42 E	0	CO
Kollumerwaard	Netherlands	KMW	RIVM	53.33 N	6.27 E	0	CO ₂ , CH ₄ , CO
Kosetice Observatory	Czech Republic	KOS	CHMI	49.58 N	15.08 E	534	CH ₄ , CO
Krvavec	Slovenia	KVV	ARSO	46.30 N	14.53 E	1740	CO
Lamezia Terme	Italy	LMT	ISAC	38.88 N	16.23 E	6	CO ₂ , CH ₄ , CO
Lampedusa	Italy	LMP	NOAA	35.52 N	12.63 E	45	CO ₂ , CH ₄ , N ₂ O, SF ₆ , ¹³ CO ₂ , C ¹⁸ O ₂ , CO
Lampedusa	Italy	LMP	ENEA	35.52 N	12.63 E	45	CO ₂ , CH ₄ , N ₂ O, SF ₆ , CCl ₄ , CH ₃ CCl ₃ , CFCs, HCFCs, HFCs, CBrClF ₂ , CBrF ₃ , CHCl ₃ , CH ₃ Cl, CH ₂ Cl ₂ , CH ₃ I, CH ₃ Br, CH ₂ Br ₂
Lecce Environmental-Climate Observatory	Italy	ECO	ISAC	40.34 N	18.12 E	36	CO ₂ , CH ₄ , CO
Lerwick	United Kingdom of Great Britain and Northern Ireland	SIS	CSIRO	60.13 N	1.18 W	84	CO ₂ , CH ₄ , N ₂ O, ¹³ CO ₂ , CO, H ₂
Lindenberg	Germany	LIN	DWD	52.22 N	14.12 E	112	CO ₂ , CH ₄
Mace Head	Ireland	MHD	NOAA	53.33 N	9.90 W	5	CO ₂ , CH ₄ , N ₂ O, SF ₆ , ¹³ CH ₄ , ¹³ CO ₂ , C ¹⁸ O ₂ , CCl ₄ , CH ₃ CCl ₃ , CFCs, HCFCs, HFCs, CBrClF ₂ , CO, CH ₃ Cl, CH ₂ Cl ₂ , CH ₃ Br, C ₂ Cl ₄ , H ₂

LIST OF OBSERVATIONAL STATIONS (continued)

Station	Country/Territory	GAW ID	Organization	Latitude (°)	Longitude (°)	Location Altitude (m)	Parameter
Mace Head	Ireland	MHD	AGAGE	53.33 N	9.90 W	5	CH ₄ , N ₂ O, SF ₆ , SO ₂ F ₂ , NF ₃ , CCl ₄ , CH ₃ CCl ₃ , CFCs, HCFCs, HFCs, PFCs, CBrClF ₂ , CBrF ₃ , C ₂ Br ₂ F ₄ , CO, CHCl ₃ , CH ₃ Cl, CH ₂ Cl ₂ , CH ₃ Br, C ₂ HCl ₃ , C ₂ Cl ₄ , H ₂
Mace Head	Ireland	MHD	LSCE	53.33 N	9.90 W	5	CO ₂ , CH ₄
Monte Cimone	Italy	CMN	AGAGE	44.17 N	10.68 E	2165	SO ₂ F ₂ , CCl ₄ , CH ₃ CCl ₃ , CFCs, HCFCs, HFCs, PFCs, CBrClF ₂ , CBrF ₃ , CHCl ₃ , CH ₃ Cl, CH ₂ Cl ₂ , CH ₃ Br, C ₂ Cl ₄
Monte Cimone	Italy	CMN	IAFMS	44.17 N	10.68 E	2165	CO ₂ , CH ₄
Monte Cimone	Italy	CMN	ISAC	44.17 N	10.68 E	2165	CO, H ₂
Monte Cimone	Italy	CMN	UNIURB	44.17 N	10.68 E	2165	CH ₄ , N ₂ O, SF ₆ , CO
Monte Curcio	Italy	CUR	IIA	39.32 N	16.42 E	1796	CO ₂ , CH ₄ , CO
Neuglobsow	Germany	NGL	UBAG	53.14 N	13.03 E	62	CO ₂ , CH ₄ , CO
Ocean Station Charlie	United States of America	STC	NOAA	54.00 N	35.00 W	0	CO ₂
Ocean Station Charlie	United States of America	STC	MGO	54.00 N	35.00 W	0	CO ₂
Ocean Station M	Norway	STM	NOAA	66.00 N	2.00 E	4	CO ₂ , CH ₄ , N ₂ O, SF ₆ , ¹³ CO ₂ , C ¹⁸ O ₂ , CO, H ₂
Ochsenkopf	Germany	OXK	NOAA	50.03 N	11.81 E	1185	CO ₂ , CH ₄ , N ₂ O, SF ₆ , ¹³ CO ₂ , C ¹⁸ O ₂ , CO
Pallas	Finland	PAL	NOAA	67.97 N	24.12 E	560	CO ₂ , CH ₄ , N ₂ O, SF ₆ , ¹³ CO ₂ , C ¹⁸ O ₂ , CO
Pallas	Finland	PAL	FMI	67.97 N	24.12 E	560	CO ₂ , CH ₄
Payerne	Switzerland	PAY	Empa	46.81 N	6.94 E	490	CO
Pic du Midi	France	PDM	LA	42.94 N	0.14 E	2877	CO
Pic du Midi	France	PDM	LSCE	42.94 N	0.14 E	2877	CO ₂ , CH ₄
Plateau Rosa	Italy	PRS	RSE	45.94 N	7.71 E	3480	CO ₂ , CH ₄
Puy de Dôme	France	PUY	LAMP	45.77 N	2.97 E	1465	CO
Puy de Dôme	France	PUY	LSCE	45.77 N	2.97 E	1465	CO ₂ , CH ₄
Ridge Hill	United Kingdom of Great Britain and Northern Ireland	RGL	UNIVBRIS	52.00 N	2.54 W	204	CO ₂ , CH ₄ , N ₂ O, SF ₆
Rigi	Switzerland	RIG	Empa	47.07 N	8.46 E	1031	CO
Schauinsland	Germany	SSL	UBAG	47.90 N	7.92 E	1205	CO ₂ , CH ₄ , N ₂ O, SF ₆ , CO
Sede Boker	Israel	WIS	NOAA	31.13 N	34.88 E	400	CO ₂ , CH ₄ , N ₂ O, SF ₆ , ¹³ CO ₂ , C ¹⁸ O ₂ , CO, H ₂
Serreta (Terceira)	Portugal	AZR	NOAA	38.77 N	27.38 W	40	CO ₂ , CH ₄ , N ₂ O, SF ₆ , ¹³ CH ₄ , ¹³ CO ₂ , C ¹⁸ O ₂ , CO, H ₂
Sonnblick	Austria	SNB	UBAA	47.05 N	12.96 E	3106	CO ₂ , CH ₄ , CO
Storhofdi	Iceland	ICE	NOAA	63.40 N	20.28 W	118	CO ₂ , CH ₄ , N ₂ O, SF ₆ , ¹³ CO ₂ , C ¹⁸ O ₂ , CO, H ₂
Summit	Denmark	SUM	NOAA	72.58 N	38.48 W	3238	CO ₂ , CH ₄ , N ₂ O, SF ₆ , ¹³ CH ₄ , ¹³ CO ₂ , C ¹⁸ O ₂ , CCl ₄ , CH ₃ CCl ₃ , CFCs, HCFCs, HFCs, CBrClF ₂ , CO, CH ₃ Cl, CH ₂ Cl ₂ , CH ₃ Br
Summit	Denmark	SUM	INSTAAR	72.58 N	38.48 W	3238	CH ₄

LIST OF OBSERVATIONAL STATIONS (continued)

Station	Country/Territory	GAW ID	Organization	Location			Parameter
				Latitude (°)	Longitude (°)	Altitude (m)	
Tacolneston Tall Tower	United Kingdom of Great Britain and Northern Ireland	TAC	NOAA	52.52 N	1.14 E	56	CO ₂ , CH ₄ , N ₂ O, SF ₆ , CO
Tacolneston Tall Tower	United Kingdom of Great Britain and Northern Ireland	TAC	UNIVBRIS	52.52 N	1.14 E	56	CO ₂ , CH ₄ , N ₂ O, SF ₆ , SO ₂ F ₂ , CH ₃ CCl ₃ , CFCs, HCFCs, HFCs, PFCs, CBrClF ₂ , CBrF ₃ , CO, CHCl ₃ , CH ₃ Cl, CH ₂ Cl ₂ , CH ₃ Br, C ₂ HCl ₃ , C ₂ Cl ₄ , H ₂
Teriberka	Russian Federation	TER	MGO	69.20 N	35.10 E	40	CO ₂ , CH ₄
Waldhof	Germany	LGB	UBAG	52.80 N	10.76 E	74	CO ₂
Wank	Germany	WNK	IMKIFU	47.51 N	11.14 E	1780	CO ₂
Westerland	Germany	WES	UBAG	54.92 N	8.31 E	12	CO ₂
Zeppelin Mountain (Ny Ålesund)	Norway	ZEP	NOAA	78.91 N	11.89 E	475	CO ₂ , CH ₄ , N ₂ O, SF ₆ , ¹³ CH ₄ , ¹³ CO ₂ , C ¹⁸ O ₂ , CO, H ₂
Zeppelin Mountain (Ny Ålesund)	Norway	ZEP	AGAGE	78.91 N	11.89 E	475	SF ₆ , SO ₂ F ₂ , NF ₃ , CH ₃ CCl ₃ , CFCs, HCFCs, HFCs, PFCs, CBrClF ₂ , CBrF ₃ , C ₂ Br ₂ F ₄ , CHCl ₃ , CH ₃ Cl, CH ₂ Cl ₂ , CH ₃ Br, C ₂ Cl ₄
Zeppelin Mountain (Ny Ålesund)	Norway	ZEP	ITM	78.91 N	11.89 E	475	CO ₂
Zeppelin Mountain (Ny Ålesund)	Norway	ZEP	NILU	78.91 N	11.89 E	475	N ₂ O, CFCs
Zingst	Germany	ZGT	UBAG	54.44 N	12.72 E	1	CO ₂ , CH ₄
Zugspitze-Gipfel	Germany	ZUG	IMKIFU	47.42 N	10.99 E	2962	CO ₂
Zugspitze-Gipfel	Germany	ZUG	UBAG	47.42 N	10.99 E	2962	CO ₂ , CH ₄ , CO
Zugspitze-Schneefernerhaus	Germany	ZSF	DWD	47.42 N	10.98 E	2671	²²² Rn, ⁷ Be
Zugspitze-Schneefernerhaus	Germany	ZSF	UBAG	47.42 N	10.98 E	2671	CO ₂ , CH ₄ , N ₂ O, SF ₆ , CO

LIST OF OBSERVATIONAL STATIONS (continued)

Station	Country/Territory	GAW ID	Organization	Latitude (°)	Longitude (°)	Altitude (m)	Parameter
ANTARCTICA							
Arrival Heights	New Zealand	ARH	NIWA	77.83 S	166.66 E	184	CH ₄ , N ₂ O, ¹³ CH ₄ , CO
Casey	Australia	CYA	CSIRO	66.28 S	110.52 E	51	CO ₂ , CH ₄ , N ₂ O, ¹³ CO ₂ , CO, H ₂
Halley	United Kingdom of Great Britain and Northern Ireland	HBA	NOAA	75.57 S	25.50 W	30	CO ₂ , CH ₄ , N ₂ O, SF ₆ , ¹³ CO ₂ , C ¹⁸ O ₂ , CO, H ₂
Halley	United Kingdom of Great Britain and Northern Ireland	HBA	BAS	75.57 S	25.50 W	30	CO
Jubany	Argentina	JBN	IAA	62.24 S	58.67 W	15	CO ₂
King Sejong	Republic of Korea	KSG	KMA	62.22 S	58.78 W	0	CO ₂
Mawson	Australia	MAA	CSIRO	67.60 S	62.87 E	20	CO ₂ , CH ₄ , N ₂ O, ¹³ CO ₂ , CO, H ₂
McMurdo	United States of America	MCM	NOAA	77.85 S	166.67 E	11	CH ₄
Palmer Station	United States of America	PSA	NOAA	64.77 S	64.05 W	10	CO ₂ , CH ₄ , N ₂ O, SF ₆ , ¹³ CO ₂ , C ¹⁸ O ₂ , CCl ₄ , CH ₃ CCl ₃ , CFCs, HCFCs, HFCs, CBrClF ₂ , CO, CH ₃ Cl, CH ₂ Cl ₂ , CH ₃ Br, H ₂
South Pole	United States of America	SPO	NOAA	90.00 S	24.80 W	2841	CO ₂ , CH ₄ , N ₂ O, SF ₆ , ¹³ CH ₄ , ¹³ CO ₂ , C ¹⁸ O ₂ , CCl ₄ , CH ₃ CCl ₃ , CFCs, HCFCs, HFCs, CBrClF ₂ , CBrF ₃ , CO, CH ₃ Cl, CH ₂ Cl ₂ , CH ₃ Br, C ₂ Cl ₄ , H ₂
South Pole	United States of America	SPO	CSIRO	90.00 S	24.80 W	2841	CO ₂ , CH ₄ , N ₂ O, ¹³ CO ₂ , CO, H ₂
Syowa	Japan	SYO	NOAA	69.01 S	39.58 E	18.4	CO ₂ , CH ₄ , N ₂ O, SF ₆ , ¹³ CO ₂ , C ¹⁸ O ₂ , CO, H ₂
Syowa	Japan	SYO	TU	69.01 S	39.58 E	18.4	CO ₂
MOBILE							
Aircraft (Western North Pacific)	Japan	AOA	JMA				CO ₂ , CH ₄ , N ₂ O, CO
Aircraft (off the coast of Sendai Plain)	Japan	PIP	TU				CH ₄
Aircraft (over Bass Strait and Cape Grim)	Australia	AIA	CSIRO				CO ₂ , CH ₄ , N ₂ O, ¹³ CO ₂ , CO, H ₂
Aircraft (over Japan and surroundings)	Japan	OAS	MRI				CH ₄ , N ₂ O, SF ₆ , CFCs
Aircraft: Orleans Alligator liberty, M/V	France	ORL	LSCE				CO ₂ , CH ₄
Atlantic Ocean	Japan	ALL	JMA				CO ₂
CONTRAIL	United States of America	AOC	NOAA				CO ₂
CONTRAIL	Japan	EOM	NIES				¹³ CH ₄ , CH ₃ D
CONTRAIL	Japan	EOM	TU				

LIST OF OBSERVATIONAL STATIONS (continued)

Station	Country/Territory	GAW ID	Organization	Location			Parameter
				Latitude (°)	Longitude (°)	Altitude (m)	
Drake Passage	United States of America	DRP	NOAA				CO ₂ , CH ₄ , N ₂ O, SF ₆ , ¹³CO ₂ , C ¹⁸ O ₂ , CO
INSTAC-I	Japan	INS	MRI				CO ₂ , CH ₄ , ¹³ CO ₂
Keifu Maru, R/V	Japan	KEF	JMA				CO ₂ , CFCs, TIC
Kofu Maru, R/V	Japan	KOF	JMA				CO ₂
MRI Research, 1978-1986, R/V	Japan	MRI	MRI				CH ₄
MRI Research, Hakuho Maru, R/V	Japan	HKH	MRI				CO ₂
MRI Research, Kaiyo Maru, R/V	Japan	KIY	MRI				CO ₂
MRI Research, Natushima, R/V	Japan	NTU	MRI				CO ₂
MRI Research, Ryofu Maru, R/V	Japan	RFM	MRI				CO ₂
MRI Research, Wellington Maru, R/V	Japan	WLT	MRI				CO ₂
Mirai, R/V	Japan	MMR	MRI				CO ₂
Mirai, R/V	Japan	MMR	JAMSTEC				CO ₂
NOPACCS - Hakurei Maru -	Japan	HAK	NEDO				TIC
Northern and western Pacific	Japan	NWP	TU				N ₂ O
Pacific Ocean	United States of America	POC	NOAA				CO ₂ , CH ₄ , N ₂ O, SF ₆ , ¹³CO ₂ , C ¹⁸ O ₂ , CO, H ₂
Pacific Ocean	New Zealand	BSL	NIWA				CH ₄ , ¹³ CH ₄
Pacific-Atlantic Ocean	United States of America	PAO	NOAA				CO ₂ , CH ₄ , N ₂ O, SF ₆ , CO
Ryofu Maru, R/V	Japan	RYF	JMA				CO ₂ , CH ₄ , N ₂ O, CFCs, TIC
Santarem	Brazil	SAN	INPE				CO ₂ , CH ₄ , N ₂ O, SF ₆ , CO
Ship between Ishigaki Island and Hateruma Island	Japan	SIH	TU				CO ₂
South China Sea	United States of America	SCS	NOAA				CO ₂ , CH ₄ , ¹³ CO ₂ , C ¹⁸ O ₂ , CO, H ₂
Soyo Maru, R/V	Japan	SOY	FRA				CO ₂
WEST COSMIC - Hakurei Maru No.2 -	Japan	HRM	NEDO				TIC
Wakataka-Maru	Japan	WAK	FRA				CO ₂
Western Pacific	United States of America	WPC	NOAA				CO ₂ , CH ₄ , N ₂ O, SF ₆ , ¹³ CH ₄ , ¹³ CO ₂ , C ¹⁸ O ₂ , CO
over Japan between Sendai and Fukuoka	Japan	TDA	TU				CH ₄

APPENDIX D LIST OF CONTRIBUTORS

Station Country/Territory	Name	Address
REGION I (Africa)		
Mt. Kenya (Kenya)	Constance Okuku	Kenya Meteorological Department MT KENYA GAW STATION P.O. Box 192 10400 NANYUKI Kenya
	Jörg Klausen	Federal Office of Meteorology and Climatology MeteoSwiss 8058 ZH,Zürich-Flughafen Operation Center 1, Switzerland
	Stephan Henne	Swiss Federal Laboratories for Materials Science and Technology Ueberlandstrasse 129 8600 Duebendorf, Switzerland
Izaña (Tenerife) (Spain)	Emilio Cuevas	State Meteorological Agency of Spain C/ La Marina, 20, Planta 6, 38001 Santa Cruz de Tenerife, Spain
Cape Point (South Africa)	Alastair Williams	ANSTO, Locked Bag 2001 Kirrawee DC, NSW 2232 Australia
Assekrem (Algeria)	Sidi Baika	Office National de la Meteorologie POBox 31 Tamanrasset 11000, Algeria
Amsterdam Island (France)	Michel Ramonet	LSCE - CEA Saclay - Orme des Merisiers - 91191 Gif-sur-Yvette, France
	Jean Sciare	LSCE - CEA Saclay - Orme des Merisiers - Bat.701 91191 Gif-sur-Yvette, France
Cape Point (South Africa)	Thumeka Mkololo	SAWS, c/o CSIR (Environmentek), P.O. Box 320,Stellenbosch 7599, South Africa
	Casper Labuschagne	SA Weather Service, c/o CSIR (Environmentek) P.O. Box 320,Stellenbosch 7599, South Africa
	Lynwill Martin	SAWS, c/o CSIR (Environmentek), P.O. Box 320,Stellenbosch 7599, South Africa
	Warren Joubert	SAWS, c/o CSIR (Environmentek) P.O. Box 320,Stellenbosch 7599, South Africa
Cape Verde Atmospheric Observatory (Cabo Verde)	Katie Read	Department of Chemistry University of York, Heslington York YO10 5DD United Kingdom
	Lucy Carpenter	Department of Chemistry University of York, Heslington York YO10 5DD United Kingdom
REGION II (Asia)		
Hamamatsu (Japan)	Mitsuo Toda	Shizuoka University 3-5-1 Jyohoku, Hamamatsu 432-8561, Japan

LIST OF CONTRIBUTORS (continued)

Station Country/Territory	Name	Address
Cape Ochiishi Hateruma Island (Japan)	Yasunori TOHJIMA	National Institute for Environmental Studies Center for Global Environmental Research 16-2, Onogawa, Tsukuba-shi, Ibaraki 305-8506, Japan
	Hitoshi MUKAI	National Institute for Environmental Studies Center for Global Environmental Research 16-2, Onogawa, Tsukuba-shi, Ibaraki 305-8506, Japan
	Takuya Saito	National Institute for Environmental Studies 16-2 Onogawa, Tsukuba 305-8506, Japan
Memanbetsu Tateno (Tsukuba) (Japan)	Kazuhiro Tsuboi	Meteorological Research Institute 1-1, Nagamine Tsukuba Ibaraki 305-0052
Minamitorishima Ryori Yonagunijima (Japan)	Kazuyuki SAITO	Japan Meteorological Agency 1-3-4 Otemachi Chiyoda-ku Tokyo 100-8122
Bering Island Kotelnyj Island Tiksi (Russian Federation)	Nina Paramonova	Voeikov Main Geophysical Observatory St. Petersburg, Karbyshev Street 7, Russian Federation, 194021
Kyzylcha (Uzbekistan)		
Mt. Waliguan (China)	ZHANG Yong	China Meteorological Administration 46 Zhongguancun S. Ave., Haidian Dist., Beijing, 100081, China
Kisai Mt. Dodaira Urawa (Japan)	Yosuke MUTO	Center for Environmental Science in Saitama 914 Kamitanadare, Kisai-machi, Kita-Saitama-gun, Saitama 347-0115, Japan
Gosan (Republic of Korea)	Haeyoung Lee	National Institute of Meteorological Sciences/Korea Meteorological Administration 33 Seohobuk-ro, Seogwipo, Jeju, 63568 Rep.of Korea
	Park Hyo-Jin	Climate Change Monitoring Division, Korea Meteorological Administration 61 Yeouidaebang-ro 16 gil, Dongjak-gu, Seoul, 07062, Republic of Korea
Takayama (Japan)	Shohei Murayama	AIST Tsukuba West, 16-1 Onogawa, Tsukuba, Ibaraki 305-8569, Japan
Hok Tsui / Cape d Aguilar King's Park (Hong Kong, China)	David H.Y. Lam	Hong Kong Observatory 134A Nathan Road, Kowloon, Hong Kong.

LIST OF CONTRIBUTORS (continued)

Station Country/Territory	Name	Address
	Olivia S.M. Lee	Hong Kong Observatory 134A Nathan Road, Kowloon, Hong Kong.
Nepal Climate Observatory - Pyramid (Nepal)	Igor Arduini	University of Urbino, Dep. of Pure and Applied Sciences (DISPEA) piazza Rinascimento 6, 61029 Urbino - Italy
Anmyeon-do Jeju Gosan (Republic of Korea)	Haeyoung Lee	National Institute of Meteorological Sciences/Korea Meteorological Administration 33 Seohobuk-ro, Seogwipo, Jeju, 63568 Rep.of Korea
	Dajeong Lee	National Institute of Meteorological Sciences/Korea Meteorological Administration 33 Seohobuk-ro, Seogwipo, Jeju, 63568 Rep.of Korea
	Sumin Kim	National Institute of Meteorological Sciences 33, Seohobuk-ro, Seoqwiyo. Jeju, 63568, Rep. of KOREA
Hok Tsui / Cape d Aguilar (Hong Kong, China)	Ka Se Lam	The Hong Kong Polytechnic University Hung Hom, Kowloon, Hong Kong, China
Pha Din (Viet Nam)	Martin Steinbacher	Swiss Federal Laboratories for Materials Science and Technology Ueberlandstrasse 129 CH-8600 Duebendorf Switzerland
	Nguyen Nhat Anh	Viet Nam Meteorological and Hydrological Administration No. 8 Phao Dai Lang street 100000 Ha Noi Viet Nam
Issyk-Kul (Kyrgyzstan)	V. Sinyakov	Kyrgyz National University Manas Street 101, Bishkek, 720033, Kyrgyz Republic
Gosan (Republic of Korea)	Seung-Yeon Kim	National Institute of Environmental Research Environmental Research Complex Gyeongseo-dong, Seo-gu, Incheon, 404-708, Republic of Korea
	Kyung-Jung Moon	National Institute of Environmental Research Environmental Research Complex Gyeongseo-dong, Seo-gu, Incheon, 404-708, Republic of Korea
Suita (Japan)	Tomohiro Oda	Universities Space Research Association Global Modeling and Assimilation Office NASA Goddard Space Flight Center 8800 Greenbelt Road, Greenbelt, Maryland 20771
	Takashi Machimura	Osaka University Green Engineering Lab Division of Sustainable Energy and Environmental Engineering 2-1 Yamadaoka, Suita, Osaka 565-0871 Japan

LIST OF CONTRIBUTORS (continued)

Station Country/Territory	Name	Address
Nagoya (Japan)	A. Matsunami	Research Center for Advanced Energy Conversion, Nagoya University Furo-cho, Chikusaku, Nagoya 464-8603, Japan
Mikawa-Ichinomiya (Japan)	Koji Ohno	Aichi Air Environment Division 1-2 Sannomaru-3chome, Naka-ku, Nagoya, Aichi 460-8501, Japan

REGION III (South America)

El Tololo (Chile)	Martin Steinbacher	Swiss Federal Laboratories for Materials Science and Technology Ueberlandstrasse 129 CH-8600 Duebendorf Switzerland
	Gaston Torres	Dirección Meteorológica de Chile Av. Portales 3450, Estación Central - Santiago
Huancayo (Peru)	Mutsumi Ishitsuka	Observatorio de Huancayo, Instituto Geofisico del Peru Apartado 46, Huancayo, Peru
Arembepe (Brazil)	Luciana Vanni Gatti	National Institute in Space Research Atmospheric Chemistry Laboratory Av. Prof. Lineu Prestes, 2242 Cidade Universitaria, Sao Paulo, SP- BRAZIL CEP 05508-900

REGION IV (North and Central America)

Alert Churchill East Trout Lake Estevan Point Fraserdale Sable Island (Canada)	Lin Huang	Environment and Climate Change Canada Climate Research Division 4905 Dufferin Street, Toronto, Ontario CANADA M3H 5T4
	Doug Worthy	Environment and Climate Change Canada Climate Research Division 4905 Dufferin Street, Toronto, Ontario CANADA M3H 5T4
Candle Lake Chibougamau Egbert Lac La Biche (Alberta) (Canada)	Doug Worthy	Environment and Climate Change Canada Climate Research Division 4905 Dufferin Street, Toronto, Ontario CANADA M3H 5T4

REGION V (South-West Pacific)

Cape Grim (Australia)	Alastair Williams	ANSTO, Locked Bag 2001 Kirrawee DC, NSW 2232 Australia
--------------------------	-------------------	--

LIST OF CONTRIBUTORS (continued)

Station Country/Territory	Name	Address
Cape Grim (Australia)	Paul Krummel	CSIRO Oceans and Atmosphere - Climate Science Centre 107-121 Station Street Aspendale Victoria, 3195 Australia
	Ray Langenfelds	CSIRO Oceans and Atmosphere - Climate Science Centre 107-121 Station Street Aspendale Victoria, 3195 Australia
	Zoë Loh	CSIRO Oceans and Atmosphere - Climate Science Centre 107-121 Station Street Aspendale Victoria, 3195 Australia
Lauder (New Zealand)	Sylvia Nichol	NIWA - Wellington Private Bag 14901, Kilbirnie, Wellington, 6241 301 Evans Bay Parade, Hataitai, Wellington 6021
	Gordon Brailsford	NIWA - Wellington Private Bag 14901, Kilbirnie, Wellington, 6241 301 Evans Bay Parade, Hataitai, Wellington 6021
Baring Head (New Zealand)	Jocelyn Turnbull	GNS Science
	Sylvia Nichol	NIWA - Wellington Private Bag 14901, Kilbirnie, Wellington, 6241 301 Evans Bay Parade, Hataitai, Wellington 6021
	Gordon Brailsford	NIWA - Wellington Private Bag 14901, Kilbirnie, Wellington, 6241 301 Evans Bay Parade, Hataitai, Wellington 6021
Danum Valley (Malaysia)	Ahmad Fairudz Jamaluddin	Malaysian Meteorological Department Jalan Sultan, 46667, Petaling Jaya, Selangor MALAYSIA
	Mohan Kumar Sammاثuria	Malaysian Meteorological Department Jalan Sultan, 46667, Petaling Jaya, Selangor MALAYSIA
Bukit Kototabang (Indonesia)	Martin Steinbacher	Swiss Federal Laboratories for Materials Science and Technology Ueberlandstrasse 129 CH-8600 Duebendorf Switzerland
	Jörg Klausen	Federal Office of Meteorology and Climatology MeteoSwiss 8058 ZH,Zürich-Flughafen Operation Center 1, Switzerland
	Ilahi, Asep Firman	Agency for Meteorology, Climatology and Geophysics Jl. Raya Bukittinggi-Medan Km. 17 Palupuh, District Agam, West Sumatera, Indonesia PO BOX 11 Bukittinggi 26100
	Nahas, Alberth Christian	Agency for Meteorology, Climatology and Geophysics Jl. Raya Bukittinggi-Medan Km. 17 Palupuh, District Agam, West Sumatera, Indonesia PO BOX 11 Bukittinggi 26100
	Reza Mehdi	Agency for Meteorology, Climatology and Geophysics Stasiun Pemantau Atmosfer Global Bukit Kototabang Jl Raya Bukittinggi-Medan Km 17 Palupuh 26100, Bukittinggi

LIST OF CONTRIBUTORS (continued)

Station Country/Territory	Name	Address
REGION VI (Europe)		
Diabla Gora / Puszcza Borecka (Poland)	Zdzislaw Przadka	Institute of Environmental Protection - NRI Kolektorska 4, 01-692 Warsaw, Poland
	Anna Degorska	Institute of Environmental Protection - NRI Kolektorska 4 01-692 Warsaw, Poland
	Krzysztof Skotak	Institute of Environmental Protection - NRI Kolektorska 4, 01-692 Warsaw, Poland
Monte Curcio (Italy)	Mariantonio Bencardino	CNR-Institute of Atmospheric Pollution Research c/o UNICAL-Polifunzionale 87036 Rende, Italy
BEO Moussala (Bulgaria)	Ivo Kalapov	Institute for Nuclear Research and Nuclear Energy Tsarigradsko shose Blvd. 1784 Sofia Bulgaria
Kloosterburen Kollumerwaard (Netherlands)	Ronald Spoor	National Institute of Public Health and the Environment PO Box 1 3720 BA Bilthoven the Netherlands
Schauinsland (Germany)	Ludwig Ries	German Environment Agency Umweltbundesamt, Umweltforschungsstation Schneefernerhaus, Zugspitze 5, 82475 Zugspitze
	Frank Meinhardt	German Environment Agency Umweltbundesamt Messstation Schauinsland Schauinslandweg 2 79254 Oberried-Hofsgrund
Brotjacklriegel Deuselbach Neuglobsow Waldhof Westerland Zingst Zugspitze-Gipfel (Germany)	Ludwig Ries	German Environment Agency Umweltbundesamt, Umweltforschungsstation Schneefernerhaus, Zugspitze 5, 82475 Zugspitze
Zugspitze-Schneefernerhaus (Germany)	Cedric Couret	German Environment Agency Umweltbundesamt, Umweltforschungsstation Schneefernerhaus, Zugspitze 5, 82475 Zugspitze
Jungfraujoch (Switzerland)	Markus Leuenberger	Physics Institute, Climate and Environmental Physics, University of Bern Physics Institute, Climate and Environmental Physics Sidlerstrasse 5, CH-3012 Bern
Tacolneston Tall Tower (United Kingdom of Great Britain and Northern Ireland)	Simon O'Doherty	Atmospheric Chemistry Research Group School of Chemistry University of Bristol Cantocks Close BS8 1TS Bristol United Kingdom

LIST OF CONTRIBUTORS (continued)

Station Country/Territory	Name	Address
	Kieran Stanley	Atmospheric Chemistry Research Group School of Chemistry University of Bristol Cantocks Close BS8 1TS Bristol United Kingdom
	Daniel Say	Atmospheric Chemistry Research Group School of Chemistry University of Bristol Cantocks Close BS8 1TS Bristol United Kingdom
Ridge Hill (United Kingdom of Great Britain and Northern Ireland)	Simon O'Doherty	Atmospheric Chemistry Research Group School of Chemistry University of Bristol Cantocks Close BS8 1TS Bristol United Kingdom
	Daniel Say	Atmospheric Chemistry Research Group School of Chemistry University of Bristol Cantocks Close BS8 1TS Bristol United Kingdom
Sonnblick (Austria)	Wolfgang Spangl	Federal Environment Agency Austria Spittelauer Lände 5 A-1090 Wien
	Iris Buxbaum	Federal Environment Agency Austria Spittelauer Lände 5 A-1090 Wien
	Marina Fröhlich	Federal Environment Agency Austria Spittelauer Lände 5 A-1090 Wien
Teriberka (Russian Federation)	Nina Paramonova	Voeikov Main Geophysical Observatory St. Petersburg, Karbshev Street 7, Russian Federation, 194021
Ocean Station Charlie (United States of America)		
Jungfraujoch (Switzerland)	Martin Steinbacher	Swiss Federal Laboratories for Materials Science and Technology Ueberlandstrasse 129 CH-8600 Dübendorf Switzerland
	Thomas Seitz	Swiss Federal Laboratories for Materials Science and Technology Überlandstrasse 129 CH-8600 Dübendorf Switzerland
Payerne Rigi (Switzerland)	Thomas Seitz	Swiss Federal Laboratories for Materials Science and Technology Überlandstrasse 129 CH-8600 Dübendorf Switzerland
Puy de Dôme (France)	Meyerfeld Yves	Laboratoire d'Aérologie 14 avenue Edouard Belin 31400 - TOULOUSE
	Pichon Jean-Marc	Laboratoire de Météorologie Physique LaMP 4 av. Blaise Pascal TSA 60026 CS 60026 63178 Aubière

LIST OF CONTRIBUTORS (continued)

Station Country/Territory	Name	Address
Monte Cimone (Italy)	Luigi Caracciolo di Torchiarolo	Italian Air Force Meteorological Service Aeronautica Militare Comando Squadra Aerea Reparto di Meteorologia Viale dell'Universita' 4 - 00185 Roma
Pallas (Finland)	Juha Hatakka	Finnish Meteorological Institute Erik Palmenin aukio 1 FI-00560 Helsinki, Finland
Monte Cimone (Italy)	Igor Arduini	University of Urbino, Dep. of Pure and Applied Sciences (DISPEA) piazza Rinascimento 6, 61029 Urbino - Italy
Hegyhatsal K-Puszta (Hungary)	Laszlo Haszpra	Hungarian Meteorological Service H-1181 Budapest, Gilice tér 39.
Plateau Rosa (Italy)	Daniela Heltai	Ricerca sul Sistema Energetico - RSE S.p.A. via Rubattino 54, 20134 Milano, Italy
	Francesco Apadula	Ricerca sul Sistema Energetico - RSE S.p.A. via Rubattino 54, 20134 Milano, Italy
	Andrea Lanza	Ricerca sul Sistema Energetico - RSE S.p.A. via Rubattino 54, 20134 Milano, Italy
Giordan Lighthouse (Malta)	Martin Saliba	University of Malta Department of Geosciences Tal-Qroqq Msida, MSD 2080
	Francelle Azzopardi	University of Malta Department of Geosciences Tal-Qroqq Msida, MSD 2080
	Raymond Ellul	University of Malta Department of Geosciences Tal-Qroqq Msida, MSD 2080
Kosetice Observatory (Czech Republic)	Milan Vana	Czech Hydrometeorological Institute Na sabatce 2050/17, 143 06 Praha 412-Komorany
Fundata (Romania)	Florin Nicodim	National Meteorological Administration Sos. Bucuresti-Ploiesti nr. 97, 71552 Bucharest, Romania
Zeppelin Mountain (Ny Ålesund) (Norway)	Hans-Christen	Department of Applied Environmental Science (ITM) Stockholm University SE-10691 Stockholm
	Birgitta Noone	Department of Applied Environmental Science (ITM) Stockholm University SE-10691 Stockholm

LIST OF CONTRIBUTORS (continued)

Station Country/Territory	Name	Address
Krvavec (Slovenia)	Marijana Murovec	<p>Ministrstvo za okolje in prostor / Ministry of Environment and Spatial Planning Agencija RS za okolje / Slovenian Environment Agency Urad za stanje okolja / State of environment Office Sektor za kakovost zraka / Air Quality Division Vojkova 1b, 1001 Ljubljana, p.p</p>
	Janja Turšič	<p>Ministrstvo za okolje in prostor / Ministry of Environment and Spatial Planning Agencija RS za okolje / Slovenian Environment Agency Urad za stanje okolja / State of environment Office Sektor za kakovost zraka / Air Quality Division Vojkova 1b, 1001 Ljubljana, p.p</p>
	Mateja Gjerek	<p>Ministrstvo za okolje in prostor / Ministry of Environment and Spatial Planning Agencija RS za okolje / Slovenian Environment Agency Urad za stanje okolja / State of environment Office Sektor za kakovost zraka / Air Quality Division Vojkova 1b, 1001 Ljubljana, p.p</p>
Summit (Denmark)	Jacques Hueber	<p>INSTAAR, Univ. of Colorado 1560, 30th Street UCB 450 Boulder, CO 80309 U.S.A.</p>
	Detlev Helmig	<p>INSTAAR, Univ. of Colorado 1560, 30th Street UCB 450 Boulder, CO 80309 U.S.A.</p>
Lampedusa (Italy)	Salvatore Chiavarini	ENEA-UTPRA Via Anguillarese, 301 00123 Rome, Italy
	Damiano Sferlazzo	<p>Italian National Agency for New Technologies, Energy and Sustainable Economic Development Laboratory for Observations and Measurements for Environment and Climate Station for Climate Observations Contrada Capo Grecale 92010 Lampedusa Italy</p>
	Alcide di Sarra	<p>Italian National Agency for New Technologies, Energy and Sustainable Economic Development Laboratory for Observations and Measurements for Environment and Climate Via Anguillarese, 301 00123 Rome, Italy</p>
	Salvatore Piacentino	<p>Italian National Agency for New Technologies, Energy and Sustainable Economic Development Laboratory for Observations and Measurements for Environment and Climate Via Principe di Granatelli 24, 90139 Palermo, Italy</p>
	Tatiana Di Iorio	<p>Italian National Agency for New Technologies, Energy and Sustainable Economic Development Laboratory for Observations and Measurements for Environment and Climate Via Anguillarese 301, 00123 Rome, Italy</p>
	Francesco Monteleone	<p>Italian National Agency for New Technologies, Energy and Sustainable Economic Development Laboratory for Observations and Measurements for Environment and Climate Via Principe di Granatelli 24, 90139 Palermo, Italy</p>

LIST OF CONTRIBUTORS (continued)

Station Country/Territory	Name	Address
Lamezia Terme (Italy)	Daniel Gullì	National Research Council, Institute of Atmospheric Sciences and Climate Area Industriale Comp. 15, 88046 Lamezia Terme
	Claudia Calidonna	National Research Council, Institute of Atmospheric Sciences and Climate Area Industriale Comp. 15, 88046 Lamezia Terme
	Ivano Ammoscato	National Research Council, Institute of Atmospheric Sciences and Climate Area Industriale Comp. 15, 88046 Lamezia Terme
Lecce Environmental-Climate Observatory (Italy)	Adelaide Dinoi	National Research Council, Institute of Atmospheric Sciences and Climate Str. Prv. Lecce-Monteroni km 1.2 73100 Lecce
Capo Granitola (Italy)	Paolo Cristofanelli	ISAC-CNR, VIA Gobetti 101 - 40129 Bologna, Italy
	Ignazio Fontana	Istituto per lo studio degli impatti Antropici e Sostenibilità in ambiente marino via del Mare n. 3 - 91021 Torretta Granitola (TP) - Italy
	Giorgio Tranchida	Istituto per lo studio degli impatti Antropici e Sostenibilità in ambiente marino via del Mare n. 3 - 91021 Torretta Granitola (TP) - Italy
Giovanni Giacalone	Giovanni Giacalone	Istituto per lo studio degli impatti Antropici e Sostenibilità in ambiente marino via del Mare n. 3 - 91021 Torretta Granitola (TP) - Italy
	Jgor Arduini	University of Urbino, Dep. of Pure and Applied Sciences (DISPEA) piazza Rinascimento 6, 61029 Urbino - Italy
	Michela Maione	University of Urbino, Dep. of Pure and Applied Sciences (DISPEA) Istituto di Scienze Chimiche piazza Rinascimento 6, 61029 Urbino - Italy
Monte Cimone (Italy)	Paolo Cristofanelli	ISAC-CNR, VIA Gobetti 101 - 40129 Bologna, Italy
	Michel Ramonet	LSCE - CEA Saclay - Orme des Merisiers - 91191 Gif-sur-Yvette, France
Mace Head (Ireland)		
Begur (Spain)		
Ille Grande Pic du Midi Puy de Dôme (France)		
Pic du Midi (France)	Meyerfeld Yves	Laboratoire d'Aérologie 14 avenue Edouard Belin 31400 - TOULOUSE

LIST OF CONTRIBUTORS (continued)

Station Country/Territory	Name	Address
	Gheusi Francois	Laboratoire d'Aérologie 14 avenue Eduard Belin 31400 Toulouse
Zugspitze-Schneefernerhaus (Germany)	Gabriele Frank	Deutscher Wetterdienst, German Meteorological Service Frankfurter Str. 135 63067 Offenbach Germany
Hohenpeissenberg (Germany)	Dagmar Kubistin	German Meteorological Service Albin-Schwaiger-Weg 10 D-82383 Hohenpeissenberg Germany
	Robert Holla	German Meteorological Service Albin-Schwaiger-Weg 10 D-82383 Hohenpeissenberg Germany
	Matthias Lindauer	German Meteorological Service Albin-Schwaiger-Weg 10 82383 Hohenpeissenberg
	Christian Plass-Dulmer	German Meteorological Service Albin-Schwaiger-Weg 10 D-82383 Hohenpeissenberg Germany
Gartow Lindenberg (Germany)	Dagmar Kubistin	German Meteorological Service Albin-Schwaiger-Weg 10 D-82383 Hohenpeissenberg Germany
	Matthias Lindauer	German Meteorological Service Albin-Schwaiger-Weg 10 82383 Hohenpeissenberg
	Christian Plass-Dulmer	German Meteorological Service Albin-Schwaiger-Weg 10 D-82383 Hohenpeissenberg Germany
Wank Zugspitze-Gipfel (Germany)	Thomas Trickl	Fraunhofer-Institute for Atmospheric Environmental Research Kreuzeckbahnstr. 19 82467 Garmisch-Partenkirchen
Zeppelin Mountain (Ny Ålesund) (Norway)	Ove Hermansen	Norwegian Institute for Air Research P. O. Box 100 Instituttveien 18, N-2027 Kjeller, Norway

ANTARCTICA

Syowa (Japan)	Shuji Aoki	Tohoku University Aoba 6-3, Aramaki, Aoba-ku, Sendai 980-8578
	Shinji Morimoto	Tohoku University Aoba 6-3, Aramaki, Aoba-ku, Sendai 980-8578
	Daisuke Goto	National Institute of Polar Research 10-3 Midori-cho, Tachikawa, Tokyo 190-8518
Jubany (Argentina)	Horacio Rodriguez	Direccion Nacional del Antartico- Istituto Antartico Argentino, Buenos Aires, Argentina Dto. Ciencias de la Atmósfera Instituto Antártico Argentino DIRECCION NACIONAL DEL ANTARTICO

LIST OF CONTRIBUTORS (continued)

Station Country/Territory	Name	Address
		Cerrito 1248 (1010) Capital Federal ARGENTINA
	Angelo Viola	National Research Council, Institute of Atmospheric Sciences and Climate via fosso del Cavaliere 100, Italy
King Sejong (Republic of Korea)	Haeyoung Lee	National Institute of Meteorological Sciences/Korea Meteorological Administration 33 Seohobuk-ro, Seogwipo, Jeju, 63568 Rep.of Korea
	Taejin Choi	Division of Polar Climate Research, KOPRI Get-Pearl Tower, 12 Gaetbeol-ro, Yeonsu-gu, Incheon, 406-840, Republic of Korea
Arrival Heights (New Zealand)	Sylvia Nichol	NIWA - Wellington Private Bag 14901, Kilbirnie, Wellington, 6241 301 Evans Bay Parade, Hataitai, Wellington 6021
	Gordon Brailsford	NIWA - Wellington Private Bag 14901, Kilbirnie, Wellington, 6241 301 Evans Bay Parade, Hataitai, Wellington 6021
Halley (United Kingdom of Great Britain and Northern Ireland)	Neil Brough	British Antarctic Survey High Cross, Madingley Road CAMBRIDGE CB3 0ET

MOBILE

CONTRAIL (Japan)	Hidekazu Matsueda	Meteorological Research Institute Nagamine 1-1, Tsukuba, Ibaraki 305-0052, Japan
	Toshinobu Machida	National Institute for Environmental Studies 16-2 Onogawa, Tsukuba 305-8506, Japan
	Yosuke Niwa	National Institute for Environmental Studies 16-2 Onogawa, Tsukuba 305-8506, Japan
	Kazuhiro Tsuboi	Meteorological Research Institute 1-1, Nagamine Tsukuba Ibaraki 305-0052
Northern and western Pacific (Japan)	Shuji Aoki	Tohoku University Aoba 6-3, Aramaki, Aoba-ku, Sendai 980-8578
	Kentaro Ishijima	Oceanography and Geochemistry Research Department Meteorological Research Institute Japan Meteorological Agency 1-1 Nagamine, Tsukuba, Ibaraki 305-0052, Japan
	Shinji Morimoto	Tohoku University Aoba 6-3, Aramaki, Aoba-ku, Sendai 980-8578
Aircraft (off the coast of Sendai Plain) over Japan between Sendai and	Shuji Aoki	Tohoku University Aoba 6-3, Aramaki, Aoba-ku, Sendai 980-8578

LIST OF CONTRIBUTORS (continued)

Station Country/Territory	Name	Address
Fukuoka (Japan)	Taku Umezawa	National Institute for Environmental Studies 16-2 Onogawa, Tsukuba 305-8506, Japan
	Shinji Morimoto	Tohoku University Aoba 6-3, Aramaki, Aoba-ku, Sendai 980-8578
Ship between Ishigaki Island and Hateruma Island (Japan)	Shuji Aoki	Tohoku University Aoba 6-3, Aramaki, Aoba-ku, Sendai 980-8578
	Shinji Morimoto	Tohoku University Aoba 6-3, Aramaki, Aoba-ku, Sendai 980-8578
CONTRAIL (Japan)	Shuji Aoki	Tohoku University Aoba 6-3, Aramaki, Aoba-ku, Sendai 980-8578
	Taku Umezawa	National Institute for Environmental Studies 16-2 Onogawa, Tsukuba 305-8506, Japan
Soyo Maru, R/V Wakataka-Maru (Japan)	Tsuneo Ono	Fisheries Research Agency Hokkaido National Fisheries Research Institute 116 Katsurakoi, Kushiro 085-0802, Japan
Mirai, R/V (Japan)	Akihiko Murata	Physical and Chemical Oceanography Research Group, Global Ocean Observation Research Center, Research Institute for Global Change (RIGC) Japan Agency for Marine-Earth Science and Technology (JAMSTEC), 2-15, Natsushima, Yokosuka, Kanagawa, Japan 237-0061
Mirai, R/V (Japan)	Hisayuki Yoshikawa-Inoue	Hokkaido University Laboratory of Marine and Atmospheric GeochemistryGraduate School of Environmental Earth Science N10W5, Kita-ku, Sapporo 060-0810, Japan
MRI Research, Wellington Maru, R/V (Japan)	Masao Ishii	Meteorological Research Institute Nagamine 1-1, Tsukuba, Ibaraki 305-0052, Japan
Aircraft (over Japan and surroundings) (Japan)	Kazuhiro Tsuboi	Meteorological Research Institute 1-1, Nagamine Tsukuba Ibaraki 305-0052
INSTAC-I MRI Research, 1978-1986, R/V MRI Research, Hakuho Maru, R/V MRI Research, Kaiyo Maru, R/V MRI Research, Natushima, R/V MRI Research, Ryofu Maru, R/V (Japan)	Hidekazu Matsueda	Meteorological Research Institute Nagamine 1-1, Tsukuba, Ibaraki 305-0052, Japan
	Masao Ishii	Meteorological Research Institute Nagamine 1-1, Tsukuba, Ibaraki 305-0052, Japan
	Kazuhiro Tsuboi	Meteorological Research Institute 1-1, Nagamine Tsukuba Ibaraki 305-0052

LIST OF CONTRIBUTORS (continued)

Station Country/Territory	Name	Address
Alligator liberty, M/V Keifu Maru, R/V Kofu Maru, R/V Ryofu Maru, R/V (Japan)	Kazutaka Enyo	Japan Meteorological Agency Global Environment and Marine Department Marine Division 1-3-4 Ote-machi, Chiyoda-ku, Tokyo 100-8122
	Koji Kadono	Japan Meteorological Agency Global Environment and Marine Department Marine Division 1-3-4 Ote-machi, Chiyoda-ku, Tokyo 100-8122
Aircraft (Western North Pacific) (Japan)	Kazuyuki SAITO	Japan Meteorological Agency 1-3-4 Otemachi Chiyoda-ku Tokyo 100-8122
NOPACCS - Hakurei Maru - WEST COSMIC - Hakurei Maru No.2 - (Japan)	General Environmental Technos	The General Environmental Technos Co., Ltd. (Old:Kansai Environmental Engineering Center, Co., Ltd.) 1-3-5, Azuchi machi, Chuo-ku, Osaka 541-0052, Japan
Santarem (Brazil)	Luciana Vanni Gatti	National Institute in Space Research Atmospheric Chemistry Laboratory Av. Prof. Lineu Prestes, 2242 Cidade Universitaria, Sao Paulo, SP- BRAZIL CEP 05508-900
Pacific Ocean (New Zealand)	Sylvia Nichol	NIWA - Wellington Private Bag 14901, Kilbirnie, Wellington, 6241 301 Evans Bay Parade, Hataitai, Wellington 6021
	Gordon Brailsford	NIWA - Wellington Private Bag 14901, Kilbirnie, Wellington, 6241 301 Evans Bay Parade, Hataitai, Wellington 6021
Aircraft: Orleans (France)	Michel Ramonet	LSCE - CEA Saclay - Orme des Merisiers - 91191 Gif-sur-Yvette, France

LIST OF CONTRIBUTORS (continued)

Station Country/Territory	Name	Address
NOAA /ESRL Flask Network		
Ushuaia (Argentina)	Pieter Tans*	(*) NOAA/ESRL
Cape Grim (Australia)	Kirk Thoning* (CO ₂)	R/GMD1 325 Broadway Boulder, CO 80305-3337
Ragged Point (Barbados)	Ed Dlugokencky* Colm Sweeney* (CO ₂ , CH ₄ , N ₂ O and SF ₆)	(**) Institute of Arctic and Alpine Research University of Colorado Campus Box 450 Boulder, CO 80309-0450 USA
Arembepe Natal (Brazil)	Sylvia Michel** James White** Bruce H Vaughn** (¹³ CH ₄ , ¹³ CO ₂ and C ¹⁸ O ₂)	
Alert Lac La Biche (Alberta) Mould Bay (Canada)	Arlyn Andrews* (CO)	
Easter Island (Chile)	Gabrielle Petron* (CO and H ₂)	
Mt. Waliguan Shangdianzi (China)	Scott Lehman** Jocelyn Turnbull (¹⁴ CO ₂)	
Hohenpeissenberg Ochsenkopf (Germany)		
Summit (Denmark)		
Assekrem (Algeria)		
Izaña (Tenerife) (Spain)		
Pallas (Finland)		
Amsterdam Island Crozet (France)		
Ascension Island Bird Island (South Georgia) Halley St. David's Head Taconeston Tall Tower Tudor Hill (Bermuda) (United Kingdom of Great Britain and Northern Ireland)		
Hegyhatsal (Hungary)		
Bukit Kototabang (Indonesia)		

LIST OF CONTRIBUTORS (continued)

Station Country/Territory	Name	Address
Mace Head (Ireland)		
Sede Boker (Israel)		
Storhofdi (Iceland)		
Lampedusa (Italy)		
Syowa (Japan)		
Mt. Kenya (Kenya)		
Christmas Island (Kiribati)		
Anmyeon-do Tae-ahn Peninsula (Republic of Korea)		
Plateau Assy Sary Taukum (Kazakhstan)		
Ulaan Uul (Mongolia)		
Dwejra Point (Malta)		
Kaashidhoo (Male Atoll) (Maldives)		
Mex High Altitude Global Climate Observation Center (Mexico)		
Gobabeb (Namibia)		
Ocean Station M Zeppelin Mountain (Ny Ålesund) (Norway)		
Baring Head Kaitorete Spit (New Zealand)		
Baltic Sea (Poland)		
Serreta (Terceira) (Portugal)		
Constanta (Black Sea) (Romania)		
Tiksi (Russian Federation)		

LIST OF CONTRIBUTORS (continued)

Station Country/Territory	Name	Address
Mahé (Seychelles)		
Lulin (Taiwan, Province of China)		
Argyle (ME) Atlantic Ocean Barrow (AK) Cape Kumukahi (HI) Cape Meares (OR) Cold Bay (AK) Drake Passage Grifton - Georgia Station (NC) Guam (Mariana Island) Key Biscane (FL) Kitt Peak (AZ) La Jolla (CA) Mauna Loa (HI) McMurdo Moody (TX) Niwot Ridge - T-van (CO) Ocean Station Charlie Olympic Peninsula (WA) Pacific Ocean Pacific-Atlantic Ocean Palmer Station Park Falls (WI) Point Arena (CA) Samoa (Cape Matatula) Sand Island Shemya Island South China Sea South Pole Southern Great Plains E13 (OK) St. Croix Trinidad Head (CA) Wendover (UT) West Branch (Iowa) Western Pacific (United States of America)		
Cape Point (South Africa)		

NOAA /ESRL HATS Network

Ushuaia (Argentina)	Debra J. Mondeel J. David Nance James W. Elkins Bradley D. Hall Geoffrey S. Dutton Stephen A. Montzka	Halocarbons and Other Atmosphere Trace Species Group (HATS)/NOAA/ESRL R/GMD1 325 Broadway Boulder, CO 80305-3337
Cape Grim (Australia)		
Alert (Canada)		
Summit (Denmark)		
Mace Head (Ireland)		

LIST OF CONTRIBUTORS (continued)

Station Country/Territory	Name	Address
Barrow (AK)		
Cape Kumukahi (HI)		
Grifton - Georgia Station (NC)		
Harvard Forest (MA)		
Mauna Loa (HI)		
Niwot Ridge - T-van (CO)		
Palmer Station		
Park Falls (WI)		
Samoa (Cape Matatula)		
South Pole		
Trinidad Head (CA)		
(United States of America)		

LIST OF CONTRIBUTORS (continued)

Station Country/Territory	Name	Address
CSIRO Flask Network		
Aircraft (over Bass Strait and Cape Grim) Cape Ferguson Cape Grim Casey Gunn Point Macquarie Island Mawson (Australia)	Zoë Loh Ray Langenfelds Paul Krummel	Commonwealth Scientific and Industrial Research Organisation (CSIRO) CSIRO Oceans and Atmosphere - Climate Science Centre Private Bag 1, Aspendale, Vic, Australia 3195
Alert Estevan Point (Canada)		
Lerwick (United Kingdom of Great Britain and Northern Ireland)		
Cape Rama (India)		
Mauna Loa (HI) South Pole (United States of America)		
ALE/GAGE/AGAGE Network		
Cape Grim (Australia)	Ray Wang Simon O'Doherty	Advanced Global Atmospheric Gases Experiment Massachusetts Institute of Technology, Center for Global Change Science
Ragged Point (Barbados)	Dickon Young Paul Krummel	Building 54-1312 Cambridge, MA 02139-2307
Jungfraujoch (Switzerland)	Ray F. Weiss Stefan Reimann Martin Vollmer Chris Lunder Michela Maione	
Adrigole Mace Head (Ireland)	Jgor Arduini	
Monte Cimone (Italy)		
Gosan (Republic of Korea)		
Zeppelin Mountain (Ny Ålesund) (Norway)		
Cape Meares (OR) Samoa (Cape Matatula) Trinidad Head (CA) (United States of America)		

APPENDIX E LIST OF ABBREVIATIONS

ORGANIZATIONS:

AEMET	State Meteorological Agency of Spain (Spain)
AGAGE	Advanced Global Atmospheric Gases Experiment Science Team
AICH	Aichi Air Environment Division (Japan)
AIST	National Institute of Advanced Industrial Science and Technology (Japan)
AMERIFLUX	AmeriFlux Network (USA)
ANSTO	Australian Nuclear Science and Technology Organisation (Australia)
ARSO	Slovenian Environment Agency (Slovenia)
BAS	British Antarctic Survey (United Kingdom)
BLG	Bowling Lab Group, Terrestrial Biogeochemistry, Department of Biology, University of Utah (USA)
BMKG	Agency for Meteorology, Climatology and Geophysics (Indonesia)
CALTECH	California Institute of Technology, Division of Geological and Planetary Science (USA)
CHMI	Czech Hydrometeorological Institute (Czech Republic)
CMA	China Meteorological Administration (China)
CSIRO	Commonwealth Scientific and Industrial Research Organisation (Australia)
DMC	Dirección Meteorológica de Chile (Chile)
DWD	Meteorological Observatory Hohenpeissenberg, German Meteorological Service (Germany)
ECCC	Environment and Climate Change Canada (Canada)
ECN	Energy Research Centre of the Netherlands (Netherlands)
Empa	Swiss Federal Laboratories for Materials Science and Technology (Switzerland)
ENEA	Italian National Agency for New Technology, Energy and the Environment (Italy)
FMI	Finnish Meteorological Institute (Finland)
FRA	Fisheries Research Agency (Japan)
GAGE	Global Atmospheric Gases Experiment
GAW	Global Atmosphere Watch (WMO)
GERC	National Institute of Environmental Research (Republic of Korea)
HATS	Halocarbons and other Atmospheric Trace Species Group, NOAA/ESRL (USA)
HKO	Hong Kong Observatory (Hong Kong, China)
HMS	Hungarian Meteorological Service (Hungary)
HU	Harvard University (USA)
IAA	Dirección Nacional del Antártico - Instituto Antartico Argentino, Buenos Aires (Argentina)
IAFMC	Italian Air Force Mountain Centre (Italy)
IAFMS	Italian Air Force Meteorological Service (Italy)
ICOS	Integrated Carbon Observation System (European Union)
IGP	Instituto Geofísico del Perú (Peru)
IIA	CNR - Institute of Atmospheric Pollution Research (Italy)
IMKIFU	Fraunhofer - Institute for Atmospheric Environmental Research (Germany)
INMH	National Meteorological Administration (Romania)
INPE	National Institute in Space Research (Brazil)
INRNE	Institute for Nuclear Research and Nuclear Energy (Bulgaria)
INSTAAR	Institute of Arctic and Alpine Research, University of Colorado (USA)

IOEP	Institute of Environmental Protection - NRI (Poland)
ISAC	National Research Council, Institute of Atmospheric Sciences and Climate (Italy)
ITM	Department of Applied Environmental Science, Stockholm University, (Sweden)
JAMSTEC	Japan Agency for Marine - Earth Science and Technology (Japan)
JMA	Japan Meteorological Agency (Japan)
KIT	Karlsruhe Institute of Technology (Germany)
KMA	Korea Meteorological Administration (Republic of Korea)
KMD	Kenya Meteorological Department (Kenya)
KRISS	Korea Research Institute of Standards and Science (Republic of Korea)
KSNU	Kyrgyz National University (Kyrgyzstan)
KUP	Physics Institute, Climate and Environmental Physics, University of Bern (Switzerland)
LA	Laboratoire d'Aérologie (France)
LAMP	Laboratoire de Météorologie Physique (France)
LSCE	Laboratoire des Sciences du Climat et de l'Environnement (France)
METRI	National Institute of Meteorological Research, KMA (Republic of Korea)
MGO	Voeikov Main Geophysical Observatory (Russian Federation)
MMD	Malaysian Meteorological Department (Malaysia)
MPI-BGC	Max-Planck Institute (MPI) for Biogeochemistry in Jena (Germany)
MRI	Meteorological Research Institute, JMA (Japan)
NAGOU	Nagoya University (Japan)
NCAR	National Center For Atmospheric Research (USA)
NEDO	New Energy and Industrial Technology Development Organization (Japan)
NEON	National Ecological Observatory Network (USA)
NIES	National Institute for Environmental Studies (Japan)
NILU	Norwegian Institute for Air Research (Norway)
NIST	National Institute of Standards and Technology (USA)
NIWA	National Institute of Water & Atmospheric Research Ltd. (New Zealand)
NOAA	National Oceanic and Atmospheric Administration (USA)
NOAA-CSD	Chemical Sciences Division, NOAA (USA)
NOAA/ESRL	Earth System Research Laboratory, NOAA (USA)
NPL	National Physical Laboratory (United Kingdom)
ONM	Office National de la Météorologie (Algeria)
OSAKAU	Osaka University (Japan)
PolyU	The Hong Kong Polytechnic University (Hong Kong, China)
PSU	Penn State University (USA)
RHUL	Royal Holloway University London (United Kingdom)
RIVM	National Institute of Public Health and the Environment (Netherlands)
RSE	Ricerca sul Sistema Energetico - RSE S.p.A. (Italy)
RUG	University of Groningen (RUG), Centre for Isotope Research (CIO) (Netherlands)
SAIPF	Center for Environmental Science in Saitama (Japan)
SAWS	South African Weather Service (South Africa)
SHIZU	Shizuoka University (Japan)
SIO	Scripps Institution of Oceanography (USA)
TU	Tohoku University (Japan)
UBAA	Federal Environment Agency Austria (Austria)
UBAG	German Environmental Agency (Umweltbundesamt) (Germany)
UBAG-SCHAU	Umweltbundesamt, Station Schauinsland (Germany)

UBAG/ZUG	Umweltbundesamt, Zugspitze GAW Station (Germany)
UEA	University of East Anglia (United Kingdom)
UHEI-IUP	University of Heidelberg, Institut für Umweltphysik (Germany)
UMLT	University of Malta (Malta)
UNIURB	University of Urbino, Dep. of Pure and Applied Sciences (DISPEA) (Italy)
UNIVBRIS	Atmospheric Chemistry Research Group School of Chemistry University of Bristol (United Kingdom)
UYRK	University of York (United Kingdom)
VNMHA	Viet Nam Meteorological and Hydrological Administration (Viet Nam)
WCC-Empa	World Calibration Centre (Empa)
WDCGG	World Data Centre for Greenhouse Gases (WMO)
WMO	World Meteorological Organization

ATMOSPHERIC SPECIES:

Be	beryllium
CCl₄	tetrachloromethane (carbon tetrachloride)
C₂Cl₄	tetrachloroethene (tetrachloroethylene)
CFC-11	trichlorofluoromethane (chlorofluorocarbon-11, CCl ₃ F)
CFC-12	dichlorodifluoromethane (chlorofluorocarbon-12, CCl ₂ F ₂)
CFC-113	1,1,2-trichloro-1,2,2-trifluoroethane (chlorofluorocarbon-113, CCl ₂ FCClF ₂)
CFCs	chlorofluorocarbons
CH₄	methane
CHBr₃	tribromomethane (bromoform)
CH₂Br₂	dibromomethane (methylene bromide)
CH₃Br	bromomethane (methyl bromide)
CH₃CCl₃	1,1,1-trichloroethane (methyl chloroform)
CH₃D	deuterated methane
CH₃I	iodomethane (methyl iodide)
CHCl₃	trichloromethane (chloroform)
CH₂Cl₂	dichloromethane (methylene chloride)
CH₃Cl	chloromethane (methyl chloride)
C₂HCl₃	trichloroethene (trichloroethylene)
CO	carbon monoxide
CO₂	carbon dioxide
COS	carbon oxide sulfide (carbonyl sulfide)
H₂	hydrogen
Halon-1211	bromochlorodifluoromethane (CBrClF ₂)
Halon-1301	bromotrifluoromethane (CBrF ₃)
Halon-2402	1,2-dibromo-1,1,2,2-tetrafluoroethane (CBrF ₂ CBrF ₂)
HCFC-141b	1,1-dichloro-1-fluoroethane (hydrochlorofluorocarbon-141b, CH ₃ CCl ₂ F)
HCFC-142b	1-chloro-1,1-difluoroethane (hydrochlorofluorocarbon-142b, CH ₃ CClF ₂)
HCFC-22	chlorodifluoromethane (hydrochlorofluorocarbon-22, CHClF ₂)
HCFCs	hydrochlorofluorocarbons
HFC-134a	1,1,1,2-tetrafluoroethane (hydrofluorocarbon-134a, CH ₂ FCF ₃)
HFC-152a	1,1-difluoroethane (hydrofluorocarbon-152a, CHF ₂ CH ₃)
HFCs	hydrofluorocarbons
N₂O	nitrous oxide
NF₃	nitrogen trifluoride
PFCs	perfluorocarbons
Rn	radon

SF₆ sulphur hexafluoride
SO₂F₂ sulphuryl fluoride

UNITS:

ppm parts per million
ppb parts per billion
ppt parts per trillion

Others:

TIC total inorganic carbon
M/V merchant vessel
R/V research vessel

APPENDIX F LIST OF WMO/WDCGG PUBLICATIONS

DATA REPORTING MANUAL:

WDCGG No. 1 January 1991

WMO WDCGG DATA REPORT:

			(period of data accepted)			
WDCGG No. 2 Part A	October	1992	October	1990	~ August	1992
WDCGG No. 2 Part B	October	1992	October	1990	~ August	1992
WDCGG No. 3	October	1993	September	1992	~ March	1993
WDCGG No. 5	March	1994	April	1993	~ September	1993
WDCGG No. 6	September	1994	September	1993	~ March	1994
WDCGG No. 7	March	1995	April	1994	~ December	1994
WDCGG No. 9	September	1995	January	1995	~ June	1995
WDCGG No.10	March	1996	July	1995	~ December	1995
WDCGG No.11	September	1996	January	1996	~ June	1996
WDCGG No.12	March	1997	July	1996	~ November	1996
WDCGG No.14	September	1997	December	1996	~ June	1997
WDCGG No.16	March	1998	July	1997	~ December	1997
WDCGG No.17	September	1998	January	1998	~ June	1998
WDCGG No.18	March	1999	July	1998	~ December	1998
WDCGG No.20	September	1999	January	1999	~ June	1999
WDCGG No.21	March	2000	July	1999	~ December	1999
WDCGG No.23	September	2000	January	2000	~ June	2000
WDCGG No.25	March	2001	July	2000	~ December	2000

WMO WDCGG DATA CATALOGUE:

WDCGG No. 4	December	1993
WDCGG No.13	March	1997
WDCGG No.19	March	1999
WDCGG No.24	March	2001

WMO WDCGG DATA SUMMARY:

WDCGG No. 8	October	1995
WDCGG No.15	March	1998
WDCGG No.22	March	2000
WDCGG No.26	March	2002
WDCGG No.27	March	2003
WDCGG No.28	March	2004
WDCGG No.29	March	2005
WDCGG No.30	March	2006
WDCGG No.31	March	2007
WDCGG No.32	March	2008
WDCGG No.33	March	2009
WDCGG No.34	March	2010
WDCGG No.35	March	2011
WDCGG No.36	March	2012
WDCGG No.37	March	2013
WDCGG No.38	March	2014
WDCGG No.39	March	2015
WDCGG No.40	March	2016
WDCGG No.41	March	2017
WDCGG No.42	October	2018

WMO WDCGG CD-ROM:

CD-ROM No. 1	March	1995	October	1990	~	December	1994
CD-ROM No. 2	March	1996	October	1990	~	June	1995
CD-ROM No. 3	March	1997	October	1990	~	June	1996
CD-ROM No. 4	March	1998	October	1990	~	December	1997
CD-ROM No. 5	March	1999	October	1990	~	December	1998
CD-ROM No. 6	March	2000	October	1990	~	December	1999
CD-ROM No. 7	March	2001	October	1990	~	December	2000
CD-ROM No. 8	March	2002	October	1990	~	January	2002
CD-ROM No. 9	March	2003	October	1990	~	December	2002
CD-ROM No.10	March	2004	October	1990	~	December	2003
CD-ROM No.11	March	2005	October	1990	~	December	2004
CD-ROM No.12	March	2006	October	1990	~	December	2005
CD-ROM No.13	March	2007	October	1990	~	November	2006
CD-ROM No.14	March	2008	October	1990	~	November	2007

WMO WDCGG DVD:

DVD No. 1	March	2009	October	1990	~	November	2008
DVD No. 2	March	2010	October	1990	~	November	2009
DVD No. 3	March	2011	October	1990	~	November	2010
DVD No. 4	March	2012	October	1990	~	November	2011
DVD No. 5	March	2013	October	1990	~	November	2012
DVD No. 6	March	2014	October	1990	~	November	2013
DVD No. 7	March	2015	October	1990	~	November	2014
DVD No. 8	March	2016	October	1990	~	November	2015

(period of data accepted)

REFERENCES

References

- Aoki, S., T. Nakazawa, S. Murayama, and S. Kawaguchi, Measurements of atmospheric methane at the Japanese Antarctic station, Syowa, *Tellus*, **44B**, 273–281, 1992.
- Cleveland, W. S., and S. J. Devlin, Locally weighted regression: an approach to regression analysis by local fitting, *J. Amer. Statist. Assn.*, **83**, 596–610, 1988.
- Conway, T. J., P. P. Tans, L. S. Waterman, K. W. Thoning, D. R. Kitzis, K. A. Masarie, and N. Zhang, Evidence for interannual variability of the carbon cycle from the National Oceanic and Atmospheric Administration/Climate Monitoring and Diagnostics Laboratory global air sampling network, *J. Geophys. Res.*, **99**, 22831–22855, 1994.
- Dlugokencky, E. J., L. P. Steele, P. M. Lang, and K. A. Masarie, The growth rate and distribution of atmospheric methane, *J. Geophys. Res.*, **99**, 17021–17043, 1994.
- Dlugokencky, E. J., B. P. Walter, K. A. Masarie, P. M. Lang, and E. S. Kasischke, Measurements of an anomalous global methane increase during 1998, *Geophys. Res. Lett.*, **28**, 499–502, 2001.
- Dlugokencky, E. J., R. C. Myers, P. M. Lang, K. A. Masarie, A. M. Crotwell, K. W. Thoning, B. D. Hall, J. W. Elkins, and L. P. Steele, Conversion of NOAA atmospheric dry air CH₄ mole fractions to a gravimetrically prepared standard scale, *J. Geophys. Res.*, **110**, D18306, doi: 10.1029/2005JD006035, 2005.
- Duchon, C. E., Lanczos filtering in one and two dimensions, *J. Appl. Meteor.*, **18**, 1016–1022, 1979.
- Haan, D., and D. Raynaud, Ice core record of CO variations during the last two millennia: atmospheric implications and chemical interactions within the Greenland ice, *Tellus*, **50B**, 253–262, 1998.
- Hall, B. D. (ed.), J. W. Elkins, J. H. Butler, S. A. Montzka, T. M. Thompson, L. Del Negro, G. S. Dutton, D. F. Hurst, D. B. King, E. S. Kline, L. Lock, D. MacTaggart, D. Mondeel, F. L. Moore, J. D. Nance, E. A. Ray, and P. A. Romashkin, Halocarbons and Other Atmospheric Trace Species, Section 5 in Climate Monitoring and Diagnostics Laboratory Summary Report No. 25, 1998–1999, R. S. Schnell, D. B. King, and R. M. Rosson (eds.), NOAA-CMDL, Boulder, CO., USA, 2001.
- Hall, B. D., G. S. Dutton, and J. W. Elkins, The NOAA nitrous oxide standard scale for atmospheric observations, *J. Geophys. Res.*, **112**, D09305, doi: 10.1029/2006JD007954, 2007.
- IPCC, Climate Change 2013: The Physical Science Basis. Contribution of Working Group I to the Fifth Assessment Report of the Intergovernmental Panel on Climate Change [Stocker, T. F., D. Qin, G.-K. Plattner, M. Tignor, S. K. Allen, J. Boschung, A. Nauels, Y. Xia, V. Bex, and P. M. Midgley (eds.)]. Cambridge University Press, Cambridge, United Kingdom and New York, NY, USA, 2013.
- Le Quéré C., R. M. Andrew, P. Friedlingstein, S. Sitch, J. Hauck, J. Pongratz, P. A. Pickers, J. I. Korsbakken, G. P. Peters, J. G. Canadell, A. Arneth, V. K. Arora, L. Barbero, A. Bastos, L. Bopp, F. Chevallier, L. P. Chini, P. Ciais, S. C. Doney, T. Grätzl, D. S. Goll, I. Harris, V. Haverd, F. M. Hoffman, M. Hoppema, R. A. Houghton, G. Hurtt, T. Ilyina, A. K. Jain, T. Johannessen, C. D. Jones, E. Kato, R. F. Keeling, K. K. Goldewijk, P. Landschützer, N. Lefévre, S. Lienert, Z. Liu, D. Lombardozzi, N. Metzl, D. R. Munro, J. E. M. S. Nabel, S. Nakaoka, C. Neill, A. Olsen, T. Ono, P. Patra, A. Peregon, W. Peters, P. Peylin, B. Pfeil, D. Pierrot, B. Poulter, G. Rehder, L. Resplandy, E. Robertson, M. Rocher, C. Rödenbeck, U. Schuster, J. Schwinger, R. Séférian, I. Skjelvan, T. Steinhoff, A. Sutton, P. P. Tans, H. Tian, B. Tilbrook, F. N. Tubiello, I. T. van der Laan-Luijkx, G. R. van der Werf, N. Viovy, A. P. Walker, A. J. Wiltshire, R. Wright, S. Zaehle and B. Zheng, Global Carbon Budget 2018, *Earth Syst. Sci. Data*, **10**, 2141–2194, doi: 10.5194/essd-10-2141-2018, 2018.
- Montzka S. A., G. S. Dutton, P. Yu, E. Ray, R. W. Portmann, J. S. Daniel, L. Kuijpers, B. D. Hall, D. Mondeel, C. Siso, J. D. Nance, M. Rigby, A. J. Manning, L. Hu, F. Moore, B. R. Miller, and J. W. Elkins, An unexpected and persistent increase in global emissions of ozone-depleting CFC-11, *Nature*, **557**, 413–417, doi: 10.1038/s41586-018-0106-2, 2018.
- Novelli, P. C., K. A. Masarie, and P. M. Lang, Distributions and recent changes of carbon monoxide in the lower troposphere, *J. Geophys. Res.*, **103**, 19015–19033, 1998.
- Novelli, P. C., K. A. Masarie, P. M. Lang, B. D. Hall, R. C. Myers, and J. W. Elkins, Reanalysis of tropospheric CO trends: Effects of the 1997–1998 wildfires, *J. Geophys. Res.*, **108**, 4464, doi: 10.1029/2002JD003031, 2003.
- Prinn, R. G., R. F. Weiss, J. Arduini, T. Arnold, H. L. DeWitt, P. J. Fraser, A. L. Ganesan, J. Gasore, C. M. Harth, O. Hermansen, J. Kim, P. B. Krummel, S. Li, Z. M. Loh, C. R. Lunder, M. Maione, A. J. Manning, B. R. Miller, B. Mitrevski, J. Mühle, S. O'Doherty, S. Park, S. Reimann, M. Rigby, T. Saito, P. K. Salameh, R. Schmidt, P. G. Simmonds, L. P. Steele, M. K. Vollmer, R. H. Wang, B. Yao, Y. Yokouchi, D. Young, and L. Zhou, History of chemically and radiatively important atmospheric gases from the Advanced Global Atmospheric Gases Experiment (AGAGE), *Earth Syst. Sci. Data*, **10**, 985–1018, doi: 10.5194/essd-10-985-2018, 2018.
- WMO, Technical Report of Global Analysis Method for Major Greenhouse Gases by the World Data Center for Greenhouse Gases, GAW Report No. 184, WMO TD

- No. 1473, 2009.
- WMO, WMO Global Atmosphere Watch (GAW)
Implementation Plan: 2016-2023, GAW Report
No.228, 2017.
- WMO, WMO Greenhouse Gas Bulletin No.14, 2018a.
- WMO, 19th WMO/IAEA Meeting on Carbon Dioxide,
Other Greenhouse Gases and Related Measurement
Techniques (GGMT-2017), GAW Report No.242,
2018b.
- Worthy, D. E. J., I. Levin, N. B. A. Trivett, A. J. Kuhlmann,
J. F. Hopper, and M. K. Ernst, Seven years of
continuous methane observations at a remote boreal
site in Ontario, Canada, *J. Geophys. Res.*, **103**, 15995–
16007, 1998.
- Zhao, C. L., P. P. Tans, and K. W. Thoning, A high
precision manometric system for absolute calibrations
of CO₂ in dry air, *J. Geophys. Res.*, **102**, 5885–5894,
1997.